CHAPTER 1

INTRODUCTION

1. Neurotrophins

1.1 The Discovery of Neurotrophins

In 1949, Viktor Hamburger and Rita Levi-Montalcini found that factors secreted from tumor cells promote neuronal cell survival and neurite growth. They called those factors "nerve growth promoting factors", later termed Nerve Growth Factor (NGF) (Levi-Montalcini 1949, Cohen & Levi-Montalcini 1957). Later on, Cohen and Levi-Motalcini purified the factor from mice salivary glands. This finding led to the discovery of the neurotrophin family, which was a milestone in the research field of the nervous system.

The neurotrophins are a family of proteins which have similar structure and functions. They have a number of shared characteristics, including similar molecular weights (13.2-15.9 kDa), isoelectric points (in the range of 9-10), and ~50% identity in primary structure. They exist in solution as noncovalently bound dimers. Six cysteine residues conserved in the same relative positions give rise to three intra-chain disulfide bonds (Maisonpierre *et al.* 1990a, Maisonpierre *et al.* 1990b). In addition to NGF, 4 other major neurotrophins have been identified. The second neurotrophin found was brain-derived neurotrophic factor (BDNF) which was purified from pig brain. BDNF is a

factor affecting several neuronal populations not responsive to NGF. Now the family consists of NGF, BDNF, neurotrophin-3 (NT-3), and neurotrophin-4/5 (NT-4/5). More recently, members of numerous other families of proteins, such as glial cell-derived neurotrophic factor (GDNF) family, were also discovered and have the capability to regulate neuronal survival, development and other aspects of neuronal function (Ernfors *et al.* 1990, Hohn *et al.* 1990, Maisonpierre et al. 1990a, Berkemeier *et al.* 1991, Dechant & Neumann 2002). Each factor has a distinct trophic effect on the proliferation and survival, axonal and dendritic growth and remodeling, assembly of cytoskeleton, and synapse formation and function in various subpopulations of neurons in the peripheral and central nervous system.

1.2 The structure of neurotrophins

The NGF gene (in mouse) has multiple small 5'exons (exon VIII). Four distinct precursors which have different sequences at the N termini are generated by RNA processing (Selby et al. 1987). The mouse NGF protein exists as a complex (7S) composed of 3 types of polypeptides, termed α, β and γ (Murphy *et al.* 1977). Spectroscopic measurement and X-Ray diffraction analysis revealed the three-dimensional structure of βNGF, and further contributes to the hypothesis of how NGF binds to p75NTR and TrkA

(Williams *et al.* 1982, McDonald *et al.* 1991, Bradshaw *et al.* 1994). The BDNF gene shares about 50% amino acid similarity with NGF, NT-3 and NT-4/5 (Dechant & Barde 2002). The human BDNF gene consists of seven upstream noncoding exons differentially spliced to the downstream coding exon, producing multiple transcripts. Upstream of the noncoding exons are promoters governing differential mechanisms of activation and tissue-specific transcript expression in the CNS (Garzon & Fahnestock 2007, Liu *et al.* 2006). Neurotrophins are synthesized in precursor forms (proneurotrophins) and proteolytically processed to generate the mature neurotrophins. The mature neurotrophins are produced by prohormone convertases, such as furin, through cleaving the proneurotrophins' cutting sites (Lee *et al.* 2001b, Chao & Bothwell 2002, Nykjaer *et al.* 2004). Both mature neurotrophins and uncleaved proneurotrophins are secreted from cells. The bioactivities of proneurotrophins could differ from those of mature, cleaved neurotrophins (Hempstead 2006).

A recent study showed that the precursor for NGF (proNGF) can bind to p75NTR with a high affinity and induces apoptosis of neurons *in vitro* (Nykjaer et al. 2004, Teng *et al.* 2005). Endogenous proNGF is secreted and then binds and activates p75NTR *in vivo*. proNGF expression is induced by CNS injury, and proNGF derived from injured spinal-cord lysates induced apoptosis of cultured oligodendrocytes in a p75NTR-dependent manner (Harrington *et al.*

2004, Beattie *et al.* 2002). proNGF binds to p75NTR *in vivo*, and inhibition of proNGF binding to p75NTR *in vivo* can rescue CNS neurons (Nykjaer et al. 2004, Lee et al. 2001b). However, proNGF was detected abundantly in central nervous system tissues whereas mature NGF was undetectable, suggesting that proNGF may have a function distinct from its role as a precursor (Fahnestock et al. 2001). Studies showed that proNGF also exhibits neurotrophic activity similar to mature 2.5S NGF on murine superior cervical ganglion neurons and PC12 cells, but are approximately fivefold less active. ProNGF binds to the high-affinity receptor, TrkA, as determined by cross-linking to PC12 cells, and is also slightly less active than mature NGF in promoting phosphorylation of TrkA and its downstream signaling effectors, Erk1/2, in PC12 and NIH3T3-TrkA cells (Fahnestock et al. 2004).

BDNF, as well as the other members of the neurotrophin family, is synthesized as a larger precursor (34 kDa), proBDNF, which undergoes posttranslational modifications and proteolytic processing by furin or related proteases. The metabolic labeling of recombinant human proBDNF in AtT-20 cells with $[^{35}SO_4]Na_2$, showed that proBDNF is N-glycosylated and glycosulfated (Lou et al. 2005). Some proBDNF is released extracellularly and biologically acts as mediator in TrkB phosphorylation, activation of ERK1/2, and neurite outgrowth. Pro-BDNF binds to and activates TrkB and could be involved in

TrkB-mediated neurotrophic activity *in vivo* (Fayard et al. 2005). The precursor undergoes N-terminal cleavage within the trans-Golgi network and/or immature secretory vesicles to generate mature BDNF (14 kDa). Small amounts of a 28-kDa protein that is immunoprecipitated with BDNF antibodies are also evident. This protein is generated in the endoplasmic reticulum through N-terminal cleavage of pro-BDNF at the Arg-Gly-Leu-Thr57--Ser-Leu site. Cleavage is abolished when Arg54 is changed to Ala (R54A) by *in vitro* mutagenesis (Mowla et al. 2001). Like mature BDNF, proBDNF is localized at nerve terminals in the superficial layers of the dorsal horn, trigeminal nuclei, nuclei tractus solitarius, amygdaloid complex, hippocampus, hypothalamus and some peripheral tissues (Zhou et al. 2004). These results suggest that proBDNF, like mature BDNF, is anterogradely transported to nerve terminals and may have important functions in synaptic transmission in the spinal cord and brain (Zhou et al. 2004). Some research suggests BDNF exists as a mixture of proBDNF and mature BDNF in all regions of the human brain tested. Reduced proBDNF may have functional consequences for the selective neuronal degeneration in Alzheimer's disease brain (Michalski & Fahnestock 2003). Mutation in Val66Met of BDNF results in reduction in hippocampal function of learning and the dysfunction of sorting and secretion of intracellular BDNF (Egan *et al.* 2003, Chen *et al.* 2004).

2. Receptors

Neurotrophins mainly activate two kinds of cell surface receptors, the high affinity of tropomyocin receptor kinase (Trk) family which includes three members, TrkA, TrkB and TrkC and the low affinity p75 neurotrophin receptor (p75NTR) which is a member of the tumor necrosis factor (TNF) receptor superfamily. The p75NTR binds to mature forms of NGF, BDNF, NT3 and NT4/5 with the same affinity (dissociation constant $K_d \approx 10^{-9}$M), and Trk receptors bind their cognate ligands with different affinities ($K_d = 10^{-9}$-10^{-10}M). The synergistic contribution of TrkA and p75NTR could increase the binding affinity ($K_d = 10^{-11}$M) of mature neurotrophins (Bibel *et al.* 1999, Kalb 2005).

2.1 The structure of neurotrophin receptors

Almost all of the survival-promoting activities stimulated by neurotrophins are activated by Trk receptors, whereas p75NTR can trigger classical apoptotic effects (Kim *et al.* 1999, Dechant *et al.* 1997). Differential splicing of TrkA, TrkB and TrkC mRNAs are translated to the receptor protein with differences in their ligand binding extracellular domains. The differences will affect the selective binding activity of neurotrophins to their receptors. NGF has high binding affinity to TrkA, brain derived neurotrophic factor (BDNF) and NT-4/5

activate TrkB, and NT-3 activates TrkC but also activates TrkA and TrkB in certain cellular contexts (Dechant 2001).

The extracellular domains of Trk receptors consist of three tandem leucine-rich motifs flanked by two cysteine clusters in the amino termini and two IgG-like domains in the membrane-proximal region. The intracellular domains are highly conserved sequences with kinase activities (Fig. 1A) (Wiesmann et al. 1999). The p75NTR is one member of the TNF-R/fas family receptor. It has four cysteine-rich domains in the extracellular part, which binds all the neurotrophins. Its intracellular domain is similar to the death domains of the TNF-R/fas receptor family (Fig. 1B). The ligand-receptor binding interface contains two patches: one binds to all neurotrophins in the same conserved manner, the other is specific for the NGF binding to TrkA. The research shows that co-expression of TrkA and p75NTR increases the NGF binding affinity. In contrast, the binding affinity of NT-3 to TrkA and TrkB and NT-4/5 to TrkB is reduced when p75NTR exists (Dechant 2001).

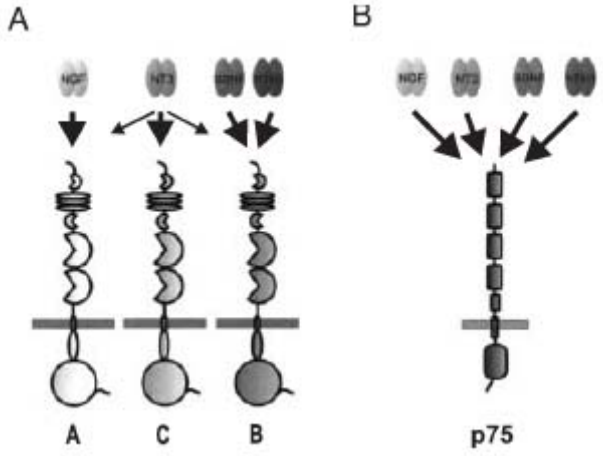

Fig. 1 Neurotrophins bind to two types of transmembrane receptors (Trk and p75NTR). (A) The structure of Trk receptors (A: TrkA, B: TrkB, C: TrkC). The extracellular domains consist of three tandem repeat leucine-rich motifs which are flanked by two cysteine clusters and two Ig-like C2 type domains which are the main contact area for binding different neurotrophins. The intracellular domains of Trk receptors are highly conserved. (B) The structure of p75NTR. The four cysteine-rich domains are the binding domain for neurotrophin ligands and its intracellular domain resembles the death domains found in several members of the TNF-R/fas family (Dechant 2001).

2.2 Molecular interactions between neurotrophin receptors

At the cellular level, the responses to neurotrophins are highly diverse. In different contexts neurotrophins can cause cells to proliferate or stop the cell cycle, to grow neurites or collapse them and to protect the cell from apoptosis or accelerate cell death. The view that neuronal survival signals occur via Trk receptor and apoptosis signals via p75NTR is too dogmatic and is not correct in most cases. For Trk receptors, the developing brains of Trk-knockout mice turn out surprisingly intact. For p75NTR knockout, the highly expressed p75NTR embryonic mice brains seem unaffected. Hence, it seems that the physiological effects of neurotrophins are highly diverse based on the molecular interactions

of their receptors in specific cellular environments (Bothwell 1995, Carter *et al.* 1996, Bibel et al. 1999).

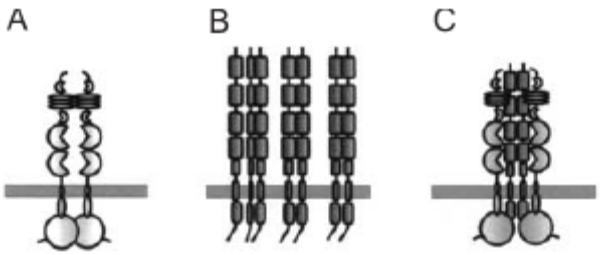

Fig. 2 Neurotrophin receptor complexes. The neurotrophin receptors form complexes within the plasma membrane. Biochemical evidence has been provided for homodimeric Trk receptors (A), for complexes between p75 monomers (B), and for mixed complexes containing both Trk and p75 receptors (C). Formation of these complexes often correlates with higher ligand affinity and specificity (Dechant 2001).

Biochemical experiments show that neurotrophin signals are triggered mainly by three types of complexes: homodimers of Trk receptors (Fig. 2A), trimers of p75NTR (Fig. 2B) and mixed p75NTR-Trk receptor (Fig. 2C). The complexes coexist and are linked through biochemical equilibria, such as receptor phosphorylation and ligand binding. A different receptor complex may cause the cross talk between different neurotrophin signals, which makes the signaling complicated (Bamji *et al.* 1998, Dechant 2001).

2.3 Trk receptor-mediated signaling pathways and functions

When neurotrophins bind to the Trk receptors, the receptors become dimerized and autophosphorylated on tyrosines of the intracellular domain, which has tyrosine kinase activity. The cytoplasmic domains of Trk receptors contain several tyrosines that can be phosphorylated by each receptor's tyrosine kinase upon binding of neurotrophins. After phosphorylation, these cytoplasmic tyrosine domains contribute to Trk-mediated signaling. The major signal pathways activated by Trk receptors are Ras, PI3-kinase, PLC-γ1 and their downstream effectors (Huang & Reichardt 2003). Among those cytoplasmic tyrosine kinase domains, two (Y490 and Y785) are the major sites for phosphorylation. The phosphorylated Y490 offers a recruitment site for both Shc and Frs2, which provide links to Ras, MAPK, PI3-kinase and other pathways. The phosphorylated Y785 recruits the enzyme PLC- γ 1 which results in Ca^{2+} and protein kinase C mobilization.

Ras is a small GTP (Guanosine-5'-triphosphate) binding protein. When this molecule is bound to GDP (Guanosine diphosphate), the molecule remains inactive. Several different adaptors appear to become engaged in promoting Ras activation. Shc is the adaptor protein which is recruited through the PTB domain by phosphorylated Y490, and then phosphorylated Shc induces the

phosphorylation of adaptor Grb2 which can bind to the Ras exchange factor son of sevenless (SOS). Additional scaffold proteins, like Src homology-2 domains (APS) and insulin receptor substrate-1 (IRS1), also link to Ras in some cell types. The adaptor proteins activate the intracellular signaling events, including Ras-Raf-Erk, PI3 Kinase-Akt, PLC-4-Ca^{2+}, NFκB and a typical protein kinase C pathway (Qian & Ginty 2001, Kaplan & Miller 2000, Foehr *et al.* 2000, Wooten *et al.* 1999). For example, activated Ras stimulates signaling through c-Raf-Erk, p38MAP kinase and class I PI3 kinase pathway (Xing *et al.* 1998, Vanhaesebroeck *et al.* 2001). Ras activation is required for normal neuronal differentiation and the survival of many neuronal subpopulations. Phosphorylated Y490 also recruits an adaptor called Frs2, which is required for the activation of MAP kinases. This signal pathway is essential for the genes' transcription which is important in the neuron differentiation and survival. PI3 kinase provides phosphoinositides (PI3) phosphorylated, which have various effects on neuronal survival and development. Firstly, those lipid products generated by PI3K recruit some phosphoinositide-dependent kinases, and they activate the protein kinase Akt, which in turn controls several proteins important in promoting cell survival through the reaction of phosphorylation. In addition, PI3 kinase also affects some targets to promote axon growth and pathfinding, and neuronal differentiation (Yuan & Yankner 2000, Brunet *et al.* 2001, Reichardt 2006).

The phosphorylation of Y785, cytoplasmic tyrosine kinase domains of Trk receptors, leads to the recruitment of the enzyme PLC-r1 which activates IP3 and DAG. IP3 can provide Ca^{2+} release from cytoplasmic stores. DAG can stimulate DAG-regulated isoforms of protein kinase C. Together, signaling through this pathway controls expression and/or activity of many proteins, including ion channels and transcription factors. In addition, neurotrophins also contribute to organization of the cytoskeleton, cell motility, growth cone behaviors and thermal sensitization through some poorly defined pathways (Corbit *et al.* 1999, Minichiello *et al.* 2002, Yuan *et al.* 2003, Klein *et al.* 2005).

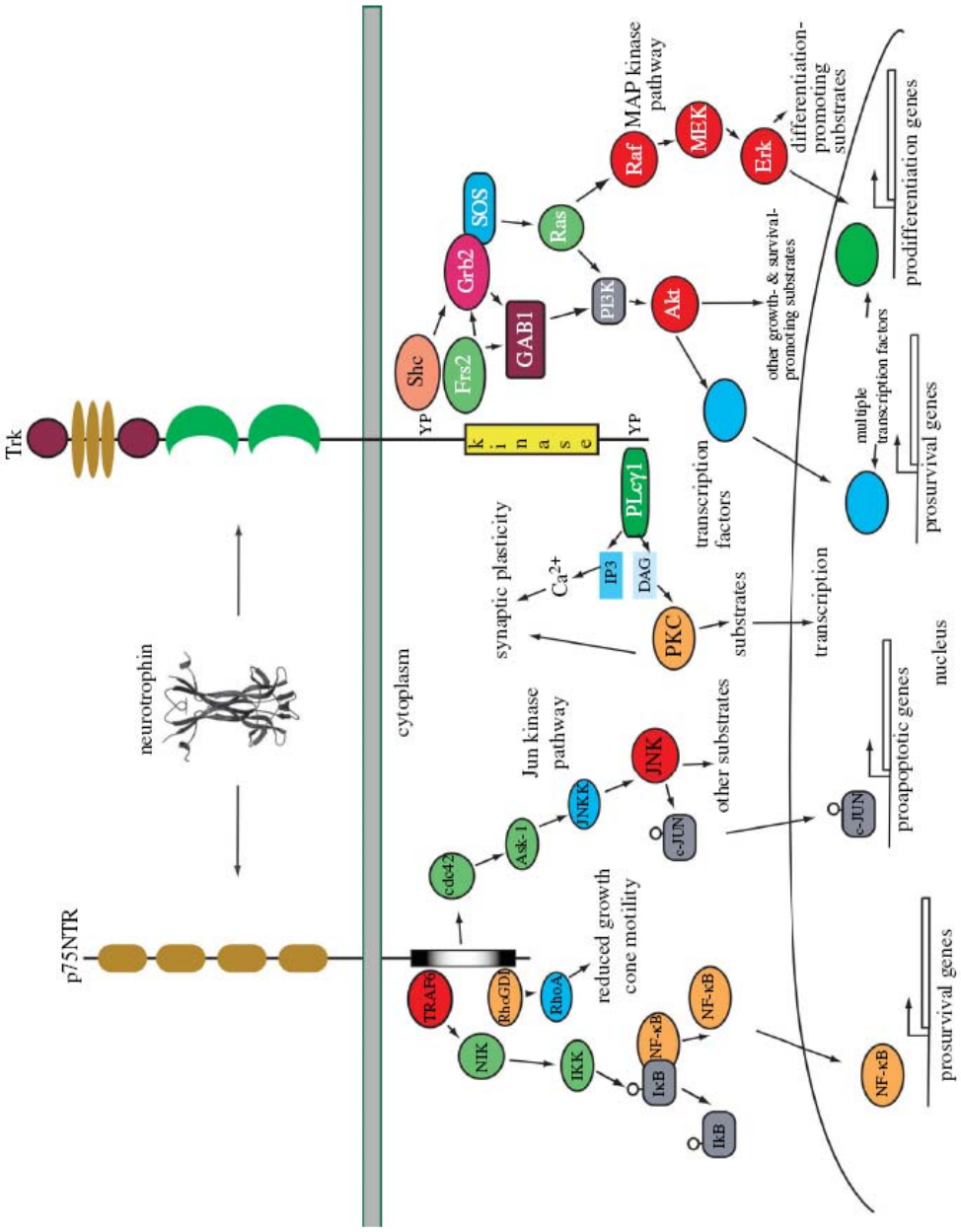
Trk
p75NTR
neurotrophin
cytoplasm
nucleus
Shc
Frs2
Grb2
SOS
GAB1
Ras
Raf
MEK
Erk
MAP kinase pathway
differentiation-promoting substrates
prodifferentiation genes
PI3K
Akt
other growth- & survival-promoting substrates
multiple transcription factors
prosurvival genes
transcription factors
PLCγ1
IP3
DAG
Ca2+
synaptic plasticity
PKC
substrates
transcription
TRAF6
RhoGDI
RhoA
reduced growth cone motility
cdc42
Ask-1
JNKK
JNK
Jun kinase pathway
other substrates
c-JUN
proapoptotic genes
NIK
IKK
NF-κB
IκB
prosurvival genes

Fig. 3 Neurotrophin signalling. This depicts the interactions of each neurotrophin with Trk and p75NTR receptors and major intracellular signalling pathways activated through each receptor. The p75NTR receptor regulates three major signalling pathways. NF-kB activation results in transcription of multiple genes, including several that promote neuronal survival. Activation of the Jun kinase pathway similarly controls activation of several genes, some of which promote neuronal apoptosis. Ligand engagement of p75NTR also regulates the activity of Rho, which controls growth cone motility. Pro-apoptosis actions of p75NTR appear to require the presence of sortilin, which functions as a co-receptor for the neurotrophins. Sortilin is not depicted in this figure, but is described in the text. Many additional adaptors for p75NTR and Trk receptors have been identified which are not depicted in this figure for simplicity, but are described in more detail in the text (Reichardt 2006).

2.4 The p75NTR-mediated signaling pathways and functions

The p75NTR has lower binding affinity to the mature forms of neurotrophins, but surprisingly has higher binding affinity to the proneurotrophins together with sortilin, a Vps 10-domain containing protein (Nykjaer et al. 2004, Chen *et al.* 2005). The p75NTR inhibits axon growth by the complex with Nogo receptor and Lingo-1 (Wang *et al.* 2002, Wong *et al.* 2002b, Yamashita *et al.*

2005).

Like Trk receptor multi adaptor proteins, the intracellular domain of p75NTR can activate several signaling pathways by binding to factors such as Traf6, neurotrophin receptor-interacting factor (NRIF), melanoma-associated antigen acting factor (MAGE), neurotrophin receptor p75NTR interacting MAGE homologue (NRAGE) and other proteins (Yamashita et al. 2005). One major signaling pathway activated by p75NTR is the Jun kinase-signaling cascade, which is implicated in neuronal cell death. p53 is activated in this pathway and this results in apoptosis. Furthermore, the activities of the Jun kinase pathway induce the expression of Fas ligand, which also results in apoptosis (Yeiser et al. 2004). The p75NTR can activate RhoA directly to inhibit neurite outgrowth. However, neurotrophins binding to p75NTR can stimulate neurite outgrowth by eliminating p75NTR-dependent activation of RhoA (Yamashita *et al.* 1999, Yamashita & Tohyama 2003). The p75NTR also can promote NF-κB-dependent neuronal survival by activation of NF-κB. In this process, both p62 and the activity of interleukin-1 receptor-associated kinase (IRAK) are necessary (Hamanoue *et al.* 1999, Middleton *et al.* 2000).

2.5 The crosstalk between the p75NTR and Trk receptors

In general, the two different receptors usually have opposing effects: the Trk receptors promote neuronal survival and differentiation, while p75NTR frequently, but not always, generate apoptosis. But this theory is overly simplistic. The life and death destinations are not segregated between one receptor or the other. Many factors contribute to the complexity of cellular responses to neurotrophins.

The Ras signaling pathway activated by the Trk receptor suppresses the major pro-apoptotic-signalling pathway stimulated by p75NTR (Yoon et al. 1998). The intermediates generated from Trk signaling pathway, such as PI3-kinase, Jnk-interacting protein 1 (JIP1) and Akt1, are involved in the various mechanisms through which Trk receptor activation suppresses the apoptotic effects of p75NTR signaling (Patapoutian & Reichardt 2001, Aloyz *et al.* 1998). On the other hand, the p75NTR pathway intermediate NF-κB increases the survival possibility of neurons (Thomas *et al.* 2005, Maggirwar *et al.* 2000) and proteins such as ARMS and caveolin adjust both p75NTR and Trk receptor signaling pathway (Bilderback *et al.* 1999, Du *et al.* 2006, Zampieri & Chao 2006, Kong *et al.* 2001, Chang *et al.* 2004). Together, all these studies about the synergistic effect of both receptors show that the pro-apoptotic signals of p75NTR are largely suppressed by p75NTR-Trk receptor interactions. Much evidence indicates that Trk receptors could also induce cell death (Muragaki *et*

al. 1997, Zampieri & Chao 2006), however the mechanism is still unknown. MAP kinase and PI3 kinase are involved in the death-promoting signaling, but the downstream effectors are unknown. The activated Trk receptors also alter the function of ligand-gated and voltage-gated ion channels (such as the NMDA receptor and $Na_v1.9$) which leads to Na^+ and Ca^{2+} current changes. The cell-type specificity, state of maturation and receptor complex may also contribute to Trk induced apoptosis (Fryer *et al.* 2000, Choi *et al.* 2004b, Kalb 2005).

3. Sensory neurons as a model for neurotrophin studies

3.1 Expression of neurotrophin receptors

The sensory neurons of ganglia are those which are the easiest to access and which also have a precise anatomical location, and the number of neurons in each sensory ganglion is comparatively constant and easy to determine. Moreover, the sensory neurons in dorsal root ganglia (DRG) supply different types of sensory receptors in multiple body locations. Thus, sensory ganglia represent good models for the analysis for neurotrophins effects.

The biological effects of neurotrophins are mediated through Trk receptors. Trk receptor expression was investigated by using *in situ* hibridizaton in DRG

(Tessarollo *et al.* 1993, Mu *et al.* 1993, Farinas *et al.* 1998). The results indicate that the time frame of Trk expression is consistent with neurotophins synthesis at early developmental stages. All Trk receptors begin expression from early embryonic stages, just a few hours after neurogenesis begins in these ganglia. Between E10 and E11, TrkB and TrkC expression is observed and TrkC is expressed in a majority of neurons but this expression stops at E13. The major quantity of TrkA is generated between E11 and E13 in DRGs. The Trk expression pattern of thoracic DRGs is similar to lumber DRGs which have more neurons expressing Trk receptors. At embryonic age, 40% of thoracic neurons express TrkA which are mainly in small neurons, 6% of neurons express TrkB which are mainly in intermediate and large neurons, and 8% of neurons express TrkC which are mainly in large neurons. In embryonic and in adult stages, TrkB and TrkC were observed coexpressed in some neurons.

The p75NTR plays a role in cell death and is constitutively expressed within a subpopulation of DRG sensory neurons. In the C7 and C8 DRG of the newborn rat, p75NTR is expressed in approximately 70% of DRG neurons. The expression of p75NTR is observed in neurons throughout the entire neuronal size range. This is the reason which is speculated to be responsible for why those neurones which constitutively express the highest levels of p75NTR are

the most vulnerable following axotomy (Murray & Cheema 2003).

NGF controls survival, differentiation, and target innervation of both peptidergic DRG sensory neurons. The common receptor for GDNF family ligands, Ret, is highly expressed in nonpeptidergic neurons. NGF controls expression of several other genes characteristic of nonpeptidergic neurons, such as TrpC3, TrpM8, MrgD, and the transcription factor Runx1, via a Ret-independent signaling pathway. These findings support a model in which NGF controls maturation of nonpeptidergic DRG neurons through a combination of GFR/Ret-dependent and -independent signaling pathways (Luo *et al.* 2007).

3.2 Neurotrophins are required for the survival of sensory neurons

It has been reported that all members of the neurotrophin family of neuronal growth factors promote survival and neurite outgrowth of dorsal root ganglion (DRG) neurons *in vitro* (Mu et al. 1993). The essential effects of neurotrophins on sensory neuron survival have been investigated *in vivo* by using the neurotrophin or Trk gene knock out animal or by injection of specific neurotrophin antibodies against endogenous neurotrophins (Farinas 1999, Crowley *et al.* 1994, Smeyne *et al.* 1994). Sensory neuron loss was observed in each of the individual neurotrophin and Trk-deficient mice. In the DRGs of

NGF or TrkA-deficient mice, approximately 70% of the normal complement of neurons are missing, while NT-3 absence causes 60-70% neuronal loss in DRG (Farinas *et al.* 1996, Crowley et al. 1994, Smeyne et al. 1994). Both NGF and NT-3 are expressed during early embryogenesis. NGF is expressed in those neurons that have already projected into the limb. The NGF expression is restricted to the limb epidermis. NT-3 is the most abundantly expressed neurotrophin during embryogenesis, but its expression domain changes as axons grow distally. BDNF and NT-4/5 are not clearly detectable at times of gangliogenensis (Coppola et al. 2001). The early death of sensory neurons and the reduction in neuron number suggest that these neurotrophins are critical in the sensory neuron development.

At embryonic stages, NGF and NT-3 contribute greatly in determining the final neuron number. After birth, BDNF plays a role in regulating neuron survival. A lack of TrkB or BDNF causes 30-35% neuron loss at 2 weeks of age (Klein *et al.* 1993, Ernfors *et al.* 1994). This suggests that BDNF is acting to maintain a normal complement of DRG neurons and a deficiency in BDNF production causes the loss of certain type of neurons (LeMaster et al. 1999).

3.3 Response to nerve injury and functions of neurotrophins on injured neurons

Unlike other regions of the body, after a nerve is injured in the periphery, no neuronal mitosis or proliferation occurs (Burnett & Zager 2004). A few hours after injury, axon and myelin start to breakdown progressively. Ultrastructurally, the microtubules, neurofilaments and axonal contour become disarrayed. In this degeneration process, Schwann cells and endoneurial mast cells play pivotal roles. Schwann cells are activated within 24 hours after injury and their mitotic rate is increased. These cells divide rapidly to form de-differentiated daughter cells which can help to remove the degenerated axonal and myelin fractions and pass them to macrophages. Through this process, the site of injury can be cleared. The endoneurial mast cells proliferate quickly within the first 2 weeks after injury. The released histamine and serotonin help macrophage activity. The inflammatory response is also one of the results of nerve injury, which is caused by the local vascular trauma hemorrhage and edema. The proliferated fibroblasts lead to the fusiform swelling of the injured segment and the enlargement of the entire nerve trunk (Richardson *et al.* 1980, Sunderland 1990, Sunderland & Bradley 1950).

Soon after nerve injury, macrophages stimulate the rapidly increasing concentration of NGF mRNA, NGF receptor (TrkA) mRNA in the vast majority of sympathetic and sensory neuron, which leads to the retrograde

transport of NGF to the cell body to act in its survival role (Farinas et al. 1998). NGF induces motoneuron apoptosis through its receptor p75NTR (Sedel et al. 1999). NGF also acts on Schwann cells to regrow axon sprouts (Yin *et al.* 1998, Burnett & Zager 2004).

The receptor of BDNF (TrkB) is widely expressed in motoneurones. BDNF increases neurite outgrowth and innervation of motoneurones. All *in vivo* and in vitro studies strongly suggest the effect of BDNF on axonal and neurite regeneration, especially on motor nerves (Ye & Houle 1997). After sciatic nerve transection, BDNF delivered on the injured side improves the rate and degree of the recovery of sciatic function (Utley et al. 1996).

NT-3 induces survival and differentiation responses in sensory and parasympathetic neurons and NT-3 increases the regenerative sprouting of transected corticospinal tract (Henderson *et al.* 1993, Schnell *et al.* 1994). The combination of NT-3 and BDNF enhances propriospinal axonal regeneration and more significantly, promotes axonal regeneration of specific distant populations of brain stem neurons into grafts at the mid-thoracic level in adult rat spinal cord (Xu et al. 1995).

4. Transport and release of neurotrophins

Generally, neurotrophins come from two sources, autocrine and paracrine. Firstly, during development, neurotrophins are synthesized and secreted by the regions being invaded by axons. This secretion offers trophic support to neurons that are targeting their final destination (Ringstedt *et al.* 1999, Wong et al. 2002b). Secondly, after peripheral nerve injury, the inflammatory response and release of cytokines induces the accurate expression of NGF and other neurotrophins in Schwann cells and fibroblasts within the injured nerve. NGF is also synthesized in mast cells and released following mast cell activation. These phenomena are believed to be essential for the survival and regeneration of injured neurons (Korsching 1993, Levi-Montalcini *et al.* 1996). Thirdly, many neurons themselves synthesize neurotrophins. For example, BDNF acts in an autocrine or paracrine fashion to support DRG sensory neurons, and it is also transported anterogradely, trans-synaptically and retrogradely to effect other neurons in the brain (Altar *et al.* 1997, Brady *et al.* 1999, Huang & Reichardt 2001).

In neuronal cells, following receptor-mediated internalization, neurotrophins can be sorted into several subcellular pathways including being recycled back to the plasma membrane either as a ligand-receptor complex or as the receptor only, they can be rapidly degraded or they can be transported via retrograde

transcytosis (von Bartheld 2004, Butowt & von Bartheld 2001). The ligand-receptor complex internalizes through clathrin-mediated endocytosis. After internalization, some of the vesicles are transported retrogradely to the cell body using the dynein-dependent and microtubule-dependent transport mechanism. The vesicle-associated Trk receptors remain autophosphorylated and capable of promoting a unique set of signals upon arrival at the cell bodies. These include PI3K and Erk5. The alternative model for retrograde signaling is that after neurotrophin binding to Trk receptors on distal axons, a wave of ligand-independent Trk phosphorylation is retrogradely propagated, or local signals emanating from Trk receptors in distal axons are themselves propagated to cell bodies where they promote activation of cell body-associated Trk and consequently cell survial (Ginty & Segal 2002, Campenot & MacInnis 2004). Once the protein has been transported to either axon terminals or to somatodendritic domains, it can be released from the neuron (von Bartheld 2004, Butowt & von Bartheld 2001).

4.1 Transport of NGF

Axonal retrograde transport of neurotrophins is essential for neuronal growth and survival (Hendry *et al.* 1974a, Hendry *et al.* 1974b). Retrograde transport of NGF is the classic model of neurotrophin transport as a target-derived

survival factor. In adult sympathetic neurons, the endocytosis of NGF is conducted through p75NTR and TrkA (Gatzinsky et al. 2001). Rapid internalization and retrograde trafficking of the NGF-TrkA complex has been demonstrated in a number of systems and this is thought to transmit trophic signals from neuronal terminals to cell bodies. The NGF-p75NTR complex is another internalization pathway. It can be internalized into early endosomes and eventually accumulates in recycling endosomes in the cell (Bronfman *et al.* 2003, Lalli & Schiavo 2002).

4.2 Transport of NT-3

Neurotrophin-3 (NT-3) retrograde transport was tested at adult peripheral nervous system (PNS) and central nervous system (CNS) neuron cell bodies by intracranial and intranerve injections of iodinated NT-3 (Altar & DiStefano 1998). Unlike NGF, NT-3 is produced in a variety of adult neural systems. The investigation of NT-3 localisation by use of highly specific and sensitive antibodies, identified NT-3 proteins in nerve terminals where no NT-3 mRNA was found (Radka et al. 1996). In the chick retinotectal pathway and zebra fish motor-cortical pathway, the anterograde transport of exogenous NT-3 depends on a complex of TrkC and p75NTR and promotes the survival of postsynaptic neurons after axotomy (Johnson *et al.* 1997, von Bartheld *et al.* 1996b, von

Bartheld *et al.* 1996a). Most newly synthesized NT-3 is released through the constitutive secretory pathway as a result of furin-mediated endoproteolytic cleavage of proNT3 in the trans-Golgi network. Sorting of the NT3 precursor can occur in both the constitutive and regulated secretory pathways, which is consistent with NT3 having both survival-promoting and synapse-altering functions (Farhadi et al. 2000).

4.3 Transport of BDNF

Nerve growth factor (NGF) is released through the constitutive secretory pathway from cells in peripheral tissues and nerves where it can act as a target-derived survival factor. In contrast, brain-derived neurotrophic factor (BDNF) appears to be processed in the regulated secretory pathway of brain neurons and secreted in an activity-dependent manner to play a role in synaptic plasticity (Mowla et al. 1999). After being synthesized, unlike most proNGF efficiently cleaved by the endoprotease furin which is also the preferred proprotein convertases (PCs) of proBDNF in the trans-Golgi network (TGN), BDNF is mainly secreted as proBDNF (Hempstead 2006, Lee et al. 2001b, Lee *et al.* 2001a). The secreted proBDNF can be converted to mature BDNF by the action of extracellular tPA/plasmin (Lee et al. 2001b, Pang *et al.* 2004). There also has a controversial study showed that proBDNF was effectively processed

by furin, PACE4 and PC516-B in coexpressed either the kidney epithelial cell line BSC40 or the furin activity-deficient colon carcinoma cell line LoVo (Seidah et al. 1996). As it was discussed in the paper, those experiments performed under conditions where both the substrate and the convertase were expressed at high levels. In vivo, the enzyme to substrate ratios may differ widely from one type of cell to the other, which may influence the nature of the convertase responsible for the processing of each neurotrophin precursor.

Although little is known about the bidirectional transport mechanisms of BDNF, many groups are investigating this issue. In the PNS, convincing studies using a double ligation of sciatic nerve have shown that endogenous BDNF accumulated on both proximal and distal sides of the ligature (Zhou & Rush 1996, Tonra *et al.* 1998). It also has been shown that the injury of sensory neurons can upregulate the expression and anterograde transport of BDNF (Tonra et al. 1998). In the CNS, anterograde transport is a common feature of BDNF trafficking. Many regions, such as medial habenula, central nucleus of the amygdala, bed nucleus of stria terminalis, lateral septum and spinal cord, were detected by immunohistochemistry containing extremely heavy BDNF-immunoreactive fiber/terminal labeling that lacked BDNF mRNA. This observation suggested that in these regions BDNF was derived from anterograde axonal transport by afferent systems (Conner *et al.* 1997, Altar et

al. 1997). In all, BDNF is bidirectionally transported in axons, but the mechanisms of how BDNF is transported is not known.

4.3.1 Anterograde transport

Anterograde transport is the process of transport of molecules from the cell body to axons and dendrites. Many kinesin superfamily proteins (KIFs) participate in this sort of transport as molecular motors. In axons and dendrites, microtubules act as rails along which a variety of cargoes including protein complexes, vesicular and cytoskeletal components can be transported (Schliwa & Woehlke 2003). Microtubules in axons and distal dendrites are unipolar, and their plus ends orient distal to the cell body. However, microtubules in proximal dendrites are of mixed polarity (Baas et al. 1989). During transport, the neurotrophins may be packed in the vesicles or fused into organelles (Mukherjee *et al.* 1997, Gunawardena & Goldstein 2004a, von Bartheld 2004).

The mechanism of anterograde transport is still incompletely understood and the identity of transport cargoes is not entirely clear. Large dense core vesicles (LDCV) may be one of these cargoes (Shakiryanova *et al.* 2005, Li *et al.* 1999a). In axon terminals, LDCVs have been associated with anterogradely transported neurotrophins. But in some cell types such as hippocampal

neurons, LDCVs rarely exist, suggesting that newly synthesized trophic factors may not be packaged and transported in LDCVs in hippocampal neurons (Smith et al. 1997).

4.3.2 Retrograde transport

Retorgrade transport is the process of transport of molecules from the axonal or dendritic terminals to the cell body. Many dynein superfamily proteins participate in this sort of transport as molecular motors (Gunawardena & Goldstein 2004a). Recent studies indicate endosomes are the main retrograde transport vehicles (Wahle *et al.* 2005, Seaman *et al.* 1998), while other studies identify multivesicular bodies (MVBs) as the major trafficking organelles for retrograde transport (Gabriely et al. 2007). Neurotrophins bind and activate their receptors at axon terminals and are internalized into cells through receptor-dependent mechanisms. Endocytosed neurotrophins and receptors enter the retrograde transport pathway along the axon. Sciatic nerve ligation experiments showed that p75NTR was transported both anterogradely and retrogradely (Johnson et al. 1987). Accumulation of Trk receptors was detected at the distal site after the sciatic nerve ligature, indicating its retrograde transport (Yano & Chao 2004). Although the retrograde transport of Trk receptors and p75NTR has been observed, the molecular mechanism of

transport has not been fully understood. Tctex-1, the light chain of the dynein motor complex, was found to interact with the juxtamembrane domain of the TrkB receptor by yeast two-hybrid screening, co-immunoprecipitation and sciatic nerve ligature experiments (Yano *et al.* 2001, Bhattacharyya *et al.* 2002). So far, whether other motor molecules are involved in the retrograde transport remains unknown.

4.3.3 Release

In general, the newly synthesized neurotrophins are packaged into vesicles and are then transported to either pre-synaptic axon terminals or post-synaptic dendrites for local secretion. The two principal cellular secretion pathways for neurotrophins are constitutive and regulated release, depending on whether the release occurs spontaneously or in response to stimuli. In acute hippocampal slices and cultured neurons overexpressing NGF, there is a transient increase above baseline of extracellular NGF following stimulation with high concentrations of potassium, glutamate or carbachol (Blochl & Thoenen 1995). Similarly, regulated BDNF secretion is also observed by high frequency burst stimulation in hippocampal slices and cultured neurons overexpressing BDNF (Griesbeck *et al.* 1999, Balkowiec & Katz 2002). After potassium-mediated depolarization and an increase in intracellular calcium levels, the regulated

secretion of NT-3 was observed in neurons (Boukhaddaoui et al. 2001).

With the development of techniques, synaptic secretion of neurotrophin was visualized by using overexpression of GFP-tagged BDNF in cultured neurons (Horch & Katz 2002, Kojima *et al.* 2001). In these studies, BDNF-GFP accumulated at glutamatergic synaptic junctions and underwent activity-dependent release. BDNF-GFP was also reported to be released from a pre-synaptic to post-synaptic neuron (Kohara et al. 2001). There exists no data for NGF, NT-3 or NT-4/5 secretion at synapses.

The different releasing pathway of BDNF from dendrites seems to have different neuronal effects than BDNF released from synapses. The dendrite-to-dendrite release of BDNF helps nearby dendritic branching without any effect on axons or spines (Horch & Katz 2002), whereas neurotrophin secretion from synapses may affect synaptic plasticity and formation of new spines (Schinder et al. 2000).

4.3.4 Proteins involved in intracellular BDNF trafficking

Two proteins have been identified to interact with BDNF within neurons. Amino acids 44-103 of the prodomain of BDNF are the BDNF-sortilin

interaction domain, and this domain is required for efficient regulated BDNF secretion. Furthermore, the highly expressed sortilin in HEK 293 cells increases the amount of BDNF secreted. Alltogether, sortilin interacts with the prodomain of BDNF and is involved in sorting to the regulated secretory pathway and release of BDNF (Chen et al. 2005).

The other interaction protein is carboxypeptidase E (CPE). CPE is the sorting receptor in secretory granule membranes and interacts with mature BDNF. It contains a three-dimensional sorting signal motif, $I_{16}E_{18}I_{105}D_{106}$, which is required for the sorting and release of BDNF to the regulated pathway for activity-dependent secretion. The mutation of the two acidic residues (E_{18} and D_{106}) results in missorting of proBDNF to the constitutive pathway (Lou et al. 2005).

5. Htt and HAP1 take part in the transport of BDNF

BDNF transportation is distinctly decreased in Huntington's disease (HD) (Charrin *et al.* 2005, Bossy-Wetzel *et al.* 2004). Htt is an important regulator in BDNF transport along microtubules in the cell. Htt could enhance its efficiency of microtubule based transport, whereas polyQ-htt could inhibit this process (Gauthier et al. 2004). This htt-mediated vesicular transport requires HAP1 and

P150^{Glued}. The complex of Htt/HAP1/P150^{Glued} enables the BDNF-containing vesicles to move along microtubules. PolyQ-htt inhibits HAP1/P150^{Glued} dynactin binding to microtubules, and this could lead to the BDNF transport deficit and result in a loss of neurotrophic support and toxicity (Gauthier et al. 2004).

5.1 Huntington's Disease

HD is an inherited neurodegenerative disease caused by mutant htt with cytosine-adenine-guanine (CAG) trinucleotide repeats in exon 1 which codes for polyglutamine (polyQ) expansion. The normal htt protein with 6 to 34 polyQs tract does not cause the disease whereas disease symptoms can be observed when polyQ extension is greater than 40 in the N-terminal fragment of htt (Karlin & Burge 1996, Bertaux *et al.* 1998, Davies & Ramsden 2001). The polyQ region contributes to the modification of the three-dimensional structure of the whole protein and differences in the physiological function of the protein (Chen 2003, Weibezahn *et al.* 2004). This is why the number of ployQ repeats plays a key role in the disease pathogenesis.

HD is characterized by cognitive decline, chorea, dementia, and other psychiatric symptoms. In HD, the mutant huntingtin is ubiquitously expressed

in the brain and peripheral organs. Although the disease affects a number of brain regions such as the cortex, thalamus and subthalamic nuclei, the neuropathological hallmark of HD is the severe atrophy of the striatum. In the striatum, medium spiny GABAergic projection neurons in the basal ganglia are preferentially lost, whereas spiny interneurons are relatively spared. In the cerebral cortex, large neurons in layer VI are most affected. The disease typically has a mean onset at an age of 35 years, and ultimately leads to death after 15-20 years of progressive neurodegeneration (Davies & Ramsden 2001, Cattaneo *et al.* 2005).

The pathological mechanisms of HD are not fully understood but many theories are proposed. Excitotoxicity plays a critical role in the pathogenesis of the disease. Nuclear inclusions form after different types of proteolytic cleavage which causes abnormal protein-protein interaction in HD. Oxidative stress, energy metabolism, apoptosis also change during the progress of HD (Davies & Ramsden 2001, Sadri-Vakili *et al.* 2006).

5.2 Huntingtin regulates neuronal gene transcription

Wild type and mutant huntingtin (Htt) are localized in several organelles as well as the cytoplasm and nucleus of neurons. Mutant huntingtin causes

transcriptional dysregulation in HD by interacting with numerous nuclear transcription factors, such as CREB-binding protein (CBP) and TATA-binding protein (TBP). The interaction of mutant huntingtin with transcription factors has been demonstrated to cause the downregulation of specific gene transcription in the brains of R6/2 and N171-82Q HD mouse models (Steffan *et al.* 2000, Nucifora *et al.* 2001, Sadri-Vakili et al. 2006).

Further investigations conducted in vitro and in vivo show that the wild type huntingtin stimulates BDNF expression in cortical neurons through regulating the activity of the BDNF promoter exon II, which consists of a sequence named repressor element 1 (RE1, also called neuron-restrictive silencer element, NRSE). Wild type huntingtin can competitively bind to this sequence with RE1-silencing transcription factor (REST, also called neuronal restrictive silencing factor, NRSF) which acts as a transcriptional silencer, whereas mutant huntingtin can not. As a consequence, REST suppresses the expression of BDNF in neurons which express mutant huntitngtin. Taken together, wild type huntingtin promotes BDNF transcription through inhibition of REST. Nevertheless, mutant huntingtin reduces the transcription by the formation of RE1/REST complex in the nucleus (Zuccato *et al.* 2001, Sugars & Rubinsztein 2003, Zuccato *et al.* 2003, Zucker *et al.* 2005, Sadri-Vakili et al. 2006, Sadri-Vakili & Cha 2006).

5.3 Htt plays a role in BDNF vesicle transport

Htt can act as a scaffold protein which enables the packaging of various proteins for transport along microtubules. As one of the components of cargo-motor molecules, Htt is required for the efficient anterograde and retrograde transport of neurotrophins (Gunawardena & Goldstein 2004a). BDNF is the most important factor supporting the survival of striatal neurons. BDNF located in striatal neurons is synthesized in and transported from the cerebral cortex (Altar et al. 1997). Down-regulation of wild type htt by RNAi can attenuate BDNF transport, the effect is gene dosage-dependent and BDNF transport is completely abolished by knockout of huntingtin (Gauthier et al. 2004). The mutant huntingtin in neuronal cells may impair the trafficking of BDNF-containing vesicles (Gauthier et al. 2004, Trushina *et al.* 2004).

Mutant Htt could interrupt the complex of wild type huntingtin/HAP1/p150Glued and thus interfere with microtubule transport. The pathogenic polyQ expansion blocks the axonal transport pathway, and retards BDNF transport to striatal neurons (Davies & Ramsden 2001, Gauthier et al. 2004, Gunawardena & Goldstein 2004b, Trushina et al. 2004). This lack of BDNF transport is one of the reasons why medium spiny neurons die in the

striatum. Thus enhancing the transportation of neurotrophins is a potential therapeutic strategy for HD. There is evidence indicating that increased BDNF, GDNF, NT-3 and NT-4/5 support provides structural and functional neuroprotection in various models of HD (Cattaneo et al. 2005).

On the other hand, as TrkB gene transcription is reduced by mutant Htt in a polyQ-length-dependent manner (Gines et al. 2006), TrkB levels in striatum and cortex were also found to be decreased in both transgenic HD mouse models and in human HD (Gines et al. 2006). This is why applying BDNF into the brains of HD patients is not as effective as expected (Kells et al. 2004). Nevertheless, in neurotoxin-injured striatal neurons and astrocytes, the GDNF receptors, GFRα-1 and Ret, are upregulated (Marco et al. 2002). The viral delivery of GDNF improves behavior and protects striatal neurons in HD transgenic mouse models (Gines et al. 2006, McBride *et al.* 2006).

6. Discovery of Huntingtin-Associated Protein 1 (HAP1)

A number of proteins are known to interact with Htt. One of these is HAP1 which was first identified in a yeast two-hybrid system as an interacting partner for Htt. It interacts with both Htt and mutant Htt, but the binding ability is increased by the polyQ expansion (Li et al. 1998c). HAP1 consists of two

isoforms (HAP1-A, 75kDa and HAP1-B, 85kDa) which have different C-terminal sequences. HAP1-A has a unique sequence of 21 amino acids, whereas HAP1-B has a different sequence of 51 amino acids (Li *et al.* 1995, Nasir *et al.* 1998).

6.1 Localization of HAP1

HAP1 is mainly present in the somatodendritic cytoplasm of neurons (Martin et al. 1999). The mRNA localization is extremely discrete (Page et al. 1998). The most prominent localizations of HAP1 mRNA are in basal forebrain, cerebral cortex, cerebellum, the accessory olfactory bulb and the pedunculopontine nuclei. HAP1 is highly expressed in the olfactory bulb, the hypothalamus, and the supraoptic nucleus (Page et al. 1998, Li *et al.* 1996). In the rat brain, the expression is more intense in the stratum, brainstem, olfactory bulb, thalamus and ventral forebrain than in cerebral cortex, hippocampus, cerebellum and spinal cord (Li *et al.* 1998a, Gutekunst *et al.* 1998). The ratios of HAP1-A to HAP1-B are different in various regions. In the olfactory bulb and spinal cord, the level of HAP1-A is lower than that of HAP1-B (Li et al. 1998a). In the striatum and other regions their levels are almost the same. The 68kDa isoform is predominant in the cerebral cortex, striatum, hippocampus and thalamus (Li et al. 1998b).

HAP1 is highly expressed throughout the cell cycle of striatal cells. In dividing cells, it radiates from spindle poles to microtubules in mitotic spindles. In the earliest stages of mitotic striatal cells, HAP1 is associated with condensed chromatin in the nucleus and large amount of punctate structures in the perinuclear and peripheral cytoplasm. During postmitosis, HAP1 is absent from the nucleus and appears on endoplasmic reticulum (ER)/Golgi-like membranes in the perinuclear region, and has a punctuate distribution in the cytoplasm (Martin et al. 1999).

In adult mouse brain neurons, HAP1 is highly enriched in large dense organelles, large endosomes (multivesicular bodies) and moderately expressed in small vesicles, tubulovesicular structures, plasma membrane, coated and budding vesicles and microtubules (Martin et al. 1999).

6.2 Molecular structure of HAP1

The common region of both HAP1 isoforms contains three predicted coiled-coil domains (H1, H2 and H3) and a huntingtin-binding domain (HB) as shown in Fig. 4.

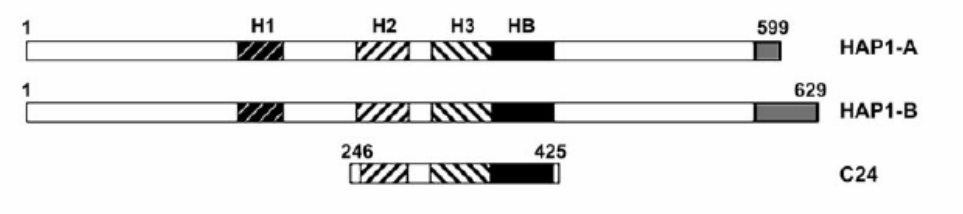

Fig. 4 Domain structure of HAP1. HAP1 isoforms, HAP1-A and HAP1-B, differ only at the C terminus. Three putative coiled-coil domains (H1,H2 and H3) and the HB are indicated (Li et al. 2002b).

6.3 The function of HAP1

6.3.1 Postnatal lethality

HAP1 plays an important role in early postnatal life. The majority of HAP1 knock out mice die at P2, and ~80% die before P3, and none can survive past P9 (Li et al. 1998b, Chan *et al.* 2002). However restored HAP1 expression in neuronal cells before birth rescues the early lethality (Dragatsis et al. 2004). A few hours after birth, HAP1 mutant mice exhibit abnormal feeding behavior (Chan et al. 2002). HAP1 is indispensable for the initiation and/or maintenance of sucking in neonatal mice (Dragatsis et al. 2004). The mechanism of the phenotype still remains to be investigated.

Nipple-searching behavior and attachment to the nipple, in most mammals, is believed to be mediated primarily by olfactory and tactile cues (Larson & Stein 1984). Absence of olfactory bulbs or surgical lesions in the olfactory system in newborns lead to a reduction in nipple attachment efficiency, and consequent early postnatal lethality due to starvation (Hongo et al. 2000). All HAP1 knock out pups exhibited a normal rooting reflex in response to manual stimulation of their mouth region, indicating normal tactile sensation and motor control. By eliminating the competition of milk sucking between wild type and heterozygous pups, HAP1 knock out pups survived into adulthood and did not display any feeding, behavioral or brain abnormalities as adults. Moreover, HAP1 knock out pups' mothers do nest, crouch over their pups in a typical nursing manner, and collect them when they are scattered, further indicating that olfaction is not affected in HAP1 knock out mice (Dragatsis et al. 2004).

Furthermore, neuronal cell number in the trigeminal ganglion, which could affect the sucking behavior, is not reduced. There is no change in the levels of satiety peptides within the hypothalamus of P1 HAP1 pups nor was any change found in the morphology of peptide-containing neurons. However, more neuronal death was found in the hypothalamus of HAP1 knockout mice (Li et al. 2002b). The precise role of HAP1 in the feeding behavior of pups needs to be thoroughly studied. For example, whether the gustatory responses have been

altered is not known. It is also possible that changes in neurotransmitter release play a role in the abnormal feeding behavior in HAP1 knock-out mice. It is known that the HAP1 knock out can alter serotonin function through the hypothalamic-pituitary-adrenal axis (Dragatsis et al. 2004).

6.3.2 Intracellular transport

Duo which is a membrane cytoskeletal protein was identified by using the yeast two-hybrid system as a HAP1-binding proteins (Goodman et al. 1995) and belongs to RhoGEF superfamily (Erickson & Cerione 2004, Colomer *et al.* 1997). Guanine exchange factors (GEF) stimulate Rho and Rac signal transduction molecules by switching them from the inactive (GDP-bound) to the active (GTP-bound) form. These molecules are often involved in organizing the cytoskeleton and act as axon guidance molecules (Schmidt & Hall 2002). Duo contains at least four or five spectrin-like repeats which enable it to bind to actin, one GEF domain (Matsudaira 1991, Goodman et al. 1995), peptidylglycine α-amidating monooxygenase (PAM) binding region, and HAP1 binding region. The cytoplasmic domain of PAM, which binds Duo is believed to be involved in the biogenesis of secretory granules and has a sorting signal for internalization from the cell surface (Milgram et al. 1996). Duo is a rac1-specific binding protein, which regulates cytoskeleton (actin)

organization, endocytosis, exocytosis and free radical production. Thus HAP1 is proposed to play a role in vesicle trafficking and cytoskeletal functions, and takes part in a ras-related signaling pathway (Colomer et al. 1997).

Furthermore, HAP1 binds to $P150^{Glued}$, a subunit of dynactin, which binds to both microtubules and dynein, and induces the microtubule-dependent retrograde transport of membranous organelles. HAP1 may influence the transport of various proteins that bind to $P150^{Glued}$ (Engelender *et al.* 1997, Li et al. 1998b).

In investigating the function of two HAP1 isoforms, it was found that the common region of HAP1-A and HAP1-B binds to other molecules which constitute the cytoplasmic inclusions, however the C-terminus of HAP1-B takes the role for inhibition of the formation of inclusions whereas the unique C-terminal region of HAP1-A seems to be critical for inclusion formation. Both isoforms can aggregate in different proportions or self-associate *in vivo*, where HAP1-A accelerates the formation of inclusions and HAP1-B suppresses this formation simultaneously. Whether there are inclusions in the cell body depends on the proportion of the two isoforms (Li et al. 1998a). The expression level of HAP1-B is normally higher than that of HAP1-A in most brain regions. This could explain in part why the majority of native HAP1 in the

brain is cytosolic and diffusely distributed in the neurons (Li et al. 1998a). It is reported that the common region also binds to Htt and $P150^{Glued}$ (Li et al. 1998b). From the colocalization experiment of HAP1 and P150Glued in transfected cells, the cytoplasmic inclusions were found to be colocalized with HAP1. Thus the cytoplasmic inclusions could be transported along microtubules with HAP1 and $P150^{Glued}$ (Li et al. 1998b).

During synaptic vesicle trafficking in axonal terminals, Htt and HAP1 may act as scaffold proteins which bind to synaptic vesicles. Mutant Htt has a much higher binding affinity to synaptic vesicles than normal Htt and reduces the association of HAP1 with the vesicle (Li *et al.* 2003a, DiFiglia *et al.* 1995). The tightly bonded complexes of mutant Htt and vesicles are separated and released, thus create a physical barrier that interferes with organelle transport and vesicle recycling in axons (Li *et al.* 2001, Li et al. 2003a). Such an effect could alter the release and uptake of various neurotransmitters and could lead to axonal degeneration (Li et al. 2003a).

HAP1 also interacts with hepatocyte growth factor-regulated tyrosine kinase substrate (Hrs), an early endosome-associated phosphoprotein which plays a role in the regulation of vesicular trafficking and signal transduction (Komada & Kitamura 2001, Raiborg *et al.* 2001) , and regulates endocytic trafficking

through early endosomes (Li et al. 2002b). HAP1 is involved in both constitutive or ligand-induced receptor-mediated endocytosis and the endosome to lysosome trafficking of epidermal growth factor (EGF) receptors (Li et al. 2002b). Endosomes containing translocated EGF receptors activate cell proliferation and survival (Li et al. 2003b). The overexpression of HAP1 blocks vesicular trafficking from early to late endosomes, causes the formation of enlarged early endosomes and inhibits the trafficking of endosomes to lysosomes. Thus, HAP-1 can inhibit the degradation of internalized EGF receptors but not affect continuous EGF receptor internalization (Li et al. 2002b). The overexpression of HAP1 could protect against the lack of EGF receptor-induced degeneration. On the other hand, the increased expression of mutant Htt causes abnormal interactions of HAP1 with Hrs, resulting in aberrant endocytic trafficking (Li et al. 2002b, Li et al. 2003b).

HAP1 may interact directly with some membrane receptors. One of these is γ-aminobutyric acid type A receptor ($GABA_AR$) which regulates neuronal excitability by its level of stability on the cell surface (Moss & Smart 2001, Sieghart & Sperk 2002). HAP1 binds the $GABA_AR$ β subunit specifically (Kittler et al. 2004). During the cell signalling pathway of $GABA_AR$, HAP1 inhibits receptor lysosomal degradation and at the same time facilitates receptor recycling back to the cell membrane. In this way, HAP1 increases

$GABA_AR$ cell surface number, therefore affecting neuronal excitability (Kittler et al. 2004). The type 1 inositol (1,4,5)-trisphosphate receptor ($InsP_3R1$) is another membrane receptor that also binds to HAP1 (Tang et al. 2003). $InsP_3R1$ is an intracellular Ca^{2+} release channel which is very important in the neuronal Ca^{2+} signal pathway (Berridge 1998). Htt may directly interact with the $InsP_3R1$ C-terminus, and this binding of Htt to the $InsP_3R1$ C-terminus is dependent on both the presence of HAP1 and the polyQ expansion. Mutant Htt can bind to the $InsP_3R1$ C-terminus either directly or indirectly through HAP1 (Tang et al. 2004). But the interesting finding is that the functional effects of mutant Htt on $InsP_3R1$-mediated Ca^{2+} release are attenuated in medium spiny striatal neurons (MSN) of HAP1 knock out mice when compared with wild-type mice MSN. Thus, HAP1 potentiates functional effects of mutant Htt on $InsP_3R1$ function in vivo. As is already known, increases in neuronal Ca^{2+} represent early events in the pathogenesis of HD (Tang et al. 2003, Zeron *et al.* 2002). HAP1 facilitates functional effects of mutant Htt on $InsP_3R1$ and suggests a role for HAP1 in altered neuronal Ca^{2+} signalling, which potentially leads to selective neuronal loss in HD (Tang et al. 2004).

7. Molecular motors

Organelle transport in cell processes is mainly controlled by molecular motors

including kinesin which are plus-end-directed motors (anterograde transport) and dynein which are minus-end-directed motors (retrograde transport). Structurally, molecular motors consist of two functional parts, a motor domain and a tail domain. The motor domain binds to cytoskeletal filaments and also offers chemical energy for movement. The tail domain is quite divergent in different motors that allow it to recognize different cargoes either directly or through accessory light chains (Gunawardena & Goldstein 2004b).

Axonal and dendritic transport is extremely complicated as some cargoes are transported selectively whereas others are transported nonselectively. Which sequences of selectively transported proteins function as selective targeting signals and what mechanism underlies the selective transport or selective retention of cargoes remains to be fully elucidated. With regard to how motors differentiate axons from dendrites, research shows that microtubules play a role in selective transport. At the transition site from the cell body to the axon there is a deficiency in rough endoplasmic reticulum compared with other parts of the cell body. This special structure has a remarkably high affinity for microtubule-associated proteins EB1 (Nakata & Hirokawa 2003). It is possible that Kinesin superfamily protein 5 (KIF5) also recognizes the same special structure as EB1 which leads to KIF5 carrying its cargo selectively to the axon. However, both selective and nonselective transport occurs in most cases, many

sequences for selective transport have been identified, but such sequence identification has not always clarified the underlying sorting mechanism (Hirokawa & Takemura 2004).

7.1 Kinesin motors

7.1.1 The structure of kinesin

Kinesins are the largest superfamily of microtubule-dependent motors for anterograde transport, with 45 members in mice and human, and they are the most abundant motors in many cell types. The kinesin superfamily can be divided into three groups on the basis of the positions of the motor domains: the amino (N)-terminal motor, middle motor and carboxy (C)-terminal motor types (referred to as N-kinesins, M-kinesins and C-kinesins). There are 39 N-kinesins, 3 M-kinesins and 3 C-kinesins. Kinesin also can be classified based on 14 large families, kinesin1 to 14 (Hirokawa & Takemura 2005). It is thought that different kinesins carry different subpolulatins of cargoes and have different anterograde pathways. Conventional kinesin, kinesin I, was originally discovered in the context of vesicle transport in axons. It is a tetramer consisting of a kinesin heavy chain (KHC) dimer and two kinesin light chains (KLC) (Fig. 5). In mammals, kinesin I KHC consist of three different subunits

(KIF5A, KIF5B, and KIF5C) (Xia et al. 1998) and kinesin I KLC consists of at least three subunits (KLC1, KLC2, and KLC3) (Rahman et al. 1998). All KIFs have a globular motor domain, an α-helical coiled coil stalk domain and a C-terminal tail domain. The globular motor domains have high degrees of homology in all KIFs and contain a microtubule-binding sequence and an ATP-binding sequence. The C-terminal has a unique sequence and interacts with the N-terminal coiled-coil domain of KLC. This diversity of domains is thought to regulate motor activity and binding to different cargoes. The C-terminal of KLC consists of six tetratrico peptide repeat domains, which are involved in protein-protein interactions and are proposed to link KLC to receptor proteins on vesicular cargoes (Schnapp 2003, Hirokawa & Takemura 2005).

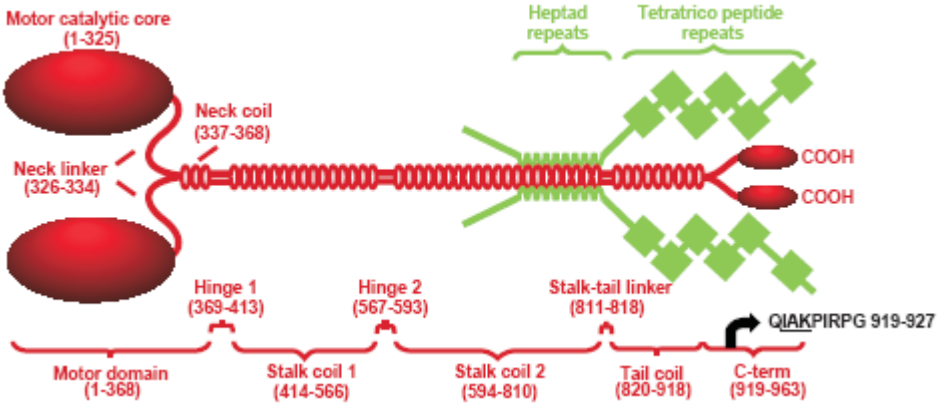

Fig. 5 Domain organization of kinesin I. Heavy and light polypeptide chains are shown in red and green, respectively. Cargo-binding domains (CBD) are located at C-terminus (Schnapp 2003).

7.1.2 Kinesins mediate cargo transport in axons

In the axon, many membranous organelles are transported from the cell body to synaptic terminals. After proteins are synthesized in the Golgi apparatus, they are packaged in different vesicles and anterogradely transported to the synaptic terminal.

KIF1A and KIF1Bβ transport synaptic vesicle precursors along axons and then the precursors are assembled into synaptic vesicles at synaptic terminals. Mutant mice that lack either KIF1A or KIF1Bβ have reduced synaptic vesicle density at nerve terminals, and sensory and motor nerve function is impaired (Yonekawa *et al.* 1998, Zhao *et al.* 2001). Moreover, *in vivo* experiments in heterozygous KIF1Bβ mutant mice show the transport of synaptic vesicle precursors is significantly decreased (Zhao et al. 2001). KIF1Bα, an isoform derived from the same gene as KIF1Bβ by alternative splicing, transports mitochondria anterogradely (Nangaku et al. 1994). KIF5 can also transport mitochondria (Tanaka *et al.* 1998, Kanai *et al.* 2000). The hypothesis is that mitochondria may have many binding sites for motor proteins. KIF5 also transports other cargoes, including vesicles that contain apolipoprotein E receptor 2, GAP43 and VAMP2 and oligomeric tubulin in a large transport complex at a speed that is compatible with slow axonal transport. The kinesin

complex KIF3A-KIF3B-KAP3 transports large vesicles with diameters of 90-160 nm, which are associated with fodrin through an interaction between KAP3 and fodrin. These sorts of transport are essential for neurite extension (Nangaku et al. 1994, Yonekawa et al. 1998, Takeda *et al.* 2000, Nakata & Hirokawa 2003, Hirokawa & Takemura 2005).

7.1.3 Kinesins mediate cargo transport in dendrites

In dendrites, there are many molecules transported from the cell body by different kinesins, including those associated with postsynaptic densities, neurotransmitter receptors, ion channels and specific mRNAs. KIF17 transports NMDA (N-methyl-D-aspartate) glutamate receptors (NMDARs). KIF17 is an N-kinesin and co-exists mainly in dendrites with the NR2B subunit of NMDARs which it anterogradely transports to postsynaptic regions (Guillaud et al. 2003). The overexpression of KIF17 enhances working or episodic-like memory and spatial learning and memory in transgenic mice (Wong et al. 2002a). This might be due to the increased phosphorylation of a transcription factor, cyclic AMP responsive element binding protein (CREB) (Wong et al. 2002a, Guillaud et al. 2003). KIF5s (KIF5A, KIF5B and KIF5C) can transport AMPA (α-amino-3-hydroxy-5-methyl-4-isoxazole propionic acid) glutamate receptors (AMPARs) and a large multisubunit complex of 42

proteins that includes the mRNAs for αCaMKII and ARC (Kanai et al. 2004). The proteins in this complex include those associated with RNA transport, those associated with protein synthesis, RNA helicases, heterogeneous nuclear ribonucleoproteins, and other RNA-associated proteins. Furthermore, KIF21B and KIFC2 are also included in dendritic transport (Setou *et al.* 2002, Hirokawa & Takemura 2005).

7.1.4 Adaptor/scaffolding proteins for cargo recognition by motors

Although transmembrane cargo proteins can bind directly to specific motors, adaptor/scaffolding proteins also participate in cargo-motor binding. For example, KIF13A transports vesicles containing the mannose-6-phosphate receptor (M6PR). The cytoplasmic side of M6PR binds to the AP1 (adaptor protein 1) adaptor complex which also binds to KIF13A. Therefore, the AP1 adaptor complex serves as an adaptor for both the motor and vesicle. Another example is that the interaction between KIF17 and its cargo vesicles which contains NMDARs is mediated by a tripartite protein complex that contains LIN10, LIN2 and LIN7 (Bonifacino et al. 1996). All those three proteins contain PDZ domains which do not bind to each other but recruit other proteins (Garner *et al.* 2000, Hung & Sheng 2002). The C-terminal tail of KIF17 binds directly with the first PDZ domain of LIN10, which then sequentially binds

with LIN2 and LIN7. LIN7 binds to the C-terminal of NMDAR subunite NR2B via a PDZ domain. In this way the vesicles containing NMDARs are transported by KIF17 through the scaffolding protein complex (Jo *et al.* 1999, Hirokawa & Takemura 2005).

7.2. Dynein motor

7.2.1 The structure of Dynein

Dyneins are the other major family of microtubule motor proteins. There are about 15 forms of dynein in vertebrates, but only two forms are cytoplasmic, dynein 1 and dynein 2. All forms of dynein contain the largest subunit heavy chain (HC) polypeptide of >500 kDa, which is termed the motor domain. The large motor domain consists of multiple ATPase units and other structures and this structure is highly conserved in all dynein heavy chain isoforms (Fig. 6) (Neuwald et al. 1999). The cargo-binding domain is diverse and is responsible for cargo binding. Dynein also has a variety of accessory subunits named intermediate, light intermediate and light chains (ICs, LICs and LCs), which take part in cargo binding through interaction with the cargo binding domain (Fig. 6) (Samso *et al.* 1998, Neuwald et al. 1999, Burgess *et al.* 2003, Vallee *et al.* 2004).

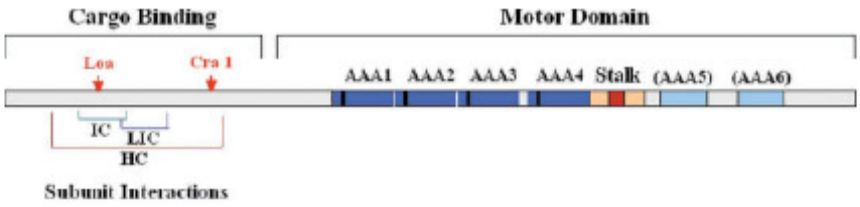

Fig. 6 Structural organization of cytoplasmic dynein. Diagram shows functional domains and binding sites within cytoplasmic dynein heavy chain. All of the accessory subunits of cytoplasmic dynein are associated with the N-terminal portion of the HC, which constitutes the base of the dynein particle. (Sites for binding of IC, LIC, and for HC dimerization are indicated by brackets.) The C-terminal portion of the HC contains six AAA ATPase domains arranged in a ring (Burgess et al. 2003).

7.2.2 Dynactin - the adaptor protein for dynein

Dynactin is one of most important multisubunit protein complex that is a necessary accessory for the dynein motor movement. Dynactin is a multifunctional adapter protein helping the cellular component to connect with microtubules and motors (Schroer 2004).

One typical structure of dynactin consists of the Arp1 rod (Arp1, Arp11, Actin, CapZ, p62, p27 and p25) and the projecting arm ($p150^{Glued}$, Dynamitin,

p24/p22). Arp1 (actin-related protein) can hydrolyze ATP and form remarkably stable, very short and of uniform length filaments and associates with spectrin-family proteins which can be found on Golgi membranes. This could be one mechanism by which dynactin binds a variety of subcellular structures. The primary sequence of p62 contains a zinc-binding motif (RING or LIM domain) near the N terminus, which commonly supports protein-protein interactions. So p62 may participate in the binding to dynactin subunits or other subcellular structures (Schroer 2004).

p150Glued is the largest subunint of dynactin which consists of two globular heads serving as microtubule binding sites and is located in the very tip of the dynactin arm. p150Glued binds microtubules and the intermediate chain of dynein, and is thought to be responsible for the movement of many cargo organelles through dynein. The globular heads contain a CAP-Gly (cytoskeleton-associated protein, glycine-rich) motif (Fig. 7), which contributes to enhancing the reaction of the dynein motor, microtubule minus-end anchoring at interphase centrosomes (Quintyne *et al.* 1999, Quintyne & Schroer 2002) and mitotic spindle poles (Gaglio et al. 1997). The $p150^{Glued}$ CAP-Gly domain also binds microtubule-binding protein, such as EB1 and CLIP-170. The two coiled coil domains (aa~220-550, aa~925-1050) (Fig. 7) support binding interactions within dynein-dynactin, and also provide a binding

platform for interactions with multiple microtubule-based motors (Waterman-Storer *et al.* 1995, McGrail *et al.* 1995). The region of aa 1023-1223 has been reported to interact with HAP1 (Li *et al.* 2002a, Vaughan *et al.* 2002, Engelender et al. 1997).

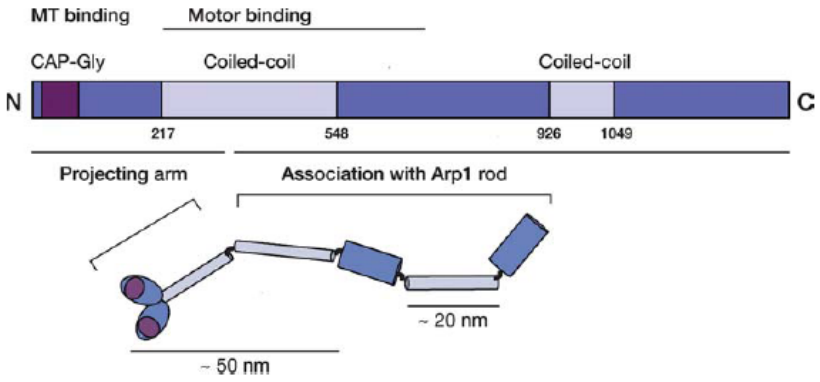

Fig. 7 Schematic illustration of the domain organization and proposed functions of p150Glued. The different functional and structural domains are defined as described in the text (Schroer 2004).

Dynactin's two structural domains are linked by dynamitin. Dynamitin associates with p150Glude and p24/22 via a series of three coiled-coil motifs. Disruption of dynamitin can cause p150Glued and p24/22 to be released from the rest of the dynactin structure. Conversely, overexpression of dynamitin could also disrupt the binding between p150Glude and p24/22. p24/22 is one of dynactin's smallest subunits and it binds dynamitin directly (Schroer 2004).

7.2.3 Dynactin polices two-way organelle traffic

The generally accepted theory is that membranous organelles are transported anterogradely by motor proteins of the kinesin superfamily and retrogradely by motor proteins of the dynein family. In most cells, organelles do not travel directly in one direction, but change direction frequently. The mechanism of this phenomenon is not very clear. But one clue is that dynactin complexes also interact with kinesin II, except for dynein, which is important for plus end-directed anterograde transport. p150Glued is the largest and most important subunit of dynactin. The treatment of extruded squid axoplasm with antibody against p150Glued inhibits both anterograde and retrograde organelle transport (Waterman-Storer et al. 1997). Drosophila embryos expressing a mutant $p150^{Glued}$ protein display impaired bidirectional organelle transport (Gross et al. 2002). It is suggested that dynactin might be involved in coordination of bidirectional transport (Dell 2003). More detailed evidence is provided by investigations using Xenopus melanophores and showing that the COOH-terminal domain of kinesin-associated protein (KAP, which is one of the motor subunits comprising kinesin II) competitively binds the same region of p150Glued (aa600-811) as dynein intermediate chain (Deacon et al. 2003). This interaction is important for kinesin II-mediated anterograde transport of melanosomes (Dell 2003).

8. Research aims and plans

Although we already know that Htt, HAP1 and p150Glued are involved in BDNF transport and polyQ Htt could interrupt the microtubule-based BDNF transport and wild type Htt could act as an anti-apoptotic factor by rescuing axonal transport (Gauthier et al. 2004), the process of how those molecules interact with each other to carry BDNF forward and backward along axons remains to be investigated. It is not known which molecule interacts with BDNF. It is also not known whether the prodomain of BDNF or mature BDNF interacts with any of these molecules. It is believed that BDNF is present within vesicles and packaged as a cargo which is carried by molecular motors. How BDNF vesicles interact with the motor accessary molecules is not clear. The first project (Chapter 2) aims to find out how BDNF interacts with molecular motor accessary proteins and how it is transported from the cell body to nerve terminals within axons. During the course of this study it was found that both the prodomain and mature BDNF interact with HAP1. Thus, the following questions have been addressed with a variety of techniques and approaches: Do BDNF fragments interact with HAP1 directly or indirectly? Do BDNF fragments co-localize with HAP1 after cotransfection? Does BDNF co-localize with HAP1 in vivo and does the ablation of HAP1 alter the

localization pattern of BDNF? Does recombinant mutant htt or mutant htt from human HD brains interfere with the interaction between HAP1 and BDNF? Is HAP1 required for the axonal transport and activity-dependent release of BDNF? Does the mutation of V66M in the BDNF prodomain affect the interaction and colocalization with HAP1?

Recent studies have shown that proneurotrophins bind p75NTR and sortilin with high affinity and trigger apoptosis of neurons *in vitro*. As the proneurotrophins are a dominant form of gene products in developing and adult animals, we wish to find out if proneurotrophins have any physiological roles *in vivo*. The second project (Chapter 3) aims to find out whether proBDNF acts as a death factor *in vivo* in a physiological condition. In this chapter, the *in vitro* role of proBDNF is investigated by using PC12 cells as a model to test whether proBDNF induces cell death and whether the apoptotic effect could be abolished by antibodies against proBDNF. Secondly, p75NTR, sortilin and proBDNF expression in DRG is investigated. Thirdly, we use the axotomized sensory neurons of neonatal rats as a model in which we have examined the potential role of proBDNF in neuronal survival *in vivo*. Finally, we examined whether soluble sortilin extracellular domain receptor rescues axotomized sensory neurons from death.

CHAPTER 2

HUNTINGTIN ASSOCIATED PROTEIN 1 INTERACTS WITH THE PRODOMAIN OF BDNF AND IS INDISPENSABLE FOR ITS AXONAL TRANSPORT AND RELEASE

1. Abstract

Brain-derived neurotrophic factor (BDNF) plays a pivotal role in brain development and synaptic plasticity. After synthesis BDNF is transported and released by a regulated pathway but the underlying mechanism remains unknown. Here, by using affinity purification and 2D-DIGE assay, we show Huntingtin-associated protein 1 (HAP1) interacts with the prodomain of BDNF and mature BDNF. The GST pull-down assays have addressed that HAP1 directly binds to the prodomain but not to mature BDNF and this binding is decreased by incubation with recombinant mutant huntingtin. HAP1 immunoprecipitation showed that less proBDNF was associated with HAP1 in the brain homogenate of Huntington's disease samples compared to those of control samples. Co-transfection of HAP1 and BDNF plasmids in PC12 cells showed HAP1 was colocalized with proBDNF and the prodomain, but not mature BDNF. ProBDNF accumulated in the proximal and distal segments of crushed sciatic nerve in wild type mice but not in $HAP1^{-/-}$ mice. The activity-dependent release of the prodomain of BDNF was abolished in $HAP1^{-/-}$ mice. HAP1 binds Val66Met prodomain with less efficiency than the wild type prodomain. We conclude that HAP1 is the cargo-carrying molecule for proBDNF-containing vesicles and plays an essential role in the transport and release of BDNF in neuronal cells.

2. Introduction

Neurotrophins are important signaling molecules regulating proliferation, differentiation, and survival of neurons and modulating synaptic plasticity and synaptogenesis (Kaplan & Miller 2000, Dechant & Neumann 2002, Barde 1990). Neurotrophins are synthesized as precursor forms (proneurotrophins), which are cleaved to generate the N-terminal prodomain and C-terminal mature neurotrophins, sorted to either the constitutive or regulated secretory pathway and released (Chao & Bothwell 2002, Chen et al. 2004). Brain-derived neurotrophic factor (BDNF) is a member of the mammalian neurotrophin family, and it promotes neurogenesis by increasing proliferation, differentiation and survival of a variety of neurons (Katoh-Semba et al. 2002). BDNF is also involved in activity-dependent synaptic plasticity and plays a role in learning and memory (Yamada & Nabeshima 2003, Binder & Scharfman 2004). BDNF is downregulated in neurological diseases such as Alzheimer's disease, Parkinson's disease and Huntington's disease and may be involved in the development of these diseases (Murer *et al.* 2001, Binder & Scharfman 2004). In Huntington's disease, the transcription and axonal transport of BDNF in cortical and striatal neurons is down-regulated by the polyQ mutant form of huntingtin (Htt) and this effect on BDNF results in the degeneration of striatal neurons and plays an essential role in the pathogenesis of Huntington's disease (Zuccato et al. 2001, Gauthier et al. 2004, Altar et al. 1997).

Htt is a scaffold protein predominantly found in the cytoplasm where it associates with various vesicular structures and molecular motors to form a cargo complex and may play a role in intracellular trafficking (Gauthier et al. 2004, Gunawardena & Goldstein 2004a). The extended (>37) glutamine stretch repeat (polyQ) in the Htt N-terminus causes abnormally assembled protein complexes. Huntingtin associated protein-1 (HAP1) is one of the interacting proteins of Htt, and is distributed throughout the brain and spinal cord. Several studies have suggested that Htt binding with HAP1 is involved in axonal transport (Li & Li 2005). BDNF vesicular transport is altered in HD, whereas wild type Htt may act as an antiapoptotic factor by rescuing axonal transport (Zuccato et al. 2001, Gauthier et al. 2004, Ferrer *et al.* 2000). Thus HAP1 is likely to be involved in BDNF vesicular transport.

Two proteins have been identified to interact with BDNF within neurons. Sortilin interacts with the prodomain of BDNF and is involved in the sorting and release of BDNF (Chen et al. 2005), whereas the sorting receptor carboxypeptidase E interacts with the sorting motif I(16)E(18)I(105)D(106) in mature BDNF and is required for the sorting and release of BDNF through the regulated secretory pathway (Lou et al. 2005). However, how BDNF is transported from cell body to the nerve terminals within axons is not known. The mutation from valine to methionine at codon 66 (Val66Mal) in the prodomain of BDNF in humans results in the retardation of the axonal transport and activity dependent release of BDNF and causes a number of neurological disorders in humans (Egan et al. 2003,

Numata *et al.* 2006). However, the mechanism underlying this mutation-derived dysfunction is not known. Since the two known interacting proteins are not involved in molecular transport, we sought to identify the mechanisms of how the post-Golgi trafficking of BDNF occurs in axons. Here we demonstrate that HAP1 directly interacts with the prodomain of BDNF and is required for the anterograde transport and activity-dependent secretion of proBDNF. Mutant Htt interferes with this interaction between the prodomain and HAP1 and the interaction is reduced with the Val66Met prodomain.

3. Materials and methods

Plasmid constructs

ProBDNF-DsRed, prodomain BDNF-DsRed, mature BDNF-DsRed and Val66Met prodomain BDNF-DsRed

To produce proBDNF, prodomain BDNF, mature BDNF and Val66Met prodomain BDNF with a red fluorescence tag, the rat cDNA sequences of proBDNF (807bp), prodomain BDNF (423bp), mature BDNF (384bp), Val66Met prodomain BDNF (423bp) were amplified by PfuTurbo DNA polymerase (STRATAGENE) from a proBDNF-EGFP construct and a Val66Met proBDNF-EGFP construct (both from Dr. Masami Kojima**,** Research Institute for Cell Engineering, National Institute of Advanced Industrial Science and Technology (AIST), Ikeda, Osaka) using the

following PCR primers (GeneWorks Pty Ltd) with added EcoR I and BamH I sites:

1. prodomain BDNF (forward) 5'-GCGAATTCCACCAGGTG-3',
2. prodomain BDNF (reverse) 5'-ATGGATCCCGCCGAACCCT-3',
3. mature BDNF (forward) 5'-GCGAATTCATGCACTCCGACCCT-3'
4. mature BDNF (reverse) 5'- ATGGCGACCGGTGGATCCCT-3'

Full-length proBDNF was amplified by using primers 1 and 4, the prodomain and the Val66Met prodomain by using primers 1 and 2, and mature BDNF by using primers 3 and 4. The amplified fragment was digested with EcoR I and BamH I and subcloned in-frame into pDsRed-Express-N1, and the sequences of the final constructs were verified by DNA sequencing.

pET100/D-TOPO prodomain BDNF, pET100/D-TOPO proBDNF and pET100/D-TOPO-Val66Met prodomain BDNF

The fragments of rat full-length proBDNF, prodomain and Val66Met prodomain BDNF (423bp) were amplified by PfuTurbo DNA polymerase (STRATAGENE) from AAproBDNF (amino acids 129 and 130, RR to AA point mutation to generate proBDNF furin-resistant recombinant protein) or Val66Met proBDNF-EGFP constructs (both from Dr. Masami Kojima**,** Research Institute for Cell Engineering, National Institute of Advanced Industrial Science and Technology (AIST), Ikeda, Osaka) with the following PCR primers (GeneWorks Pty Ltd):

1. prodomain (forward) 5'- CACCACCATCCTTTTCCTTACTATG

2. prodomain (reverse) 5'- CTAGCGCCGAACCCTCATAGA
3. proBDNF (reverse) 5'- CTACCTTCCCCTTTTAATGGT -3'

Full-length proBDNF was amplified by using primers 1 and 3 and the wild type prodomain and the Val66Met prodomain by using primers 1 and 2. The amplified fragments were subcloned in-frame into pET100/D-TOPO by following the instruction manual of Champion pET Directional TOPO Expression Kit (Invitrogen), and the sequences of the final constructs were verified by DNA sequencing.

HAP1-A/EGFP, HAP1-B/EGFP

To produce HAP1-A and HAP1-B conjugated with green fluorescence protein, fragments of rat HAP1-A cDNA (1799bp) and HAP1-B cDNA (1889bp) were amplified by PfuTurbo DNA polymerase (STRATAGENE) from PRK-HAP1-A and PRK-HAP1-B constructs (from Dr. Xiao-Jiang Li, Department of Human Genetics, Emory University School of Medicine) using PCR primers

1. HAP1-A(forward) 5'-TAGCTAGCATGCGCCCGAAGGAC-3' ,
2. HAP1-A(reverse) 5'-CGCTCGAGTAGGGTTGATGATGC-3',
3. HAP1-B(forward) 5'-TAGCTAGCATGCGCCCGAAGGAC-3',
4. HAP1-B(reverse) 5'-ATCTCGAGGGAGGACCAAGAAGG-3' (GeneWorks Pty Ltd) with added NheI and XhoI sites. The amplified fragments were digested with NheI and XhoI and subcloned in-frame into pEGFP-Express-N1, and the sequences of the final constructs were verified by DNA sequencing.

Expression of recombinant proteins

The plasmids pET100/D-TOPO-AAproBDNF, pET100/D-TOPO-prodomain BDNF, and pET100/D-TOPO-Val66Met prodomain BDNF were transformed into E. coli BL21, and the bacterial host was grown in 1000 ml LB media with 100ug/ml of ampicillin as a selective agent (300rpm, 37°C) until the optical density (OD) at 580 nm reached ≈0.8. After adding Isopropyl-b-D-thiogalactopyranoside (IPTG) to a final concentration of 0.5mM and shaking at 300 rpm overnight at 30°C, the bacteria were harvested by centrifugation at 11,000×g for 20 mins at 4°C. The pellet was resuspended in 40ml of binding buffer (50mM K-phosphate buffer,pH 7.4, 0.3M NaCl, 10% glycerol, 0.005% Triton- 100, 10mM imidazole and 1mM DTT and 1mM of PMSF as a protease inhibitor). Lysozyme (Sigma) was added to the solution to a final concentration of 0.2mg/ml to lyse the cells and the solution was kept on ice for 25 mins. The solution was then sonicated 10 times on ice for a 30 second period at a power of 50 watts. The solution was then centrifuged at 11,000×g for 20 mins at 4°C and the pellet was resuspended with 50 ml of buffer I (20mM Tris pH 8.0, 0.2M NaCl and 1% deoxycholic acid sodium salt) and subjected to agitation on ice for 30 mins. The suspension was then centrifuged at 3000×g for 10 mins. The pellet was then resuspended in 50ml of cold buffer II (10mM Tris pH8.0, 1mM EDTA and 0.25% deoxycholic acid sodium salt). The solution was then centrifuged at 3000×g for 10 mins. The pellet was washed using 40ml of buffer II three times, as above. After

the final wash, the proteins in the pellet were denatured and solublized in 40ml of 8M urea solution. A nickel column was prepared according to the manufacturer's instructions. The protein solution was centrifuged at 11,000×g for 25 mins at 4°C. The cleared supernatant was added to the column. After all the supernatant passed through the column, the column was then washed with the wash buffer (8M urea, 5mM imidazole and 0.5M NaCl). The OD of the wash eluate was monitored until it had dropped to baseline levels. The elution buffer (8M urea, 1M imidazole and 0.5M NaCl) was added to the column to elute the target proteins. The collected proteins were subjected to commassie brilliant blue staining after separation by electrophoresis. The elution solution containing proteins was diluted 10 times with refolding solution (0.75M L-Arginine, 5mM of GSH, 0.5mM GSSH, 5mM EDTA and 0.1M Tris pH 9.5). After refolding, the protein solution was dialysed against 2L of PBS for 4 hours at 4°C, followed by 5L for 4 hours and then by 10L overnight. The final protein concentration was measured using a BCA™ Protein Assay Kit (Pierce). For full-length proBDNF, supernatant lysate was generate from buffer I (20mM Tris pH 8.0, 0.2M NaCl and 1% deoxycholic acid sodium salt) purified on the nickel column. The mature BDNF recombinant protein was obtained from Protech (Rocky Hill, NJ). All recombinant proteins were characterized by SDS-PAGE with Coomassie Blue staining and Western blot analysis.

The fusion protein of HAP1 (PC43) (middle portion of HAP1, amino acids 280-445) was subcloned into pGEX-4T-2 vector (from Dr. Xiao-Jiang Li, Department

of Human Genetics, Emory University School of Medicine). One shot ® Top10 competent E Coli (Invitrogen) was used as the host strain in plasmid constructions. The construct was amplified and expressed in Top 10 E. coli and purified as GST fusion proteins, following the procedures as described (Li et al. 1998b). Briefly, competent bacterial cells were transformed with the plasmid by heat shock at 42°C for 1 minute. After this the bacteria were seeded into Luria-bertani (LB)/agar/Amp^+ selection plates. Bacterial clones were then selected and grown in 10ml Amp^+ medium (150 rpm, 37°C) overnight. After confirmation by mini-preparation of the plasmid, the remaining bacteria were further grown in 1000ml LB/Amp^+ medium (150 rpm, 37°C) until the OD at 580 nm reached ≈0.8. Following the addition of Isopropyl-b-D-thiogalactopyranoside (IPTG) to a final concentration of 0.5mM and shaking overnight at 30°C, the bacteria were harvested and pulse-sonicated.

For soluble proteins, supernatant obtained following centrifugation (15,000×rpm at 4°C, 20 min) was collected and 1% Triton-100 added. The supernatant was immediately mixed with glutathione agarose beads (Sigma) by rotating at room temperature for 1 hour. The glutathione agarose beads were collected and washed thoroughly using phosphate buffered saline (PBS, 29mM Na_2HPO_4, 15mM $KH_2PO_4$1.36M NaCl, 27mM KCl). After proteins were eluted with elution buffer (50mM Tris-HCl, 5mM Glutathione, pH 8.0), the collected protein was subjected to Commassie brilliant blue staining after separation by electrophoresis. Then the

protein was dialysed against 2L of PBS for 4 hours at 4°C, followed by 5L for 4 hours and then by 10L overnight. The final protein concentration was tested using a BCA™ Protein Assay Kit (Pierce).

Animals

All procedures involving animals were approved by the Animal Welfare Committee of Flinders University and undertaken according to the guidelines of the National Health and Medical Research Council of Australia. All animals were kept under standardized barrier breeding conditions (12-h light/12-h dark cycle) with free access to water and food.

Sheep anti HAP1 antibody generation

Colloidal gold particles were prepared by adding 0.5ml 1% gold chloride (Sigma) and 1.5ml 1% sodium citrate to 50ml boiling distilled water. The mixture was kept boiling until the color changed to red. 100ul 1M K_2CO_3 pH10.8 was then added to the solution.

For the first injection, the adult sheep was subcutaneously (SC) injected with immunization emulsion [2ml Freund's Complete Adjuvant (Chemicon), 0.5ml HAP1-GST peptide (400ug) and 1.5ml sterilized PBS] and intravenously (IV) injected with immunization mixture [4.85ml gold solution, 150 µl HAP1-GST

peptide (100μg)]. The injections were repeated every two weeks but incomplete Freund's Adjuvant was used in all subsequent injections with half the amount of HAP1 protein. One week before every injection, 20ml of sheep blood was sampled for immunoreactivity. The injections were conducted 6 times before the animal was bled out. The antibodies were affinity purified against the immunizing peptide which was immobilized on Sepharose 4B gel.

Preparation of BDNF binding proteins from rat brain homogenate

Male and female Sprague-Dawley rats (200-300g) were used. The entire purification process was performed at 4°C. Six rat brains were minced in liquid nitrogen and then homogenized by sonication in 10 volumes of RIPA buffer (150 mM NaCl, 0.1% SDS, 0.5% sodium deoxycholate, 1% NP-40, 50 mM Tris,1 mM EDTA, pH 7.8) containing protease inhibitors (protease inhibitor cocktail, Roche). The crude homogenate was centrifuged for 20 min at 5,000 × g. The supernatant was used for affinity purification.

One gram of CNBr-activated Sepharose^{TM} 4B (Amersham Biosciences) was swollen in ice-cold distilled water for 2 h and washed twice with 100 ml of ice-cold 1 mM HCl for 30 min. The gel was drained by suction through a glass filtering crucible. It was then washed twice with 100 ml of ice-cold distilled water and twice with ice-cold 0.1 M $NaHCO_3$ (pH 9.0) and partially dried by using the same apparatus. One milligram of prodomain BDNF or mature BDNF in 1 ml of

0.1 M $NaHCO_3$ (pH 9.0) was added to 1 g of the gel at 4°C and left overnight with gentle shaking. The gel was filtered and then washed successively with 100 ml each of 0.1 M $NaHCO_3$ (pH 9.0), 1 M NaCl, and distilled water until the absorbency value was 0.001 OD units at 280 nm. Two ml of 1 M ethanolamine (pH 9.0) was added to the gel and left at room temperature for 2 h with gentle shaking to block the free amino groups of the gel. The gel was drained by suction, washed successively with 100 ml each of distilled water and 1 M NaCl, and then equilibrated with 50 ml of elution buffer. The gel was finally washed three times with 100 ml of binding buffer and stored at 4°C.

The gels containing the immobilized prodomain BDNF and mature BDNF were suspended in binding buffer (3.84 mM NaH_2PO_4, 6.16 mM Na_2HPO_4, 0.15 M NaCl, pH 7.2) and equilibrated with 30 ml of the binding buffer. The brain lysate of Sprague-Dawley rats was added to the columns. The columns were washed using gravity flow with washing buffer A (56 mM NaH_2PO_4, 144 mM Na_2PO_4, 2 M NaCl [pH 7.2] plus 1% Tween 20) and then with washing buffer B (56 mM NaH_2PO_4, 144 mM Na_2PO_4, 1 M NaCl, pH 7.2) to remove the detergent (Tween 20). Samples were monitored for OD at 280 nm throughout the entire washing procedure until the absorbence of the outflow was approximately 0.001 OD units. The elution buffer (buffer C, 0.1 M glycine-HCl, pH 2.5) was then added to the column. The elution fractions were collected, and the pH was adjusted immediately to 7.2 with 2M NaOH. The proteins were dialysed using distilled water at 4°C. Each protein preparation was cleaned by using PlusOne 2-D clean-

up kit (GE Healthcare) and quantified by using PlusOne 2-D Quant Kit (GE Healthcare).

2D-DIGE and Image analysis

For sample labeling, 50 μg of each protein was labeled with 400 pmol of cyanine dyes, Cy3 for prodomain binding proteins and Cy5 for mature BDNF binding proteins according to a standard protocol. Cy2 was used for labeling of the internal standard that includes equal amounts of mature BDNF- and prodomain-binding proteins. The labeling was terminated by the addition of 1 μl of 10 mM lysine. The labeled samples were mixed to allow the gel to contain 50 μg each of Cy2-labelled internal standard, Cy3- and Cy5-labelled samples respectively. For the first-dimension separation, the labeling mixture was applied to Immobiline DryStrips (13 cm, pH 3-11 linear) by cup loading with a total running time of 55 kV.h of isoelectric focusing. The second dimension was carried out with 10% SDS-PAGE gels, and gel images were subsequently acquired at the recommended wavelengths by using a Typhoon™ Variable Mode imager (GE Healthcare).

2-D SDS-PAGE was performed (Choi et al. 2004a). 100 μg prodomain BDNF binding proteins were separated in 2-D SDS-PAGE. After the 2-D electrophoresis, the gel was stained with SYPRO Ruby. The 2-D gel was rinsed with three changes of distilled water for 5 min, and then fixed in 30% methanol- 7.5% acetic acid for 30 min. The gel was placed in the SYPRO Ruby staining solution for 3 h

overnight. Following this step, the gel was rinsed with 10% methanol-7% acetic acid for 30-60 min to remove excess stain from the gel surface. The spots on the gel were analysed using a PE Biosystems MALDI-TOF Voyager-DE STR Mass Spectrometer. For the database searches, the peptides were selected in the mass range of 750-900 Da and evaluated using the ExPasy server on the Worldwide Web at http://prospector.ucsf.edu/.

Pull-down assay

4 µg HAP1-GST proteins were diluted in binding buffer (250 mM NaCl, 50mM pH 7.9 HEPES, 0.5 mM EDTA, 0.1% Triton) and immobilized on 25µl glutathione agarose beads (Sigma). 500 ng of recombinant protein (proBDNF, prodomain BDNF, Val66Met prodomain BDNF and mature BDNF) were incubated with the beads at 4°C for 2 h without or with the presence of equal quantity of PC12 cell lysate transfected with PolyQ 23 or PolyQ103, or with the same quantity of normal or Huntington disease human brain lysate. The beads were washed three times and boiled in loading buffer to release the bound proteins. Resolved by SDS-PAGE, the proteins were transferred to a PVDF membrane (Amersham Biosciences) and were detected by immunoblotting using rabbit anti HAP1 antibody, rabbit-anti prodomain BDNF (Zhou et al. 2004) and rabbit anti-mature BDNF (Zhou et al. 1999).

Immunoprecipitation of Human brain samples

Brain samples from HD cases (2 males; age 75 and 73) and control cases (2 males, age 68 and 73) were obtained from the Flinders University Brain Bank. Cortex samples were minced in liquid nitrogen and then homogenized by sonication in 10 volumes of RIPA buffer (150 mM NaCl, 0.1% SDS, 0.5% sodium deoxycholate, 1% NP-40, 50 mM Tris,1 mM EDTA, pH 7.8) containing protease inhibitors (protease inhibitor cocktail, Roche). The crude homogenate was centrifuged for 20 min at 5,000 × g and the supernatant used for immunoprecipitation.

50 µl Sepharose beads prebound to rabbit anti-HAP1 antibody were washed in 1.0 ml of TBS (10 mM Tris-HCl, 0.14 M NaCl, pH 7.5) with 0.1% Tween-20 (Sigma) and were gently shaken for 15 min. This mixture was centrifuged at 6000 g for 10 s at 4°C; the supernatant discarded and the pellet rewashed. Next, brain samples were pre-cleared by incubation with an excess of protein A+G agarose. The cleaned 1mg of protein lysate (1 mg/ml) was added to an Eppendorf tube containing the washed HAP1-antibody immobilized Sepharose beads and the mixture was incubated for 2 h at 4°C. The incubated lysate was centrifuged at 6000 g for 10 min at 4°C. The resultant supernatant was discarded, and the pellet was washed in 3 times using 1.0 ml TBS with 0.1% Tween 20 with gentle shaking for 15 min and then centrifuged at 6000 g for 10 min. Then, 25 µl of loading buffer (50 mM Tris-HCl, pH 6.8, 5% β-mercaptoethanol, 0.2% SDS, 0.1% bromophenol blue, 10% glycerol) was added to the washed pellet. The sample was mixed by

vortexing, then placed in a boiling water bath for 10 min and centrifuged at 10,000 g for 2 min at room temperature. The resultant supernatant was detected by Western blot using sheep anti-HAP1 antibody, rabbit anti-prodomain BDNF, mouse anti-mature BDNF, rabbit anti-sortilin antibody (Abcam), and rabbit anti-prodomain BDNF antibody plus proBDNF recombinant protein.

Cell culture and transfection

PC12 cells were maintained in DMEM supplemented with 10% fetal bovine serum, 5% heat-inactivated horse serum, 50 μg/ml streptomycin, and 50 IU/ml penicillin in a humidified atmosphere at 37°C and 5% CO_2 as described previously (Gueorguiev et al. 1999). 3 days before transfection, the PC12 cells were seeded onto poly-l-ornithine (mol. wt.= 40,000;15 μg/ml) coated 42mm coverslips in 3 ml of PC12 cell culture medium containing 100ng/ml NGF. The corresponding plasmids were mixed with reconstituted Neuroporter in a ratio of 5 μl to 5 μl according to the instructions of Neuroporter Transfection kit (Sigma), and then the mixtures were added to PC12 cells. The cells were incubated with the transfection mixtures for 4 h at 37°C in an incubator with 5% CO_2. The transfection mixtures were removed and the cells were washed twice with phosphate-buffered saline, which was then replaced with 5 ml fresh NGF containing culture medium, and the cells were incubated for an additional 48 h at 37°C in humidified air containing 5% CO_2. The living cell images were taken using confocal microscopy (Leica TCS SP5).

Primary cultures of cortical neurons were prepared as described previously (Lesuisse & Martin 2002). Briefly, cells from the cerebral cortex of postnatal day 1 wild type and homozygous HAP1$^{-/-}$ mice were seeded in serum-free medium on 24-well cell culture plates (10×10^5 cells/well). The culture medium included Neurobasal medium (Invitrogen), B27 supplements (Invitrogen), 300 μM glutamine (Invitrogen), 25 μM β-mercaptoethanol, and streptomycin/ amphotericin B (Invitrogen). Three days after plating, 50% of the medium was changed and subsequently the medium was changed every 3 days. The primary cultured cortical neuronal cells were transfected with prodomain BDNF DsRed plasmids according to the instruction of Neuroporter Transfection kit (Sigma). The cells were incubated with the transfection mixtures for 4 h at 37 °C in an incubator with 5% CO_2. The transfection mixtures were removed and the cells were washed twice with phosphate-buffered saline, which was then replaced with 1 ml fresh culture medium, and the cells were incubated for an additional 48 h at 37 °C in humidified air containing 5% CO_2.

Subcellular fractionation

Subcellular fractions of wild type and HAP1$^{-/-}$ mice cortex were prepared essentially as described (Sharp *et al.* 1995, Gray & Whittaker 1962). The postnatal day 1 wild type or HAP1$^{-/-}$ mice were killed by decapitation, and cortices were rapidly collected. Cortices were homogenized in 10 ml per gram wet weight ice-

cold 0.32 M sucrose in 4 mM HEPES (pH 7.4) and a cocktail of protease inhibitors using 10 strokes of a glass/teflon homogenizer. The homogenate was centrifuged for 10 min at 1000 x g to produce a pellet (P1), which was washed by resuspension in an equal volume of homogenization buffer and recentrifuged for 10 min at 1000 x g to yield a nuclear fraction (P1). The original supernatant combined with the wash (S1) was then centrifuged at 17,500 x g for 20 min to produce a pellet (P2) and a supernatant (S2). The P2 fraction was resuspended in an amount of homogenization buffer equal to the original homogenization buffer and layered on two-step sucrose gradients consisting of 1 ml each of 0.8 and 1.2 M sucrose. The gradients were centrifuged at 25,000 rpm for 2 hr in an SW28 rotor. Three fractions were collected corresponding to material at the 0.32-0.8 M sucrose interface (myelin-enriched fraction, LP1), at the 0.8-1.2 sucrose interface (synaptosome-enriched fraction, LP2), and below 1.2 M sucrose (mitochondria-enriched fraction, LP3). The S2 fraction was centrifuged at 100,000 x g for 60 min to produce a high speed pellet (P3) and a high speed supernatant (S3). The SDS polyacrylamide gels were loaded with equal amounts of protein from each fraction (65ug per lane) to conduct western blotting using sheep anti-HAP1, rabbit-anti proBDNF.

ELISA

Forty-eight hours after transfection, transfected and non-transfected cortical neurons were washed three time with Krebs'–Ringer's–Henseleit (KRH) buffer

with the following composition (in mM): 125 NaCl, 4.8 KCl, 2.6 $CaCl_2$, 25 HEPES, 1.2 $MgSO_4$, 5.6 glucose, 1 sodium ascorbate, and 1.2 KH_2PO_4, adjusted to pH7.4 with NaOH. The conditioned media were collected after 16 h incubation at 37°C and used as a measure of constitutive secretion. To determine regulated secretion, cells were washed three times with KRH buffer, followed by 10 min incubation at 37°C in stimulated media [KRH buffer with an increased KCl concentration (56 mM) and decreased NaCl concentration (75 mM)]. Secretions resulting from these constitutive secretion conditions were normalized to 10 min. The prodomain BDNF protein concentrations in the respective media samples were determined using the prodomain BDNF ELISA system with recombinant prodomain BDNF as a standard (The ELISA assay established within our laboratory).

Polystyrene plates (number 3590, Costar, Cambridge, MA, USA) were coated with monoclonal prodomain BDNF antibody (PB17-2A, 1:3000) in 0.1 M carbonate coating buffer (pH 9.6) and incubated overnight at 4°C. The wells were blocked with 5% skim milk in 1% Tween 20 phosphate buffered saline (PBST) for 2 hours at room temperature. Then the plates were washed with 1% Tween 20 PBS (PBST). The collected media were added to the wells, in triplicate. For preparation of the protein standard, prodomain BDNF recombinant proteins were diluted in 10ng/ml, and 1:2 serial dilutions were then performed. Plates were incubated overnight at 4°C. After an additional wash step with PBST, 100 µl of monoclonal anti prodomain BDNF-HRP (PB5E-2) was added to the wells (20µg/ml) and

incubated for 2 hours at room temperature. After washing with PBST 5 times, 50 µl TMB solution was added to each well. The plates were incubated for 20 to 30 minutes at room temperature, and then the reaction was stopped with 1 M sulfuric acid (50ul/well) and the absorbance was measured at 490 nm with a model 3550 reader (Bio Rad Laboratories, California, Hercules, USA). Standards and samples were assayed in triplicate, and each group contained six independent samples. After collecting conditioned media, cells were fixed and observed under fluorescence microscopy to determine the transfection efficiency. Each sample had a transfection efficiency of ~80%.

Sciatic nerve crush

All the experiments were done on postnatal day 1. For anaesthesia, the pups were wrapped with a piece of cloth and put on ice. After 1 to 2 minutes, the mice were put on an ice cold plate. When the mouse was motionless, an incision 0.5 cm long was made in the left thigh and the left sciatic nerve was exposed and crushed at the mid-thigh level for 10 seconds with a pair of fine forceps. One drop of lidocaine (5mg/ml) was put over the wound skin. The skin was closed with 9/0 monofilament polyether sutures. Animals were kept on a warm blanket for recovery. After recovery, the neonates were returned to their mother. Six hours after sciatic nerve crush, puppies were anaesthetized on ice again and killed by perfusion through the heart with 4% paraformaldehyde. The sciatic nerve was

dissected and processed for immunohistochemistry.

ProBDNF immunohistochemistry

Antibodies to prodomain BDNF were generated by immunization of rabbits with synthetic peptide (corresponding the pre-region sequence 69–82 of the human proBDNF gene), which were conjugated to hemocyanin (KLH). We chose the unique sequence in the proBDNF region which has no homology with known sequences of other proteins in mammals, to avoid potential cross-reaction of generated antibodies to other molecules. Antibody specificity was verified after affinity purification by reaction with the immunizing antigen, and characterized by Western blot. This antibody recognises endogenous proBDNF and recombinant proBDNF (Zhou et al. 2004).

After overnight immersion in 30% sucrose in PBS at 4°C, the dissected tissues were serially cryostat sectioned at 10 μm. The sections were washed, treated with 50% ethanol and 0.3% H_2O_2 for 45 minutes. Then the sections were blocked in 20% normal horse serum (NHS) and incubated overnight in affinity-purified polyclonal antibodies raised in rabbit against proBDNF (1:1000) or normal rabbit IgG (1μg/ml) diluted in PBS containing 1% NHS and 0.3% Triton X-100 at room temperature (RT). After extensive washes, the sections were incubated in biotin-conjugated antibody to rabbit IgG (raised in sheep, 1:250 diluted with 1% NHS in

PBS, SILENUS) for 2 hours at RT, followed by ABC reagent (1:100, Vector Labs) for 1 hour at RT. The sections were washed in PBS and incubated with glucose oxidase-DAB-nickel for 5 minutes.

Image Analysis

Image analysis was accomplished using the public domain software ImageJ (available at http:// rsb.info.nih.gov/ij). All acquired images were grouped in a stack and subsequently analysed in an automated procedure using the program explained in http://www.uhnres.utoronto.ca/facilities/wcif/imagej/particle_ analysis.htm. Operations during analysis consisted of converting the images to 8-bit (256 scales of grey, ranging from 0 (black) to 255 (white), all images show a typical distribution of grey values which is used for particle counting), plotting the area of grey values, adjusting threshold and analysing particles. Summarized total area pixel^2 was displayed as filled black particles. For each particle the following parameters were recorded: area in pixels, minimum/maximum/mean grey value.

Statistics

Data are presented as mean ±S.E. Statistical significances were calculated using Student's t-test for unpaired samples. Statistically significant difference was set at $p<0.05$.

4. Results

Huntingtin-associated protein 1 is a prodomain BDNF binding protein

To investigate mechanisms underlying the axonal transport of BDNF, we attempted to identify the proteins that interact with BDNF. To do this, we first made recombinant prodomain and mature BDNF and affinity purified the interacting proteins from the rat brain. We analyzed the binding proteins by using 2D-DIGE to compare the difference in proteins in two different sets of samples. The results showed that the proteins interacting with mature BDNF from the rat brain are obviously different from the proteins interacting with prodomain BDNF (Fig. 1A). Most proteins detected from the two sets of samples are not co-localized and displayed different colors, suggesting the prodomain BDNF interacts with different proteins from the mature BDNF.

To further identify which proteins interact with the prodomain BDNF, the protein samples isolated from the prodomain affinity column were subjected to 2-D SDS-PAGE and the protein spots determined by MALTI-TOF Voyager-DE STR Mass Spectrometer and database search. One of these proteins was huntingtin-associated protein 1 (HAP1). To confirm that this protein is indeed HAP1, the prodomain BDNF binding proteins and mature BDNF binding proteins were analyzed by western blot using anti-HAP1 rabbit antibody (Gift from Defiglia). HAP1 consists of two HAP1 isoforms, HAP1-A and HAP1-B, which differ only at

the C terminus (Li et al. 1995). The Western blot showed that the smaller species, HAP1-A, was found in proteins isolated from the mature BDNF column, whereas the longer species, HAP1-B, as well as a minor band of HAP1-A were identified in the proteins isolated from the prodomain BDNF column (Fig. 1B). These results indicate that HAP1-B and HAP1-A are associated with the prodomain BDNF whereas only HAP1-A is associated with mature BDNF. To find the molecular weight of the affinity-purified BDNF domain binding proteins, the proteins isolated from the affinity columns were electrophoresed, transferred to a membrane and probed with biotinylated prodomain BDNF. In the lane of prodomain binding proteins we found a number of bands between 18 to 80 kD. A strong band corresponding to the size of 68kD (HAP1-B) was detected (Fig. 1C). Furthermore, based on the fact that p75NTR is the receptor of mature BDNF, p75NTR antibody was used to probe the membrane. It was found that a positive band at 75kDa was present in mature BDNF binding proteins but not in the prodomain BDNF-binding proteins (Fig. 1D), suggesting that p75NTR was not present in the prodomain binding proteins.

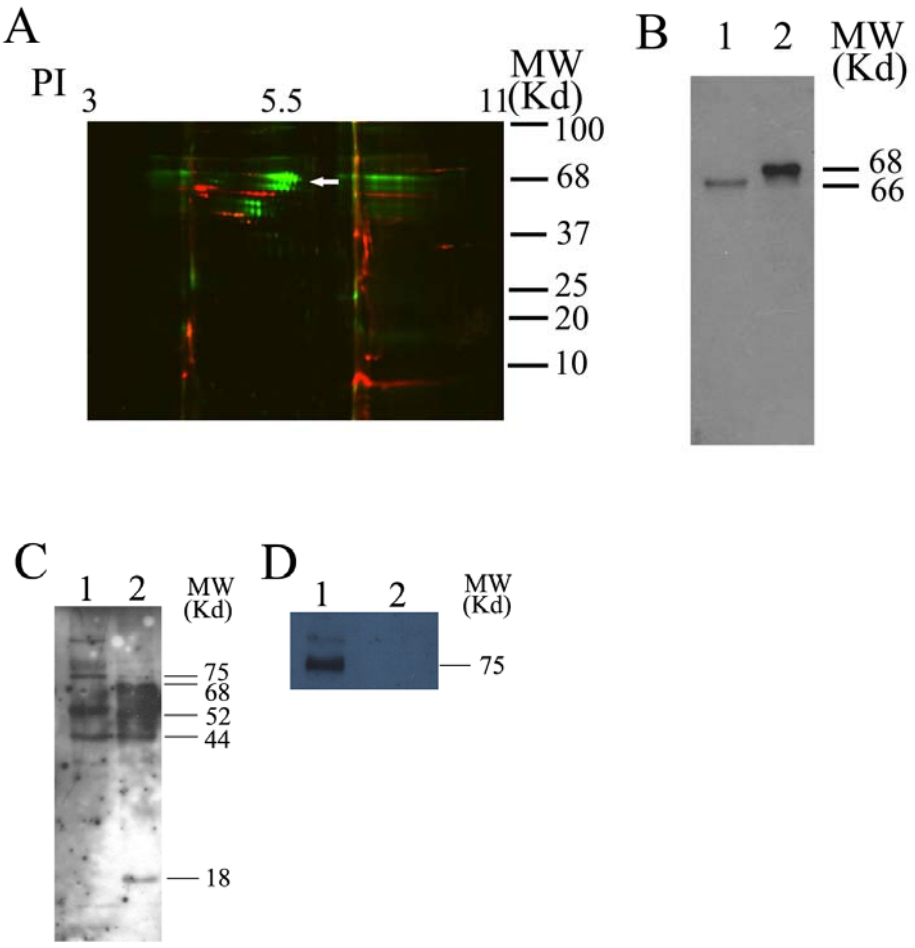
A
PI
3
5.5
11
MW
(Kd)
100
68
37
25
20
10
B
1
2
MW
(Kd)
68
66
C
1
2
MW
(Kd)
75
68
52
44
18
D
1
2
MW
(Kd)
75

Fig. 1 Interaction of prodomain BDNF with HAP1. (A) The binding proteins were collected by passing rat brain lysate through affinity columns which were immobilized with recombinant prodomain BDNF and mature BDNF. DIGE 2D-gel was used to reveal all proteins bound to the recombinant prodomain BDNF (green) and mature BDNF (red) affinity columns. When sequenced by MALTI-TOF, one of these proteins was shown to be HAP1 (white arrow). **(B)** Affinity purified mature BDNF binding proteins (lane 1) and prodomain BDNF binding proteins (lane 2) were probed with rabbit anti-HAP1 antibody. The antibody recognized a smaller band (66 Kd) in mature BDNF binding proteins and a larger band (68 Kd) in prodomain BDNF binding proteins. **(C)** Affinity purified materials from mature BDNF (lane 1) and prodomain BDNF (lane 2) were separated, transferred, and probed with biotinylated prodomain BDNF. A strong band was present around 68 Kd which is likely HAP1-B. The nature of other small bands remains to be determined. **(D)** Affinity purified material from the mature BDNF (lane 1) and prodomain BDNF (lane 2) were probed with mouse monoclonal anti-p75NTR antibody 192. p75NTR was present in the mature BDNF binding proteins, but not in the prodomain BDNF binding proteins.

Interaction of HAP1 with proBDNF, prodomain BDNF and mature BDNF in vitro.

We next tested whether HAP1 associates directly or indirectly with prodomain BDNF and mature BDNF. For this purpose, we expressed recombinant proteins of HAP1 fragment fused with GST. The pull-down assay showed that the HAP1 fragment (280-445 aa) could bind both the prodomain BDNF and full-length proBDNF, but not mature BDNF (Fig. 2A). Next, we quantified the density of the blot image. The percentages of input in pull-down assays were calculated using the input as 100%. Quantitative analysis showed 56% proBDNF and 84% prodomain BDNF were pulled-down by HAP1-GST (Fig. 2B). In contrast, no mature BDNF bound to the fragment of HAP1. These results suggest that HAP1 (280-445 aa) directly interacts with the prodomain of BDNF but not mature BDNF. The lack of interaction between HAP1-GST and mature BDNF suggests that the fragment of 280-445 aa HAP1-GST is not the binding domain for mature BDNF or that the binding of HAP1-A to mature BDNF could be caused by an indirect interaction.

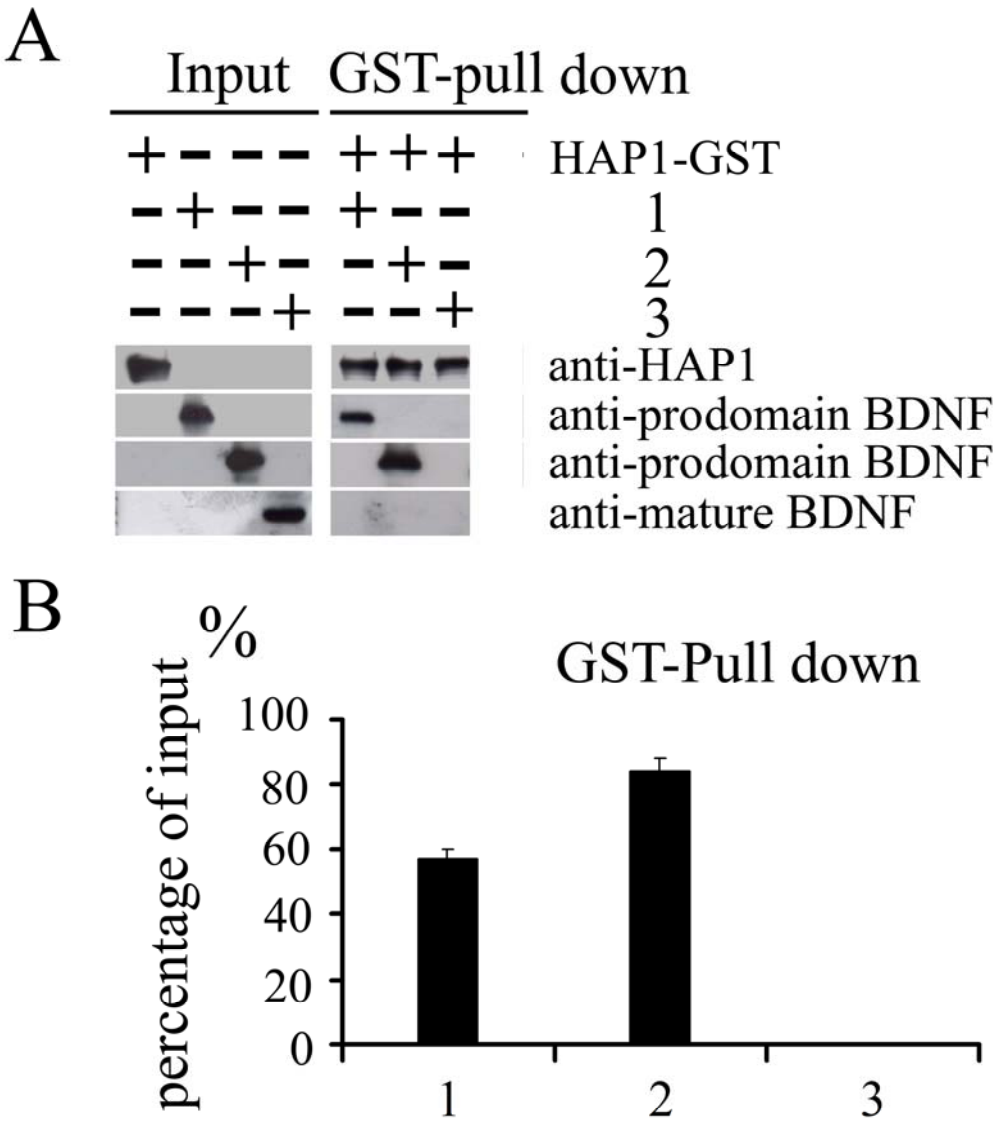
A
Input
GST-pull down
+ − − − + + +
− + − − + − −
− − + − − + −
− − − + − − +
HAP1-GST
1
2
3
anti-HAP1
anti-prodomain BDNF
anti-prodomain BDNF
anti-mature BDNF
B
%
GST-Pull down
percentage of input
100
80
60
40
20
0
1
2
3

Fig. 2 Interaction of HAP1 with proBDNF, prodomain BDNF and mature BDNF in vitro. HAP1 GST fusion proteins were immobilized on glutathione-argarose beads and incubated with proBDNF **(1)**, prodomain BDNF **(2)** and mature BDNF **(3)**. Bound proteins were detected by immunoblotting, respectively. **(A)** The quantity of input proteins is shown in the blot and the quantity of proteins after GST pull-down being performed. **(B)** Analysis of percentage of pull-down proteins. The staining intensity of each band was quantified by the NIH ImageJ program (n=3). The percentage of input was calculated using input proteins as 100%. The data are presented as mean ±SEM.

As HAP1 is known to interact with dynactin p150glued, an accessesory molecule of dynein (Engelender et al. 1997, Li et al. 1998b) and is involved in molecular transport within neurons, we hypothesize that HAP1 may be a dynein motor accessory protein playing a role in the transport and release of BDNF. However, as HAP1 is known as a cytosolic protein, the question which arises is how a vesicular protein, BDNF, interacts with the cytosolic protein, HAP1. Thus, we first needed to eliminate the possibility of an artifact where HAP1 interacted with BDNF under the non-physiological conditions of a protein mixture obtained from a brain homogenate. To address this question we carried out two different experiments (Fig. 3-1). First we co-transfected two different sets of plasmids conjugated with different fluorescent markers in PC12 cells through Live Cell Image. HAP1-A (green fluorescence) was highly colocalized with proBDNF (83.2%) and the prodomain (76.8%), as indicated by yellow fluorescence (Fig. 3-1 A and B: 1, 2), while mature BDNF (red fluorescence) was partially colocalized with HAP1-A (green fluorescence) (36.9%, Fig. 3-1 A and B: 3). The results on colocalization of HAP1-B with the BDNF fragment were similar to those of HAP1-A (Fig. 3-2).

To further investigate the significance of the interactions between HAP1 and proBDNF, we fractionated the brain lysate of wild type and $HAP1^{-/-}$ mice with sucrose gradients as reported (Sharp et al. 1995). In wild type and $HAP1^{-/-}$ mice brain lysate, proBDNF was present in both the crude nuclear fractions (P1) and high speed (P3) pellets, as well as in medium speed supernatant (S2). proBDNF was only detected in medium speed pellet (P2) of wild type mice but not in $HAP1^{-}$

$^{/-}$ mice. Subfractionation of the P2 fraction using sucrose gradient centrifugation (Sharp et al. 1995, Gray & Whittaker 1962) showed that proBDNF was located in the synaptic vesicle-enriched and synaptosome-enriched fraction (LP2, 0.8-1.2M sucrose gradient fraction) in the wild type mice but not in the $HAP^{-/-}$ mice. In wild type mice brain lysate proBDNF is widely distributed in most cellular fractions and enriched in the synaptic vesicle subcellular fraction. HAP1 was present in all subcellular fractions (Fig. 3-1 C). In $HAP1^{-/-}$ mice brain lysate, no HAP1 was detected in all fractions, indicating the specificity of the antibodies and complete knockout of HAP1 in these mice. Interestingly, no proBDNF was detected in subcellular fractions P2 and LP2 but a larger amount of proBDNF was detected in S1, P1, S2 and P3. These results suggest that the deletion of HAP1 leads to the redistribution of proBDNF and loss of proBDNF in synaptic vesicles (LP2). These data suggest that interaction between HAP1 and proBDNF is specific and may have physiological significance.

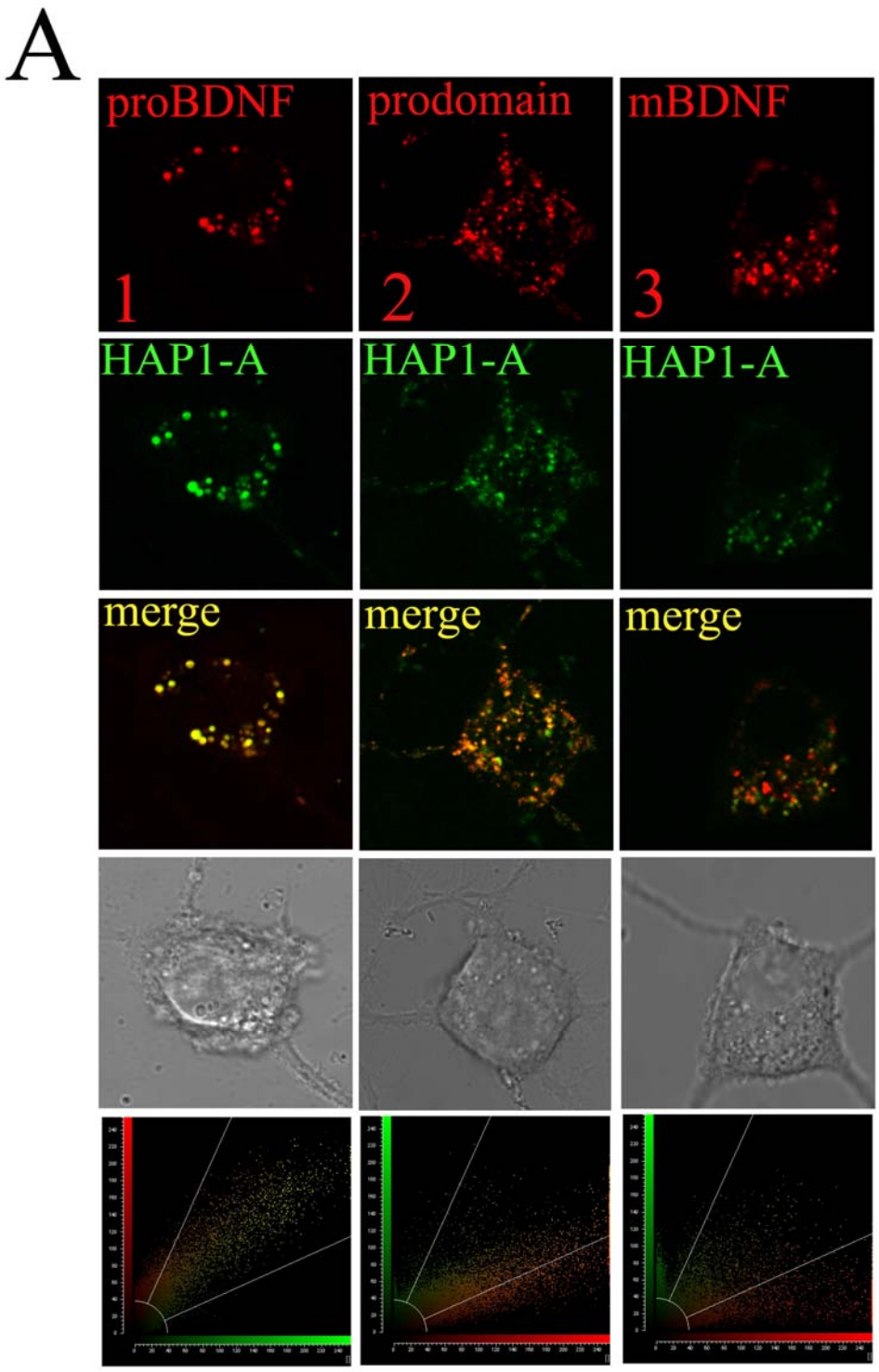
A
proBDNF
1
prodomain
2
mBDNF
3
HAP1-A
HAP1-A
HAP1-A
merge
merge
merge

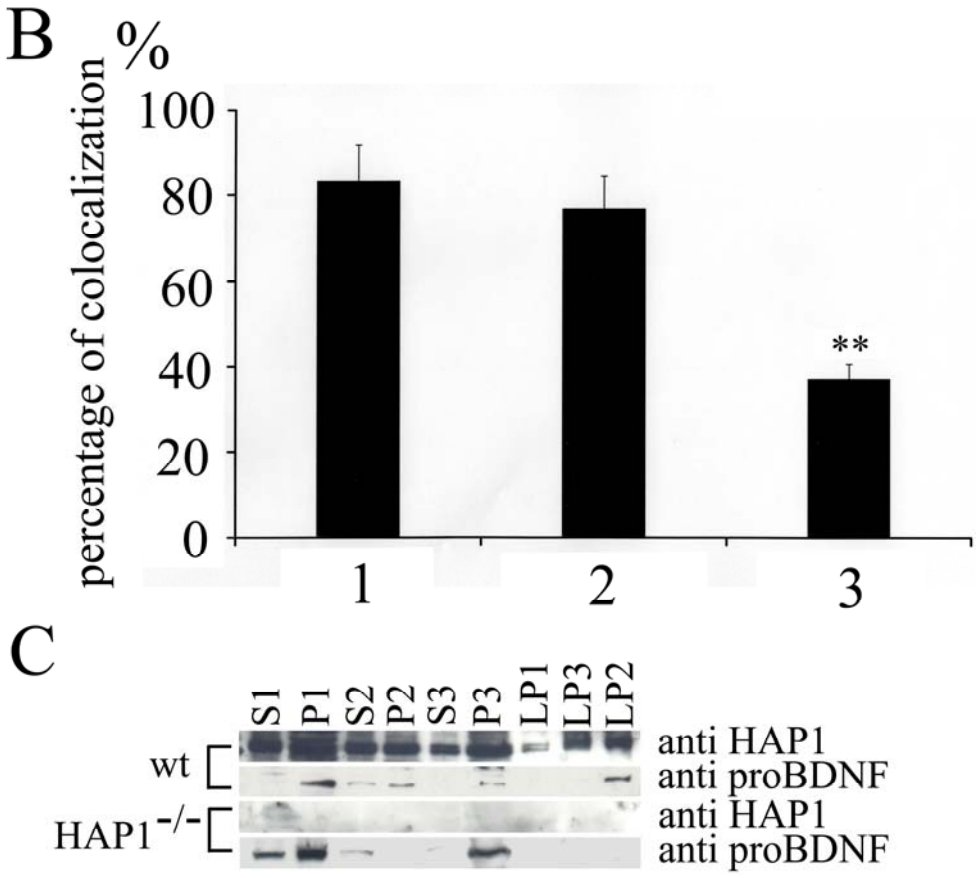
B
%
percentage of colocalization
100
80
60
40
20
0
**
1
2
3
C
S1
P1
S2
P2
S3
P3
LP1
LP3
LP2
wt
HAP1 -/-
anti HAP1
anti proBDNF
anti HAP1
anti proBDNF

Fig. 3-1 Colocalization of HAP1-A with BDNF sub-domains in PC12 cells. (A) PC12 cells were transfected with plasmids HAP1-A/EGFP (green) in combination with either full-length proBDNF-Ds-Red **(1)**, prodomain BDNF-Ds-Red **(2)** or mature (m) BDNF-Ds-Red **(3)** (red) respectively. Confocal images were taken and merged (yellow). Yellow dots indicate vesicles with both HAP1-A and BDNF sub-domains. The snapshot represents the rate of colocalization quantitatively analysed by the quantitative analysis software on Lieca SP5 Confocal Microscope. **(B)** The quantitative data showed proBDNF and prodomain BDNF highly colocalized with HAP1-A, whereas mature BDNF was partially colocalized with HAP1-A. The data are presented as mean ±SEM. The statistical analyses revealed significant differences of proBDNF and prodomain BDNF with mature BDNF (n=20, **$p<0.01$). **(C)** Subcellular fractions of sucrose gradient from P1 neonatal wild type and $HAP1^{-/-}$ mice cortex were prepared, resolved by SDS-PAGE, blotted to nitrocellulose membranes, and reacted with rabbit anti proBDNF, and sheep anti HAP1. Equal amounts of protein (65 μg) were loaded in each lane.

A

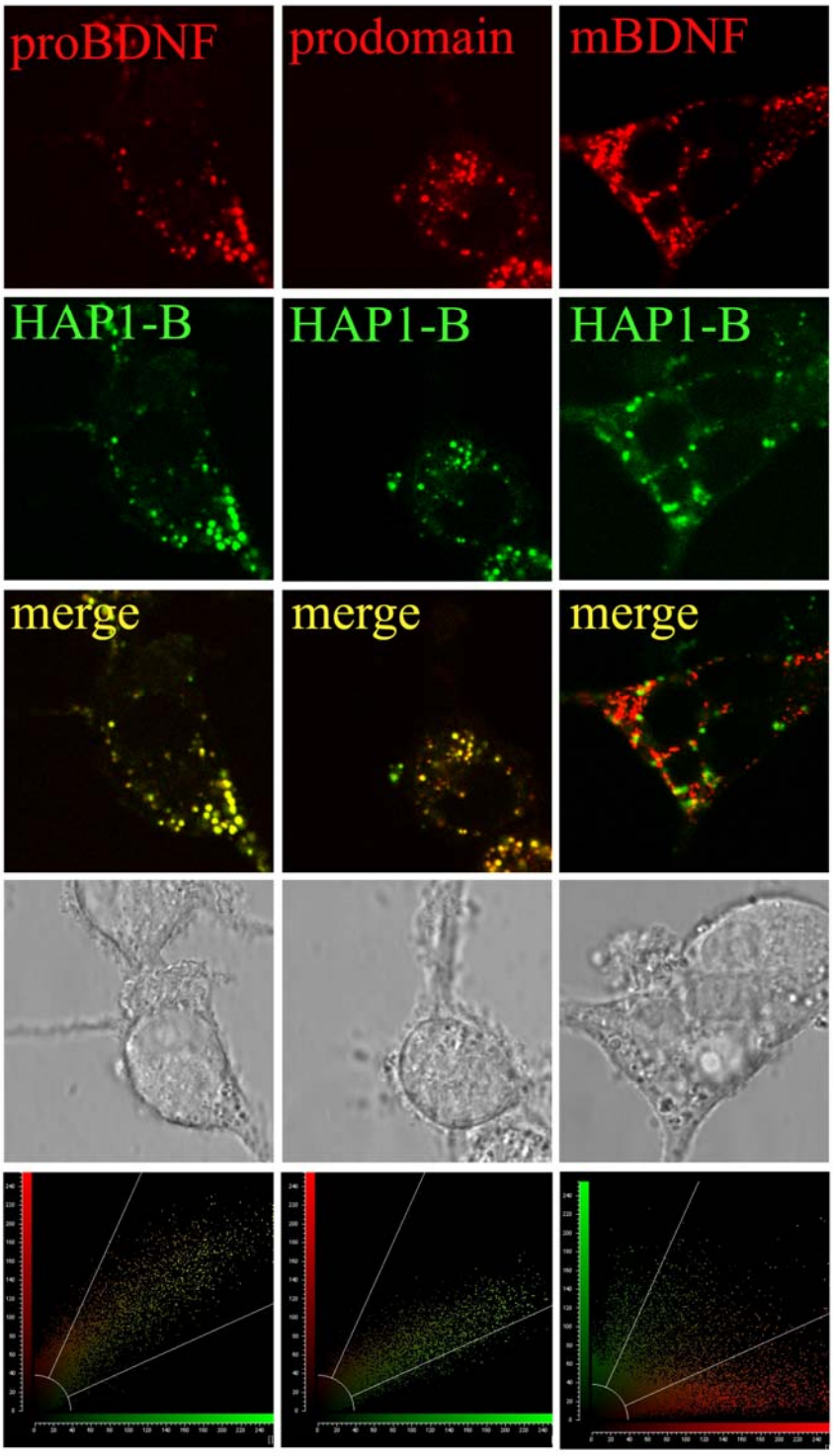
proBDNF
prodomain
mBDNF
HAP1-B
HAP1-B
HAP1-B
merge
merge
merge

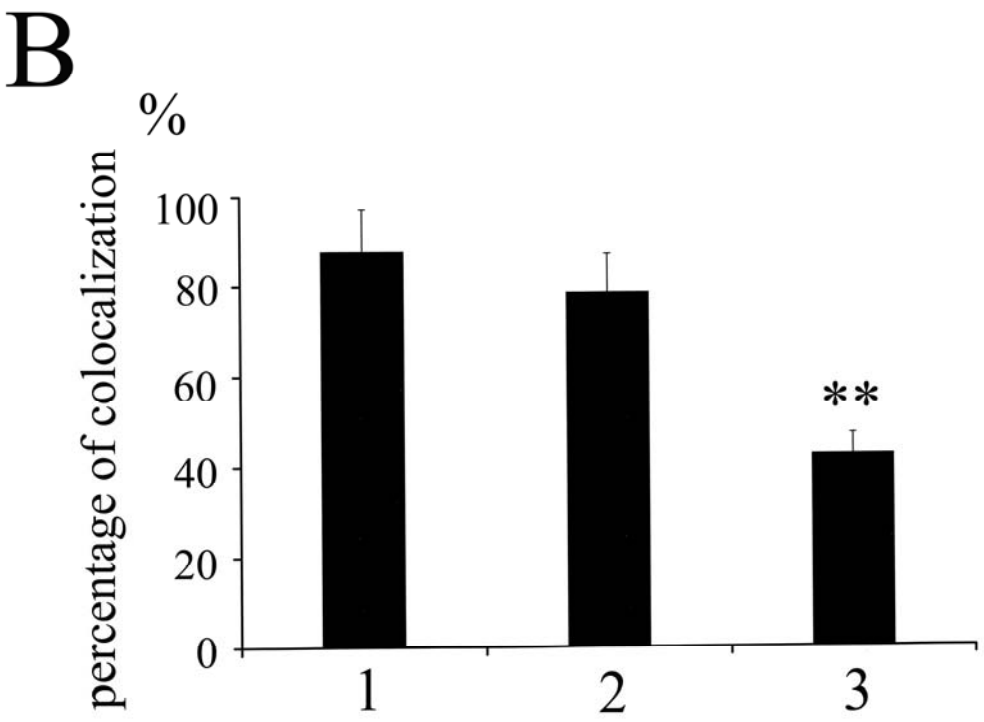
B
%
percentage of colocalization
100
80
60
40
20
0
**
1
2
3

Fig. 3-2 Colocalization of HAP1-B with BDNF sub-domains in PC12 cells. (A) PC12 cells were transfected with plasmids HAP1-B/EGFP (green) in combination with either full-length proBDNF-Ds-Red **(1)**, prodomain BDNF-Ds-Red **(2)** or mature (m)BDNF-Ds-Red **(3)** (red) respectively. Confocal images were taken and merged (yellow). Yellow dots indicate vesicles with both HAP1-B and BDNF sub-domains. The snapshot represents the rate of colocalization quantitatively analysed by the quantitative analysis software on Lieca SP5 Confocal Microscope. **(B)** The quantitative data showed proBDNF and prodomain BDNF highly colocalized with HAP1-B, whereas mature BDNF was partially colocalized with HAP1-B. The data are presented as mean ±SEM. The statistical analyses revealed significant differences between proBDNF and prodomain BDNF compared to mature BDNF ($n=20$, $^{**}p<0.01$).

HAP-1 is colocalized with internalized mature BDNF but not with de novo synthesized mature BDNF.

As our pull-down assay showed no interaction between HAP1 and mature BDNF (Fig. 2), the partial colocalization between HAP1 and mature BDNF in PC12 cells after co-transfection (Fig. 3) is intriguing. As we illustrated in the brain homogenate (Fig. 1B), HAP1-A can be pulled down by mature BDNF. We therefore hypothesized that the interaction between HAP1 and mature BDNF could be indirect. We further hypothesized that HAP1 is likely colocalized with exogenous mature BDNF which is internalized by a receptor mediated-mechanism but not colocalized with the *de novo* synthesized mature BDNF. To test this hypothesis, PC12 cells were co-transfected with two kinds of plasmids, mature BDNF/DsRed and HAP1-A/EGFP. Four hours after transfection the culture medium was changed to fresh medium which contained 100ng/ml sheep anti-mature BDNF antibody to absorb the secreted mature BDNF. The live cell images showed that there was very low colocalization rate (12%) between HAP1-A (green) and mature BDNF (red) (Fig. 4-1 A and B: 1) in the presence of neutralizing antibodies against mature BDNF. To further demonstrate the colocalization was due to the receptor-mediated internalization of mature BDNF, we transfected PC12 cells with only HAP1-A/EGFP plasmid and then added the culture medium containing recombinant DsRed labeled mature BDNF (Fig. 4-1 A and B: 2), or containing recombinant DsRed labeled mature BDNF plus 100 times unlabeled mature BDNF (Fig 4-1 A and B:3), or containing recombinant DsRed

labeled mature BDNF with antibodies against extracellular domain of p75NTR (Fig. 4-1 A and B:4). The medium only containing exogenous DsRed labeled mature BDNF (Fig.4-1 A and B:2) resulted in 91.8% colocalizations, but the medium containing unlabeled mature BDNF (Fig.4-1 A and B:3) or p75NTR antibody (Fig.4-1 A and B:4) showed very low percentage of colocalization (9% and 10%). These results strongly suggested that the colocalization of HAP1-A with mature BDNF was caused by internalization and retrograde transportation of the exogenous mature BDNF, which could be blocked by competing with mature BDNF or by blocking p75NTR, the only BDNF receptor in PC12 cells. Altogether, these findings illustrated HAP1 was colocalized with proBDNF and the prodomain, but not mature BDNF, after *de novo* synthesis. However, the internalized mature BDNF was colocalized with HAP1 by a receptor mediated mechanism and indirectly interacted with HAP1 (Fig. 1B). The results on colocalization of HAP1B with the internalized mature BDNF were similar to those of HAP1-A (Fig. 4-2).

A

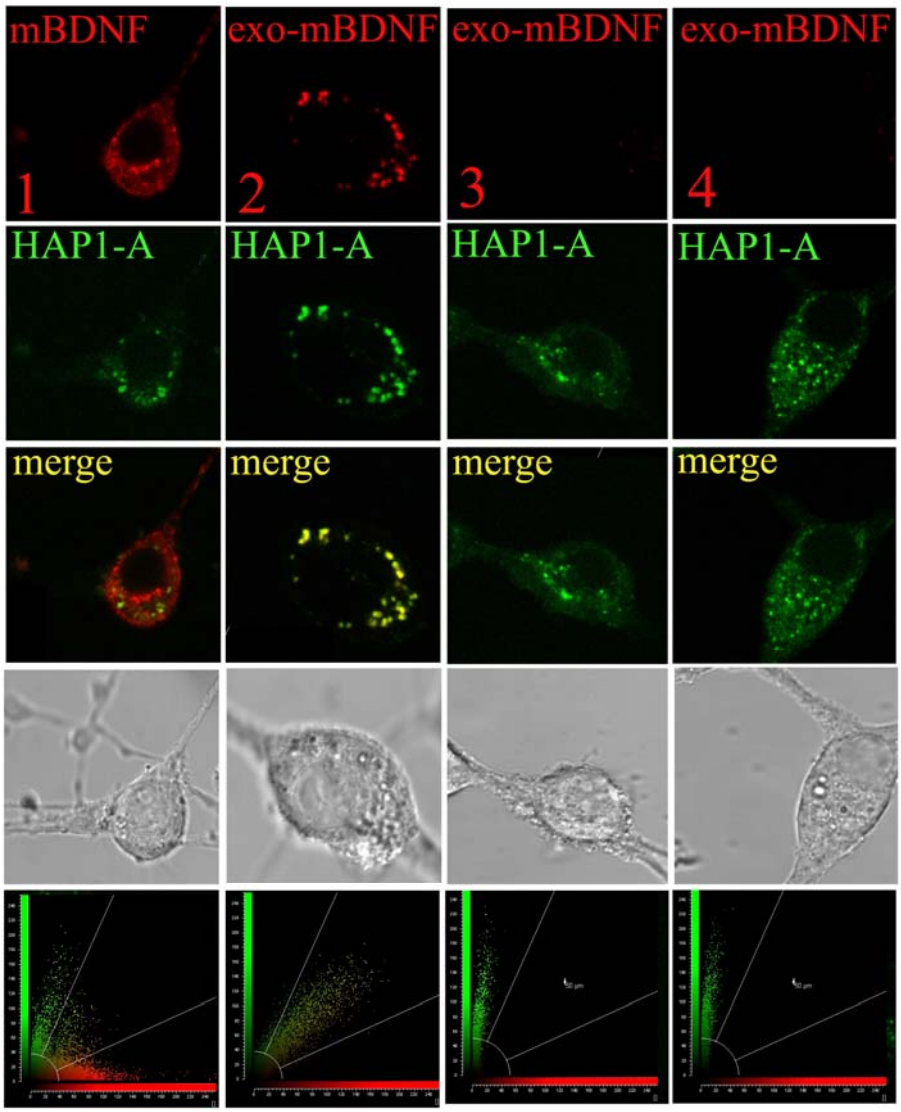
mBDNF
exo-mBDNF
exo-mBDNF
exo-mBDNF
1
2
3
4
HAP1-A
HAP1-A
HAP1-A
HAP1-A
merge
merge
merge
merge

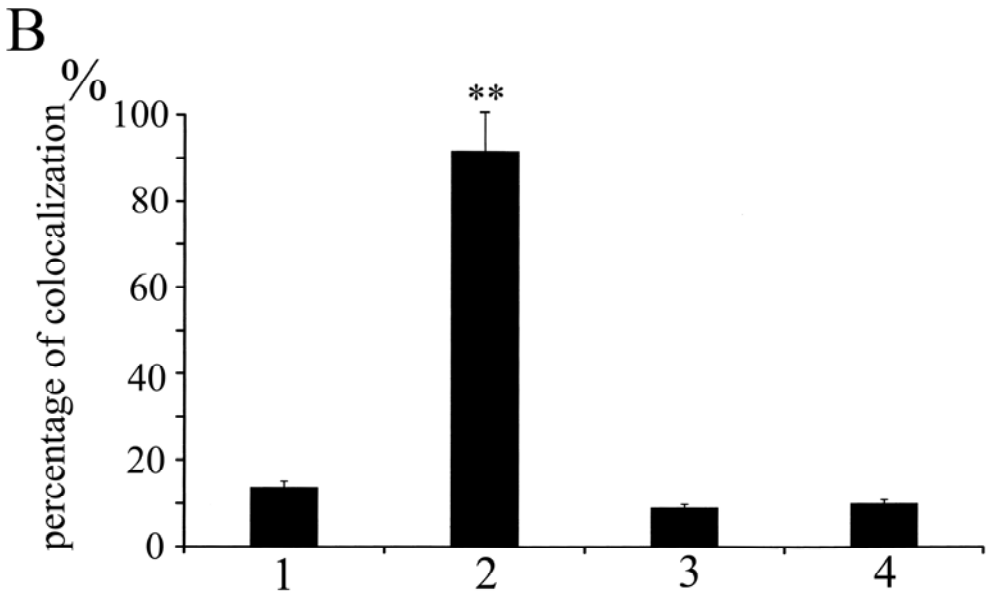
B
%
percentage of colocalization
100
80
60
40
20
0
**
1
2
3
4

Fig. 4-1 HAP-1 is colocalized with internalized mature BDNF but not with *de novo* synthesized mature BDNF (A) PC12 cells were co-transfected with plasmids of mature BDNF-Ds-Red and HAP1-A/EGFP. Immediately after transfection, the cells were cultured in the presence of sheep anti-mature BDNF to neutralize the secreted BDNF **(1)**. Very low colocalization of mature BDNF-Ds-Red and HAP1-A/EGFP was observed. **(2), (3),** and **(4)** show that PC12 cells were transfected only with HAP1-A/EGFP plasmid. Two days later, cells were incubated with either recombinant Ds-Red-labeled mature BDNF only **(2),** or recombinant Ds-Red-labeled mature BDNF with sheep anti-BDNF antibodies **(3),** or recombinant Ds-Red-labeled mature BDNF with p75NTR antibody which is against the extracellular domain of p75NTR **(4).** The high colocalization of HAP1-A/EGFP with internalized Ds-Red tagged mature BDNF was observed **(2)**. The antibodies to mature BDNF and p75NTR extracellular domain abolished internalization of Ds-red tagged exogenous mature BDNF **(3)** and **(4)**. **(B)** The percentages of colocalization were calculated from data acquired from 20 HAP1 transfected neurons. The cotransfected mature BDNF and HAP1-A/EGFP PC12 cell cultured with the medium containing mature BDNF antibody **(1)** have 12% colocalization. HAP1-A/EGFP transfected PC12 cells cultured with exogenous Ds-Red labeled mature BDNF shows 91.8% colocalization **(2)**, and culture with exogenous Ds-Red plus anti mature BDNF antibody **(3)** or anti p75NTR antibody **(4)** show 9% or 10% colocalization respectively. The data are presented as mean ±SEM. The statistical analyses revealed significant differences between the 4 groups (n=20, **p<0.01).

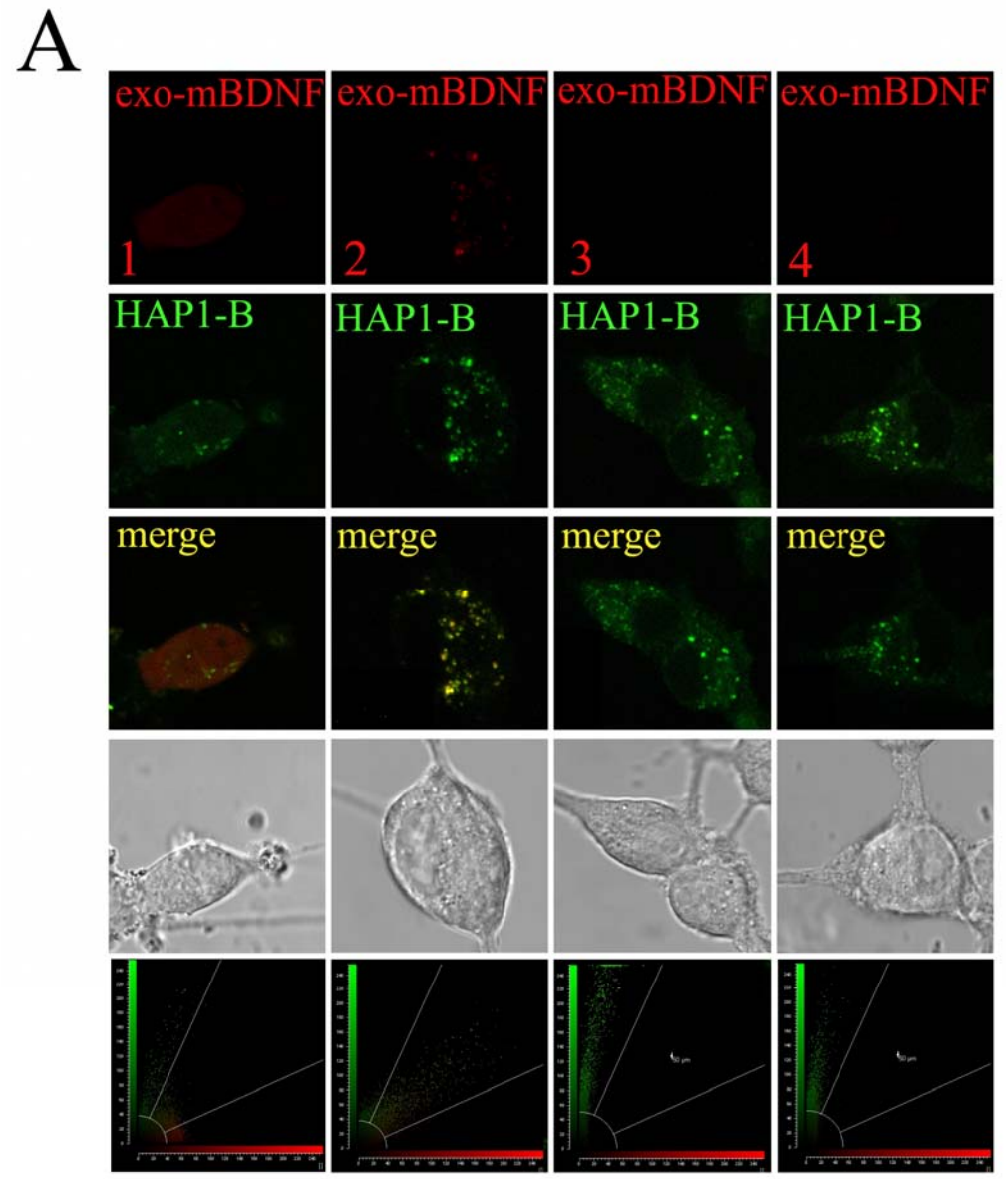
A
exo-mBDNF
exo-mBDNF
exo-mBDNF
exo-mBDNF
1
2
3
4
HAP1-B
HAP1-B
HAP1-B
HAP1-B
merge
merge
merge
merge

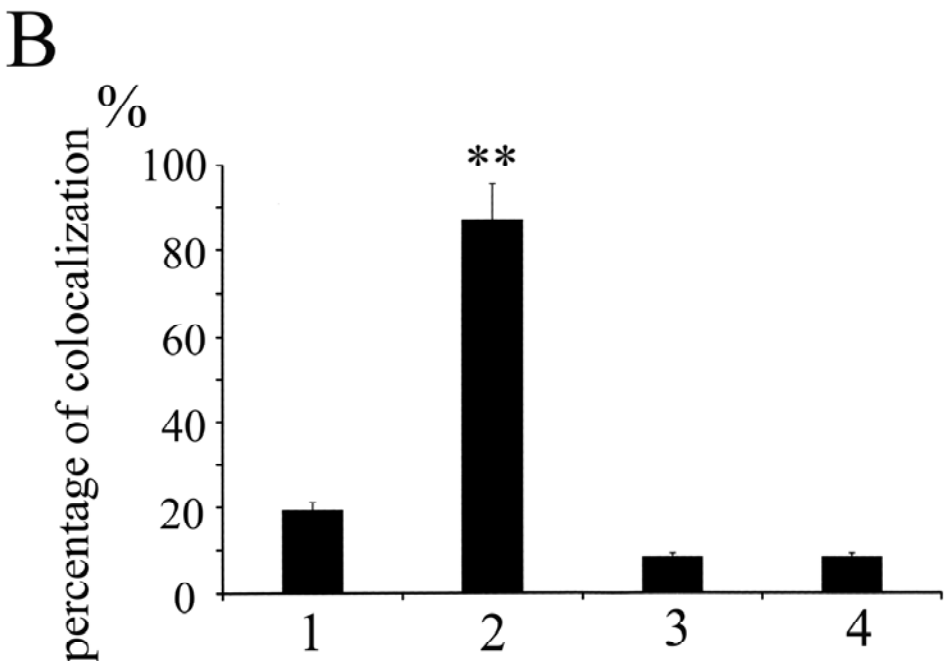
B
%
percentage of colocalization
100
80
60
40
20
0
**
1
2
3
4

Fig. 4-2 HAP1-B is colocalized with internalized mature BDNF but not with de novo synthesized mature BDNF (A) PC12 cells were co-transfected with plasmids of mature BDNF-Ds-Red and HAP1-B/EGFP. Immediately after transfection, the cells were cultured in the presence of sheep anti-mature BDNF to neutralize the secreted BDNF **(1)**. Very low colocalization of mature BDNF-Ds-Red and HAP1-B/EGFP was observed. Figure **(2), (3),** and **(4)** show that PC12 cells were transfected only with HAP1-B/EGFP plasmid. Two days later, cells were incubated with either recombinant Ds-Red-labeled mature BDNF only **(2),** or recombinant Ds-Red-labeled mature BDNF with sheep anti-BDNF antibodies **(3),** or recombinant Ds-Red-labeled mature BDNF with p75NTR antibody which is against the extracellular domain of p75NTR **(4).** The high colocalization of HAP1-B/EGFP with internalized Ds-Red tagged mature BDNF was observed **(2)**. The antibodies to mature BDNF and p75NTR extracellular domain abolished internalization of Ds-red tagged exogenous mature BDNF **(3)** and **(4)**. **(B)** The percentages of colocalization were calculated from data acquired from 20 HAP1 transfected neurons. The cotransfected mature BDNF and HAP1-B/EGFP PC12 cell cultured with the medium containing mature BDNF antibody **(1)** had 19% colocalization. HAP1-B/EGFP transfected PC12 cells cultured with exogenous Ds-Red labeled mature BDNF showed 87% colocalization **(2)**, and the culture with exogenous Ds-Red plus anti mature BDNF antibody **(3)** or anti p75NTR

antibody **(4)** showed 8% or 8% colocalization, respectively. The data are presented as mean ±SEM. The statistical analyses revealed significant differences between the 4 groups (n=20, **p<0.01).

HAP1 deletion blocked mature BDNF internalization

As the results showed that HAP1 colocalized with internalized mature but not *de novo* synthesized mature BDNF, the next question was whether internalization and retrograde transport of mature BDNF would be blocked after HAP1 deletion. To test the hypothesis, we added the conditioned medium from PC12 cells transfected with Ds-Red-BDNF plasmid, containing secreted Ds-Red labeled mature BDNF into the primary cortical neurons from P1 wild type and $HAP1^{-/-}$ mice. 30 minutes later, the cells were fixed and images taken. The red fluorescence labeled mature BDNF was observed in almost all wild type cortical neurons in 4 duplicate culture wells, but no red fluorescence particles were seen in $HAP^{-/-}$ cortical neurons (Fig. 5). No red fluorescence was seen in wt cortical neurons after the medium was replaced with conditioned medium of PC12 cells transfected with Ds-Red blank plasmid (data not shown). This suggests that HAP1 deletion blocked mature BDNF internalization and retrograde transport.

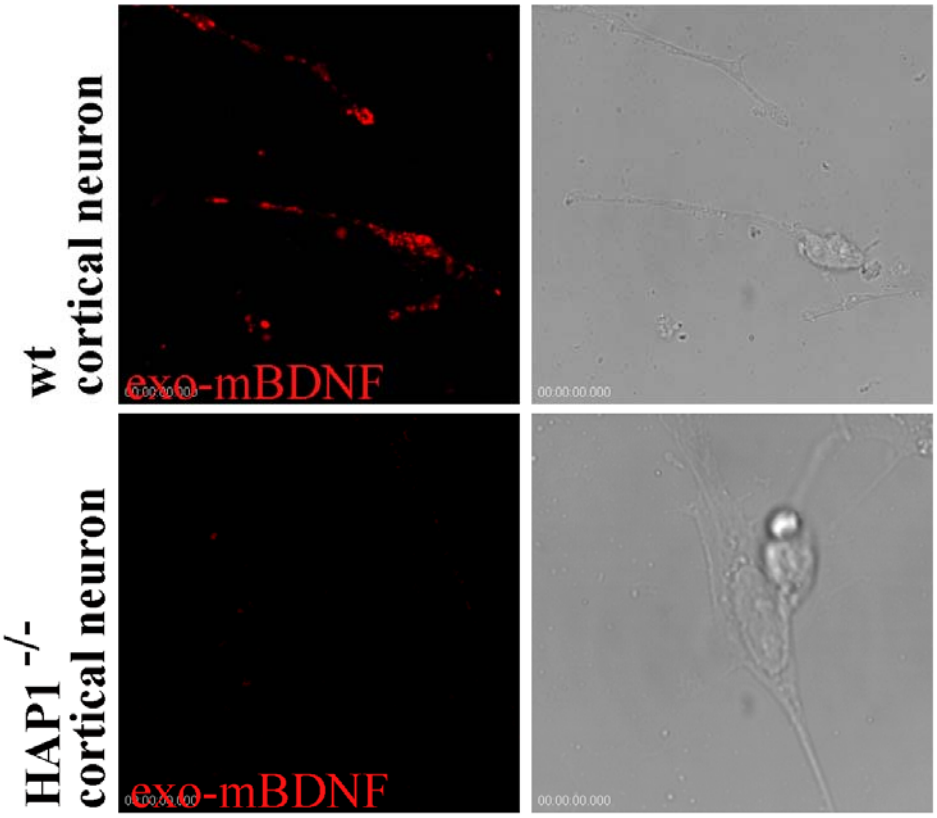

Fig. 5 Mature BDNF internalization in primary cortical neurons from wild type and HAP1$^{-/-}$ mice. The experiments were performed on primary cultured wild type and HAP1$^{-/-}$ cortical neurons from P1 mice. Two days after neurons were cultured, the culture medium was replaced with the medium containing Ds-Red labeled mature BDNF (Ds-Red-mBDNF transfected PC12 cell condition medium). 30 minutes latter, the cells were fixed in 4% paraformaldehyde and images were taken.

Anterograde and retrograde transport of endogenous proBDNF in wild type and HAP1$^{-/-}$ sciatic nerve

Sciatic nerve crush in wild type P1 mice resulted in the accumulation of proBDNF immunoreactivity (IR) on both the proximal and distal sides of the crush site (Fig. 6A). In contrast, no proBDNF IR accumulated on either side of the crushed sciatic nerve in HAP1$^{-/-}$ mice (Fig. 6B). The particle area represents the proBDNF-IR staining. On the proximal side of crushed sciatic nerve from wild type mice, the staining area was 31715 ± 3125 pixel^2. In contrast, the same proximal side of crushed sciatic nerve from the HAP1$^{-/-}$ mice was 2752 ± 133 pixel^2. The stain area from the distal side of the crush from wt mice was 14282 ± 1635 pixel^2 and for the HAP1$^{-/-}$ mice sciatic nerve was 288 ± 52 pixel^2 (Fig. 6C). No immunoreactivity was detected in control sections incubated with normal rabbit IgG or antibody pre-absorbed with immunized peptide or in the absence of antibodies. Similarly, there was a significant accumulation of proBDNF in the stumps of sectioned spinal cord of wt mice but the accumulation of proBDNF was abolished in HAP1$^{-/-}$ mice (Fig. 6 D-G). Interestingly, based on the morphology, proBDNF-ir is likely detected in glial cells (astrocytes) in both HAP1$^{-/-}$ and wild type mice (Fig. 6F and G). These results suggest that HAP1 is essential for the anterograde and retrograde transport of BDNF.

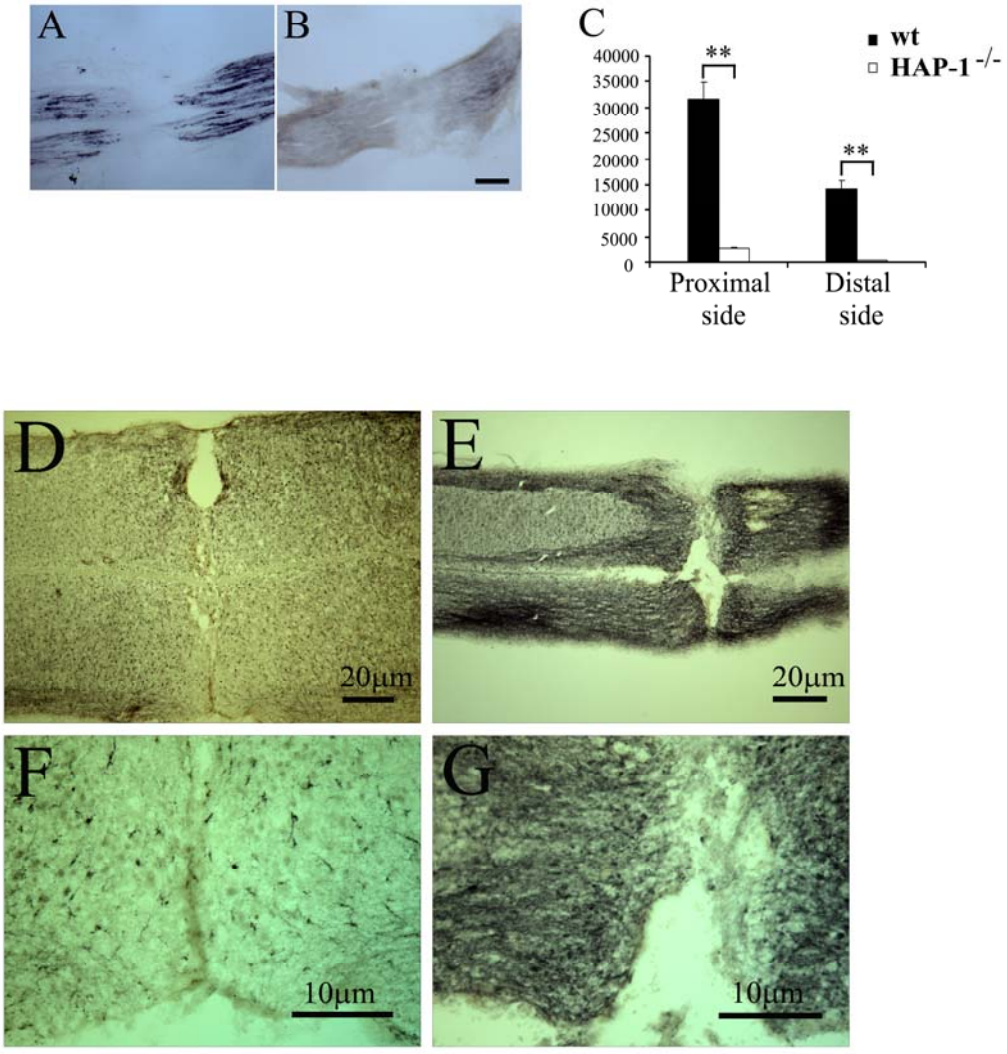
A
B
C
wt
HAP-1 -/-
40000
35000
30000
25000
20000
15000
10000
5000
0
**
**
Proximal side
Distal side
D
20μm
E
20μm
F
10μm
G
10μm

Fig. 6 Anterograde and retrograde transport of endogenous proBDNF in wild type and HAP1$^{-/-}$ sciatic nerve and spinal cord. ProBDNF immunohistochemistry of crushed sciatic nerve from P1 neonatal wt and HAP1$^{-/-}$ mice. **(A)** The proximal and distal side of sciatic nerve from a P1 neonatal wt mouse 6 hours after crush. **(B)** The P1 proximal and distal side of sciatic nerve from a neonatal HAP-1$^{-/-}$ mouse 6 hours after crush. **(C)** The graph shows the relative staining intensity of P1 neonatal wt (black bar) and HAP1$^{-/-}$ (white bar) mice proximal and distal side of sciatic nerve (The area of particles which stands for the relative staining intensity was quantified by the NIH ImageJ program. The data are presented as mean ±SEM. n=3, **p<0.01, Student's t test, scale bar=15μm). (**D**) and (**E**), 6 hours after transection of the spinal cord from HAP1-/- and wild type mice respectively. ProBDNF was detected in the axons and transected stumps in wild type mice but not in HAP1-/- mice. **F** and **G** are high magnification of **D** and **F** respectively.

Mutant huntingtin in PC12 cell lysate decreases the efficiency of the interaction of HAP1 with proBDNF, prodomain BDNF, mature BDNF

Accumulating evidence has shown that mutant Htt affects the transcription and axonal transport of BDNF (Li et al. 1995, Gauthier et al. 2004, Li & Li 2005, Zuccato et al. 2001), but the mechanisms of how mutant Htt impairs the transcription and transport of BDNF is not known. We hypothesize that mutant Htt impairs the axonal transport of BDNF by interfering with the interaction between HAP1 and the prodomain of BDNF, as it is known that mutant Htt has higher affinity binding to HAP1 than wild-type Htt (Block-Galarza *et al.* 1997, Engelender et al. 1997, Gauthier et al. 2004). To test this hypothesis, we conducted the GST-pull down assay in the presence of wild type or mutant huntingtin. PC12 neuronal cell lines overexpressing two copies of wild-type Htt (PolyQ25) or two copies of mutant Htt (PolyQ103) (gift from Schweitzer ES, Departments of Physiological Science and Neurology, Brain Research Institute, University of California, Los Angeles, USA) were homogenized. Equal amounts of total proteins in each cell lysate were incubated with HAP1-GST and proBDNF, prodomain BDNF, or mature BDNF. The pull-down of proBDNF and prodomain BDNF in the presence of PolyQ103 PC12 cell lysates was significantly decreased compared with the samples in the presence of wt Htt (PolyQ 25) cell lysate (Fig. 7A). Quantitative analysis showed the

pull down of proteins in the presence of mutant Htt was 32.5% for proBDNF and 46% for prodomain BDNF of the samples in the presence of wt Htt (Fig. 7B).

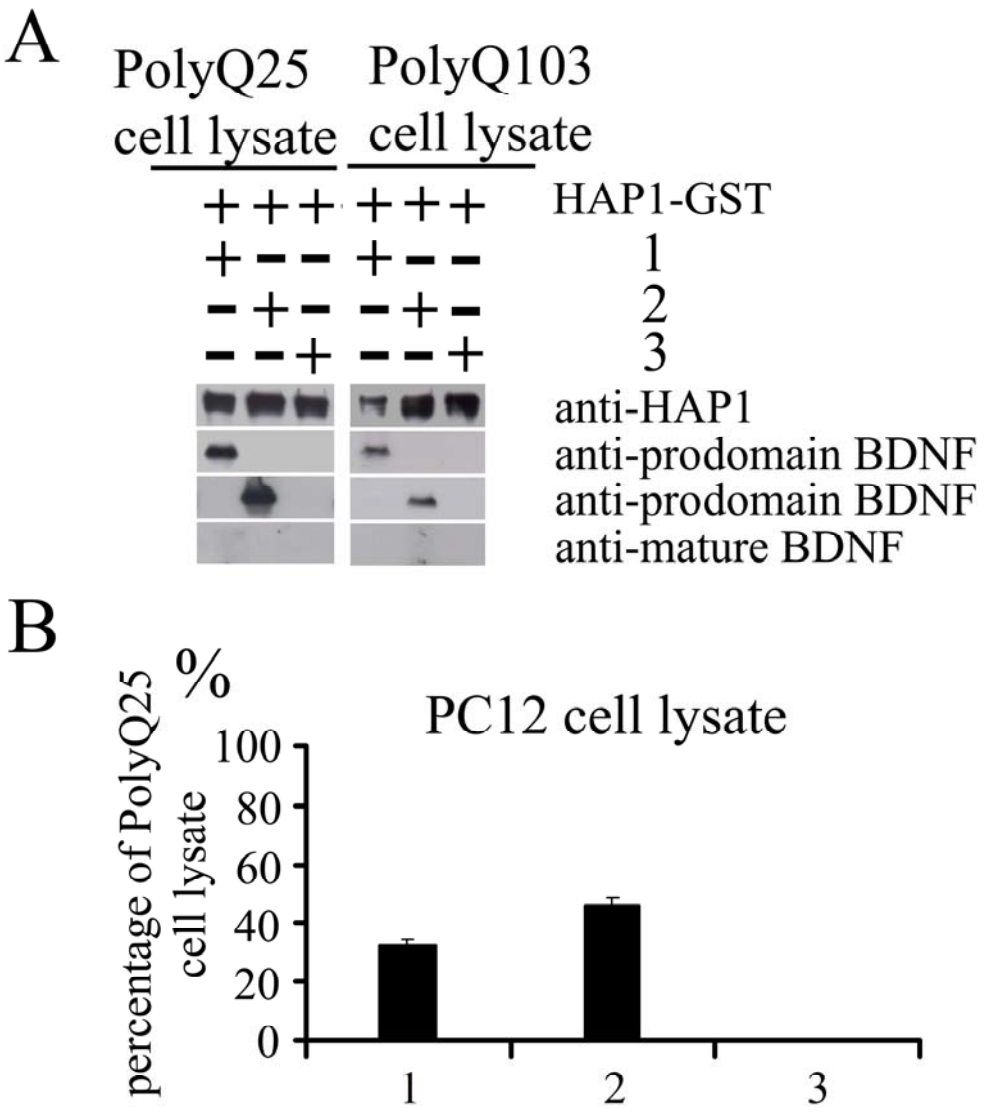
A
PolyQ25 cell lysate
PolyQ103 cell lysate
+ + + + + +
+ - - + - -
- + - - + -
- - + - - +
HAP1-GST
1
2
3
anti-HAP1
anti-prodomain BDNF
anti-prodomain BDNF
anti-mature BDNF
B
PC12 cell lysate
% percentage of PolyQ25 cell lysate
100
80
60
40
20
0
1
2
3

Fig. 7 Mutant Htt in PC12 cell lysate decreases the efficiency of the interaction of HAP1 with proBDNF, the prodomain, and mature BDNF. HAP1 GST fusion protein was immobilized on glutathione-agarose beads and incubated with proBDNF (**1**) the prodomain BDNF (**2**) and mature BDNF (**3**) in the presence of polyQ25 or polyQ103 Htt transfected PC12 cells lysate. Binding proteins were detected by immunoblotting. **(A)** The quantity of proteins in the presence of polyQ25 PC12 cell lysate and in the presence of polyQ103 PC12 cell lysate is shown in the blot. **(B)** The percentages of proteins in the presence of polyQ103 PC12 cell lysate were calculated using the quantity of proteins in the presence of polyQ25 PC12 cell lysate as 100% (The area of pixels which stands for the relative staining intensity was quantified by the NIH ImageJ program. The data are presented as mean ±SEM, from 3 separate experiments, n=3).

.

HD brain lysate decreases the efficiency of the interaction of HAP1 with proBDNF and prodomain BDNF

To further understand the mechanisms by which polyQ Htt causes the abnormality of BDNF transcription and axonal transport, we examined the interaction of HAP1 and proBDNF or HAP1 and prodomain BDNF in the presence of cell lysates of normal human brain or Huntington disease human brain by the pull down experiments. The result showed that the pull-down of proBDNF and the prodomain in the presence of HD human brain cell lysates was significantly decreased compared with the normal human brain cell lysates (Fig. 8A). The quantitative data showed the pull down proBDNF in the presence of HD brain lysate was decreased to 23.6% and the prodomain to 28.7% of normal brain lysates. No mature BDNF was detected (Fig. 8B). This finding is in agreement with the transfected PC12 cell lysates but the quantity of proteins from the brain lysates added in the incubation mixture was lower than the proteins from the cell line.

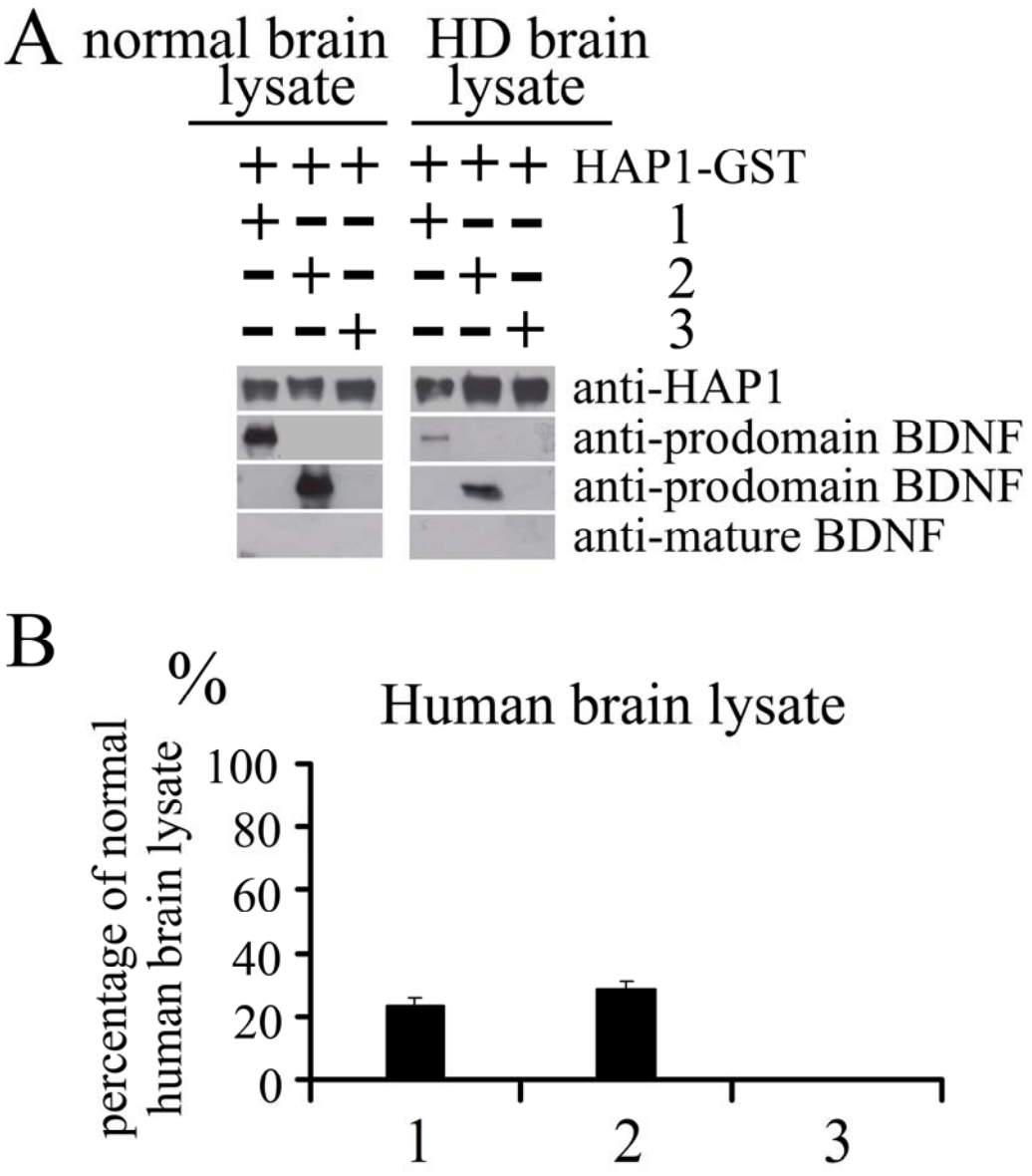
A
normal brain lysate
HD brain lysate
+ + + + + + HAP1-GST
+ − − + − − 1
− + − − + − 2
− − + − − + 3
anti-HAP1
anti-prodomain BDNF
anti-prodomain BDNF
anti-mature BDNF
B
%
Human brain lysate
percentage of normal human brain lysate
100
80
60
40
20
0
1
2
3

Fig. 8 Mutant huntingtin in HD brain lysate decreases the efficiency of the interaction of HAP1 with proBDNF, pro domain BDNF, mature BDNF. HAP1 GST fusion protein was immobilized on glutathione-agarose beads and incubated with proBDNF **(1)**, prodomain BDNF **(3)** and mature BDNF **(3)** in the presence of normal or Huntington disease human brain lysate. Binding proteins were detected by immunoblotting. (**A)** The quantity of proteins in the presence of normal brain lysate and HD brain lysate is shown in the blot. (B) The percentages of proteins in the presence of HD brain lysate were calculated using the quantity of proteins in the presence of normal brain lysate as 100% (The area of pixels which stands for the relative staining intensity was quantified by the NIH ImageJ program. The data are presented as mean ±SEM, from 3 separate experiments, n=3).

.

HAP1/proBDNF complex is altered in HD

To see whether the HAP1 and proBDNF complex is present in the human brain and whether the complex is altered in the brain of Huntington disease, HAP1 immunoprecipitation was performed using the lysates of normal and HD brain. As shown in Fig. 9, there are several species of proBDNF detected in the HAP1 immunoprecipitated sample at MW of 32 and 64 Kd of normal human brain. The bands disappeared when the membrane was probed with the antibodies pre-absorbed with the immunizing peptide (Fig. 9A). The amount of proBDNF in the complex immunoprecipitated from the HD brain was significantly reduced. Quantification result showed that amount of proBDNF immunoprecipitated from HD brain was 66.9% (32 kDa band) and 51.7% (64 kDa band) of the normal brain, probed with rabbit anti prodomain BDNF, and was 59.3% (32 kDa) and 51.6% (64 kDa) of normal brain, probed with monoclonal anti mature BDNF antibody. As sortilin is known to interact with prodomain BDNF (Chen et al. 2005, Teng et al. 2005), we also probed the complex with sortilin antibodies. The results showed that sortilin-like immunoreactivity was present in HAP-1 immunoprecipitated samples and the amount in the HD brain was reduced to 73.1% of normal brain (Fig. 9B). For positive controls, we also loaded the prodomain and mature BDNF respectively. As shown in Fig. 9A, the antibody to the prodomain does not

recognize mature BDNF, and the mature BDNF antibody does not recognize the prodomain but both antibodies recognize the endogenous full-length proBDNF. Interestingly, the recombinant prodomain formed dimers and oligomers as seen in lane 1. To further confirm this we made the fresh recombinant prodomain and incubated the prodomain at 4^{o}C for 1 week. The SDS gel showed that the fresh purified prodomain was a single band with 95% purity but Western blot analysis showed that the purified prodomain monomer forms dimers and oligomers with time at 4^{o}C in water (Fig. 9 C and D). Based on these data we concluded that several bands detected in lane 1 probed with proBDNF antibody are dimers and oligomers of the recombinant prodomain. It is possible that these oligomers are also present *in vivo* in the human brain, as we detected minor bands with higher molecular weight in lane 3 and 4 and these bands disappeared when the antibody was pre-incubated with excessive amount of the immunizing peptide, suggesting these bands are likely specific prodomain oligomers. The significance of the prodomain oligomers *in vivo* requires further investigation.

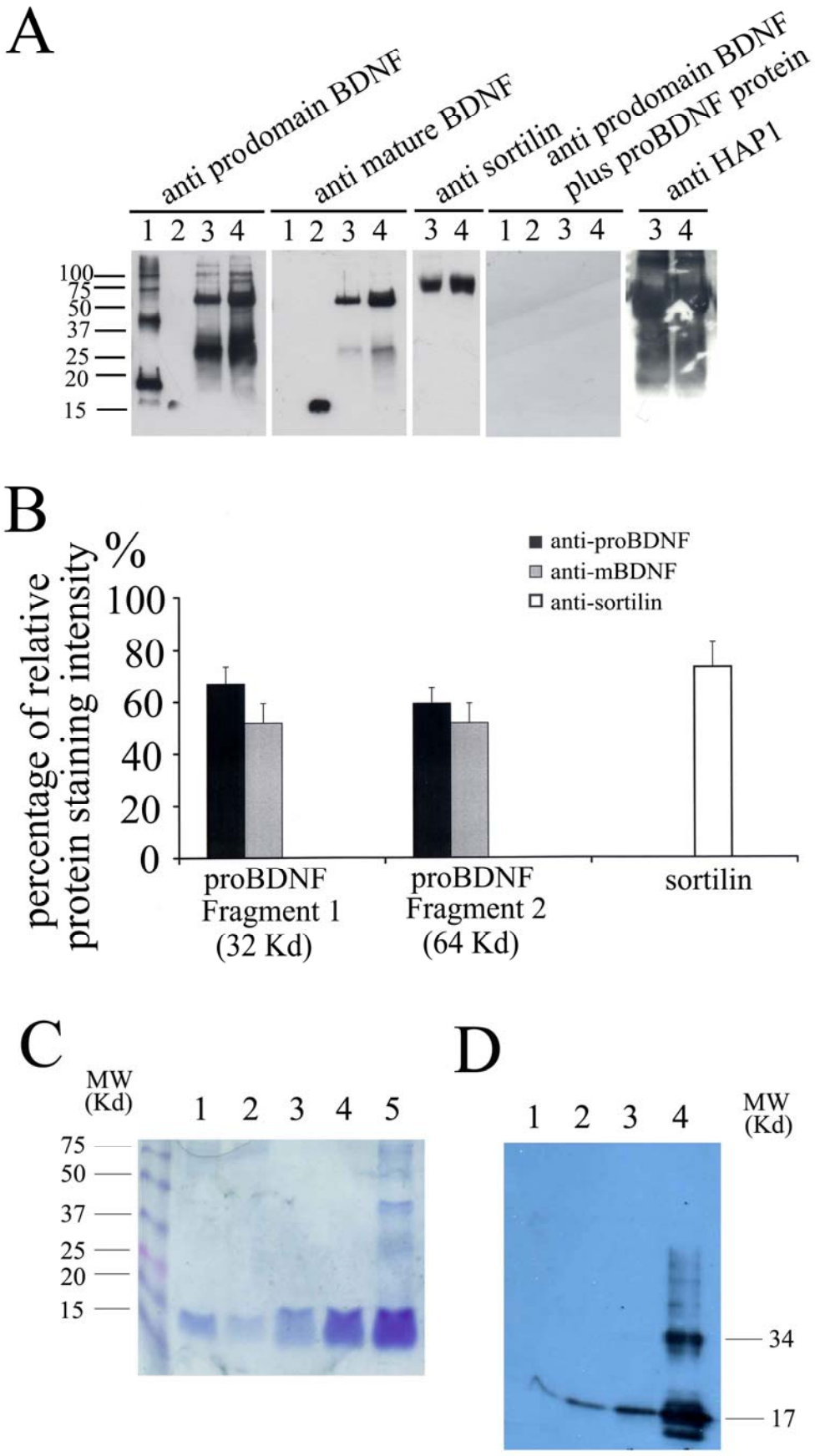
A
anti prodomain BDNF
anti mature BDNF
anti sortilin
anti prodomain BDNF plus proBDNF protein
anti HAP1
1 2 3 4 1 2 3 4 3 4 1 2 3 4 3 4
100
75
50
37
25
20
15
B
percentage of relative protein staining intensity %
100
80
60
40
20
0
anti-proBDNF
anti-mBDNF
anti-sortilin
proBDNF Fragment 1 (32 Kd)
proBDNF Fragment 2 (64 Kd)
sortilin
C
MW (Kd)
1 2 3 4 5
75
50
37
25
20
15
D
1 2 3 4
MW (Kd)
34
17

Fig. 9 HAP1/proBDNF complex is altered in HD. (A) Rabbit anti-HAP1 antibody was immobilized on Protein A beads and incubated with normal human brain lysate and HD brain lysate. The membrane was detected with anti proBDNF antibody, anti mature BDNF antibody, anti sortilin antibody and anti proBDNF antibody plus the immunizing peptide, respectively. Lane 1 proBDNF input; Lane 2 mature BDNF input; Lane 3: HAP1 immunoprecipitation from HD human brain; Lane 4: HAP1 immunoprecipitation from normal human brain. **(B)** Percentages of relative protein staining intensity of HD human brain lysate compared with normal human brain lysate (The area of pixels which stands for the relative staining intensity was quantified by the NIH ImageJ program. The data are presented as means ± SEM of three separate experiments, n=3). **(C)** Expression and purification of prodomain of BDNF from E coli. SDS gel stained with Coomasie blue showing the purity of the recombinant protein. Lanes 1, 2, 3 and 4 are proteins purified immediately from four different clones and Lane 5 is the protein from clone 4 left in $4^{o}C$ for 7 days after purification which shows the dimers and oligomers of the prodomain. **(D)** Western blot of purified proteins from clone 4: Lanes 1, 2, and 3 are different eluted fractions immediately from the column and lane 4 is the sample left in $4^{o}C$ for 1 week. The membrane was probed by antibodies to the prodomain of BDNF.

HAP1 plays a critical role in activity-dependent secretion of prodomain BDNF

BDNF is produced by cortical neurons and transported from the cortex to the striatum to support the survival of striatal neurons (Altar et al. 1997, Baquet *et al.* 2004, Saudou *et al.* 1998, Gauthier et al. 2004). To assess whether HAP1 affects regulated and constitutive secretory pathways, we performed two series of experiments on the constitutive and regulated secretion in primary cultured $HAP1^{-/-}$ and wild type mice cortical neurons (Fig. 10A) and in primary cultured cortical neurons transfected with the prodomain plasmid (Fig. 10B). The secreted prodomain was then detected by ELISA. In the case of non-transfected $HAP1^{-/-}$ and wild type mice cortical neurons, a similar quantity of the prodomain was secreted in a constitutive manner (0.32ng/ml/hour from $HAP1^{-/-}$ and 0.35ng/ml/hour from wt). In contrast, in high potassium stimulated samples, there was a significant difference between $HAP1^{-/-}$ and wild type mice cortical neurons (1.4ng/ml/hour from $HAP1^{-/-}$ vs 3.82ng/ml/hour from wt). A similar result was obtained from cortical neurons transfected with the prodomain plasmid. Equal but increased amounts of the prodomain (0.77ng/ml/hour from $HAP1^{-/-}$ and 0.80ng/ml/hour from wt) were secreted from cortical neurons of $HAP1^{-/-}$ and wt mice under basal release conditions. In contrast, the release of the prodomain of BDNF from $HAP1^{-/-}$ mice was

significantly impaired compared to the wt mice after stimulation with high potassium (8.52ng/ml/hour from HAP1$^{-/-}$ vs 2.08ng/ml/hour from wt). These results suggest that HAP1 is required for the activity dependent secretion of prodomain BDNF.

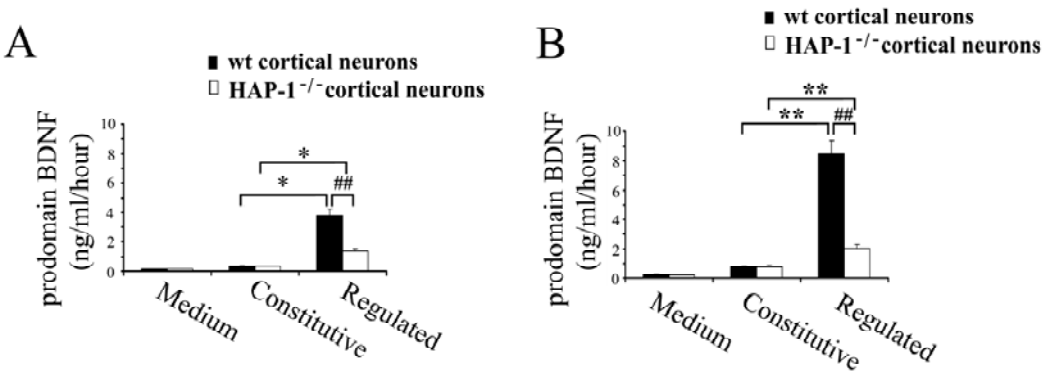
A
wt cortical neurons
HAP-1 -/- cortical neurons
prodomain BDNF (ng/ml/hour)
Medium
Constitutive
Regulated
B
wt cortical neurons
HAP-1 -/- cortical neurons
prodomain BDNF (ng/ml/hour)
Medium
Constitutive
Regulated

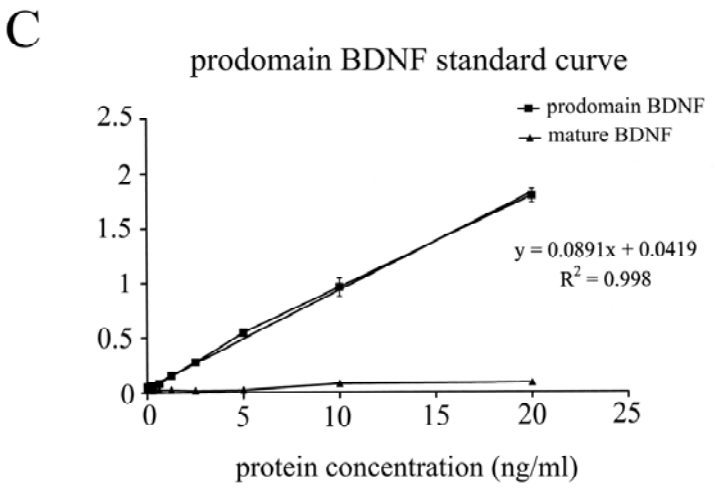
C
prodomain BDNF standard curve
prodomain BDNF
mature BDNF
y = 0.0891x + 0.0419
R2 = 0.998
protein concentration (ng/ml)

Fig. 10 HAP1 plays a critical role in the activity-dependent secretion of the prodomain. (A) The experiment was performed on naïve cortical neurons**.** Neurons were conducted under constitutive secretion and depolarization secretion conditions. All collected media were subjected to quantification of the prodomain with an ELISA assay developed in our laboratory. **(B)** The experiment was performed on neurons transfected with the prodomain plasmid**.** After 48 h, neurons were treated with constitutive secretion and depolarization secretion conditions. All collected media were subjected to quantification of the prodomain with an ELISA assay developed in our laboratory. All results are presented as a mean ± SEM determined from analysis of six independent experiments (*$p<0.05$; **$p<0.01$, $^{\#\#}p<0.01$, n=6, Student's t-test). **(C)** The prodomain BDNF ELISA standard curve was performed using prodomain BDNF and mature BDNF recombinant protein. The standard protein concentration was started from 10ng/ml and included 1:2 dilution serial to 0.0195ng/ml (n=3).

Effects of the V66M mutation on the interaction between HAP1 and BDNF prodomain.

20-30% of humans have an allele of the V66M mutation in the prodomain of the BDNF gene (Shimizu et al. 2004). The mutation is known to cause the retardation of axonal BDNF transport and activity-dependent release, leading to a reduction in the volume of the hippocampus and development of various mental disorders (Bath & Lee 2006, Hashimoto 2007, Chen et al. 2005). The mechanism underlying the retardation of BDNF transport is not known. Here we examined whether the V66M mutation affects the interaction between HAP1 and the prodomain. As shown in Fig. 11A and B, compared to the wt prodomain, the amount of V66M prodomain pulled down by HAP1 was significantly reduced (84% vs 60%). The reduction in the interaction between HAP1 and V66M prodomain was further reduced by incubation in the presence of polyQ Htt in PC12 cell lysates (46% vs 19%) or in HD brain lysates (28.7% vs 13%). These results indicate that the V66M mutation in the BDNF prodomain can reduce the interaction with HAP1, which may cause the retardation of BDNF transport and release. To test the idea, we cotransfected HAP1 with V66M prodomain to see whether there is less colocalization between HAP1 and the mutated prodomain. Our data illustrate that the level of colocalization of HAP1 and V66M prodomain (HAP1-A: 82%, HAP1-B:

86.1%) was not significantly different from that between HAP1 and the wt prodomain (HAP1-A: 76.8%, HAP1-B: 78.4%) (Fig. 11C, D, E and F).

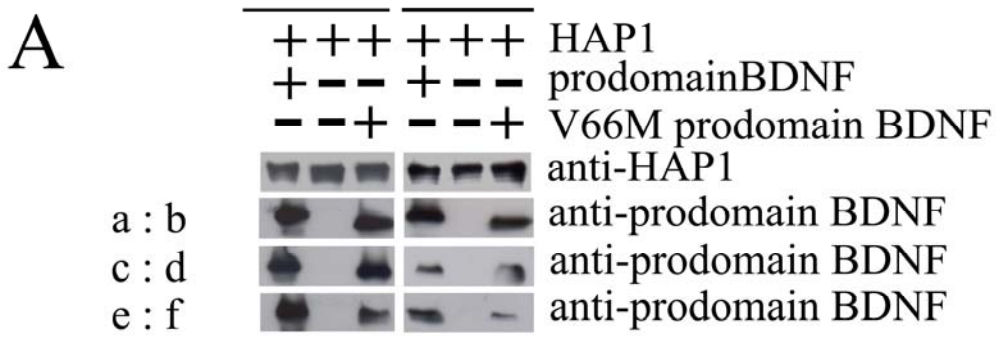
A
+++ +++ HAP1
+−− +−− prodomainBDNF
−−+ −−+ V66M prodomain BDNF
anti-HAP1
a : b
anti-prodomain BDNF
c : d
anti-prodomain BDNF
e : f
anti-prodomain BDNF

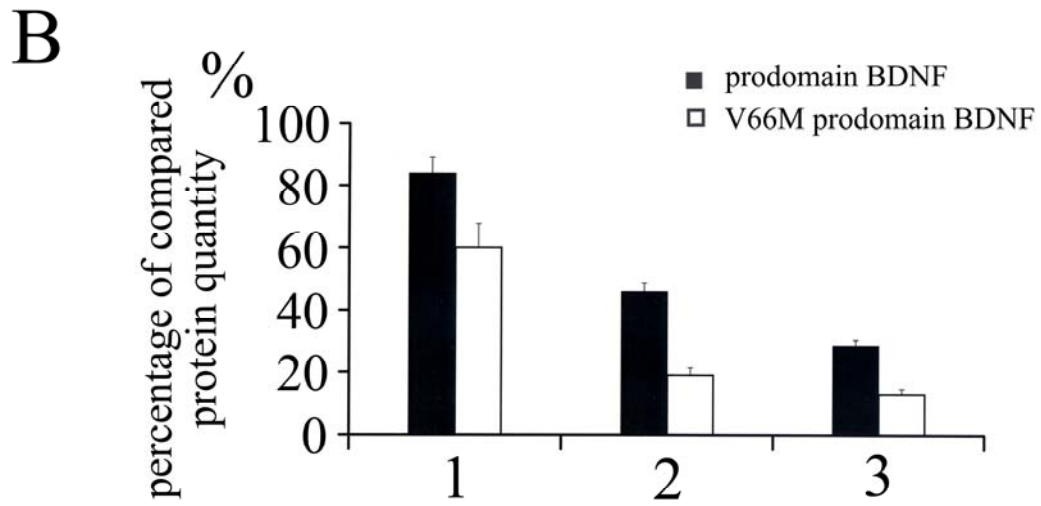
B
%
percentage of compared protein quantity
100
80
60
40
20
0
1
2
3
prodomain BDNF
V66M prodomain BDNF

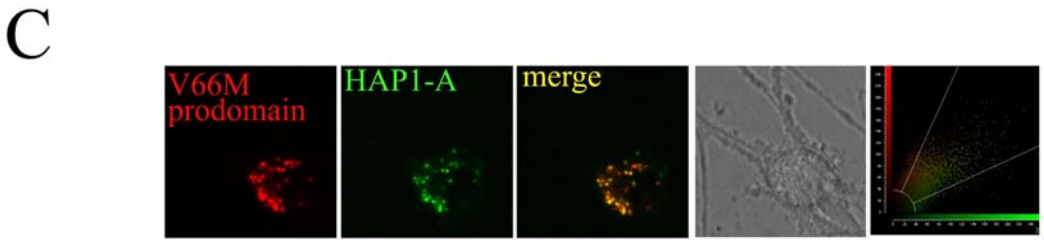
C
V66M prodomain
HAP1-A
merge

D

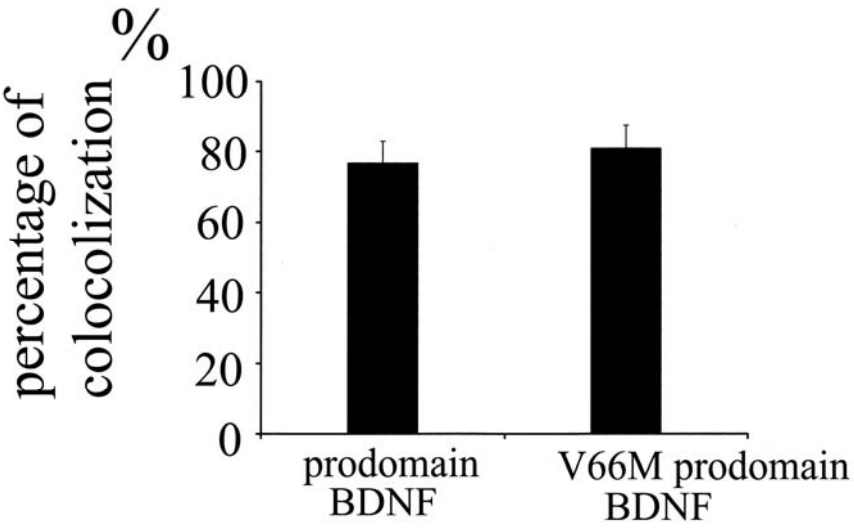
%
percentage of colocolization
100
80
60
40
20
0
prodomain BDNF
V66M prodomain BDNF

E

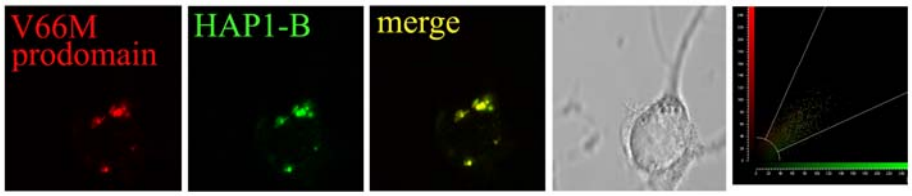
V66M prodomain
HAP1-B
merge

F

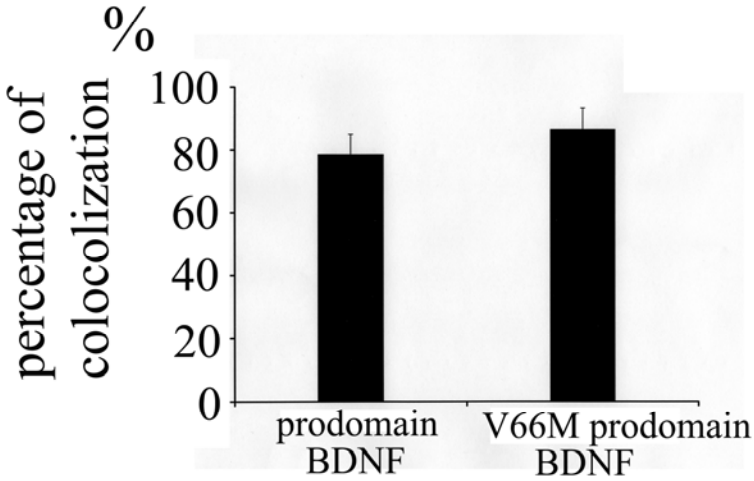
%
percentage of colocolization
100
80
60
40
20
0
prodomain BDNF
V66M prodomain BDNF

Fig. 11 Effect of the V66M mutation on the interaction between HAP1 and BDNF prodomain. **(A)** HAP1 GST fusion proteins were immobilized on glutathione-agarose beads and incubated with the wt prodomain and the V66M prodomain **(b)**, in the presence of polyQ25 **(c)** or polyQ103 Htt **(d)** transfected PC12 cell lysate, and in the presence of normal **(e)** or Huntington disease **(f)** human brain lysate. Input of prodomain BDNF and V66M prodomain are shown in **(a)**. The quantities of binding proteins were detected by immunoblotting. **(B)** The percentage of pull-down proteins are calculated using the input proteins as 100% as shown in (**1**) **(b:a)**. The percentages of proteins pulled down in the presence of polyQ103 PC12 cell lysate are calculated using the quantity of proteins pulled down in the presence of polyQ25 PC12 cell lysate as 100% as shown in **(2) (d:c)**. The percentages of proteins pulled down in the presence of HD brain lysate are calculated using the quantity of proteins pulled down in the presence of normal brain lysate as 100% as shown in **(3) (f:e)**. (The staining intensity of each band was quantified by the NIH ImageJ program and data are presented as means ± SEM of 3 separate experiments, n=3). **(C)** PC12 cells were transfected with HAP1-A/EGFP (green) and V66M prodomain BDNF-Ds-Red plasmids. Confocal images were taken and merged (yellow). Yellow dots are colocalized HAP1-A and the V66M prodomain. The snapshot represents the rate of colocalization quantitatively analysed by the software on the Lieca SP5 Confocal Microscope. **(D)** The V66M prodomain

was highly colocalized with HAP1-A, similar to the result of prodomain BDNF (Fig. 3-1 A and B: 2). The statistical analyses revealed no significant difference in HAP1 colocalization between the wt prodomain and the V66M prodomain. **(E)** PC12 cells were transfected with HAP1-B/EGFP (green) and V66M prodomain BDNF-Ds-Red plasmids. Confocal images were taken and merged (yellow). Yellow dots are colocalized HAP1-B and the V66M prodomain. The snapshot represents the rate of colocalization analysed by the quantitative analysis software on Lieca SP5 Confocal Microscope. **(F)** The V66M prodomain was highly colocalized with HAP1-B, similar to the result of the wild type prodomain (Fig. 3-2 A and B: 2). The statistical analyses revealed no significant difference in HAP1 colocalization between the wild type prodomain and the V66M prodomain.

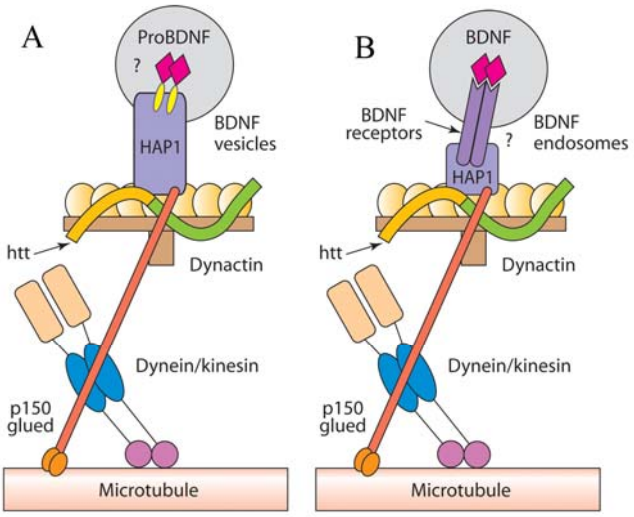

Fig. 12 Schematic diagrams depicting possible mechanisms by which proBDNF and mature BDNF are transported within neurons. A: Prodomain BDNF directly interacts with HAP1 which acts as a cargo-carrying molecule. HAP1 likely interacts with kinesin light chain, the component of the kinesin motor which carries and transports cargoes anterogradely towards the plus end of microtubules. Htt may affect the transport of BDNF by interacting with HAP1. **B**: Mature BDNF binds BDNF receptors and is internalized in endosomes. HAP1 acts as a BDNF-containing endosome-carrying molecule by interacting with BDNF receptors or the endosome components. The dynein motor accessary molecule, dynactin subunit p150glued, interacts with HAP1 and transports BDNF-containing endosomes retrogradely towards the minus ends of microtubules.

5. Discussion

BDNF is sorted into the regulated secretory pathway, anterogradely transported to presynaptic nerve terminals, released in an activity-dependent manner and plays a critical role in synaptic plasticity. In the present study we have uncovered the mechanism of how proBDNF is transported anterogradely and retrogradely along axons. The molecular motor accessory protein HAP1 directly interacts with the BDNF prodomain and indirectly with mature BDNF and plays an essential role in the anterograde and retrograde transport and activity-dependent release of proBDNF. We also found that mutant Htt interferes with the interaction between HAP1 and the prodomain and the V66M mutation reduces the binding of the prodomain to HAP1.

HAP1 directly binds to proBDNF and plays a critical role in anterograde transport and activity-dependent release.

Defects in BDNF transport and secretion may underlie a wide range of nervous system diseases, such as epilepsy, neurodegenerative diseases and neuropsychiatric diseases (Binder *et al.* 2001, Spires *et al.* 2004, Ferrer 1999, Howells *et al.* 2000, Zuccato et al. 2003, Gauthier et al. 2004). However, how BDNF-containing vesicles are transported is not known. Substantial evidence

suggests that the anterograde transport of BDNF is dependent on the prodomain sequence. The BDNF homologue nerve growth factor is normally released constitutively from dendrites of neurons (Gu *et al.* 2001, Hibbert *et al.* 2003, Mowla et al. 1999) but can be sorted into the regulated pathway and released in an activity-dependent manner when its prodomain is replaced with the BDNF prodomain (Chen et al. 2005). However, how the prodomain plays a role in this transport is not known. In the present study, we sought to elucidate the transport mechanism by identifying proteins interacting with the prodomain. The DIGE experiments and Western blot results demonstrated HAP1 interacts with both the prodomain and mature domain of BDNF. Further interaction studies using GST pull down assays with recombinant proteins showed that the BDNF prodomain directly interacts with a HAP1 fragment between aa 280-445. As the sequence of HAP1 is conserved for both HAP1-A and HAP1-B, it is highly expected that this domain may be the binding domain of the prodomain BDNF. However, prodomain BDNF binds less HAP1-A than HAP1-B *in vitro* (Fig. 1), might be caused by the rest of different region of HAP1-A and HAP1-B. HAP1 is an Htt-associated protein which interacts with both the dynactin subunit of p150Glued (Li et al. 1998b), which is the accessory protein of dynein motor (Schroer 2004, Vallee et al. 2004, Gunawardena & Goldstein 2004b), and the kinesin light chain (McGuire et al. 2006), which is a subunit of the kinesin motor (Hirokawa & Takemura 2004,

Gunawardena & Goldstein 2004b). As it is known that the dynein motor carries cargos retrogradely and the kinesin motor carries cargos anterogradely along axons (Gunawardena & Goldstein 2004b), we hypothesize that HAP1 may be the BDNF cargo-carrying molecule for these motors. Co-transfection studies showed that HAP1 is highly colocalized with the prodomaimBDNF and proBDNF but only partially with mature BDNF. Biochemical analysis of brain homogenates from wild type mice showed that BDNF is present in all precipitated components with different spin forces and is associated with the synaptic vesicles fraction, where HAP1 is also present. However, in HAP1 knockout mice, the normal pattern of BDNF distribution is disrupted (Fig. 3) and BDNF is not detectable in either the synaptic vesicle fraction (LP2) or in the pellet of moderate speed centrifugation (P2) but was increased in P1, S1 and P3 fractions. The data support that, in the absence of HAP1, BDNF failed to reach synaptic vesicles. These results support the hypothesis that HAP1 is the BDNF cargo-carrying molecule.

To further test the hypothesis, we examined the transport of endogenous proBDNF in the sciatic nerve and spinal cord in HAP1 knockout mice. Sciatic nerve is an ideal model to test the hypothesis, as the BDNF gene is highly expressed in primary sensory neurons and proBDNF and mature BDNF are both anterogradely and retrogradely transported within the sciatic nerve (Zhou

& Rush 1996, Wang *et al.* 2006). However, as HAP1 mutant mice die in the first two postnatal days and sciatic nerve is hardly seen in neonatal mice even under a surgical microscope, it is impossible to ligate the nerve to block the axonal transport as in our previous studies. Instead, we crushed the sciatic nerve in these mice, as a crush injury also interrupts axonal transport, leading to the accumulation of BDNF at the crush site. Our data showed that the inactivation of the HAP1 gene completely blocks the transport of endogenous proBDNF in both the sciatic nerve and spinal cord. These data indicate that HAP1 is essential for the transport of proBDNF. Interestingly, both anterograde and retrograde transport is abolished in these animals, suggesting that HAP1 may not only be essential for carrying BDNF forward by the kinesin motor by directly interacting with its prodomain but also essential for carrying the receptor-mediated internalized cargos of proBDNF and/or mature BDNF back toward the cell body.

It is logical to hypothesize that the activity-dependent release of BDNF requires anterograde transport and that the releasable pool of BDNF requires efficient transport from the cell soma to the dendrites and axonal terminals. Thus, if axonal transport is disrupted, activity-dependent release should be impaired. To test the hypothesis, we examined the release of proBDNF from cortical neuronal cultures from wt mice and $HAP1^{-/-}$ mice. Consistent with the

axonal transport data where BDNF transport is completely disrupted in HAP1$^{-/-}$ mice, the activity-dependent release of proBDNF is abolished, whereas constitutive release is not affected. Interestingly, activity-dependent release of BDNF in HAP$^{-/-}$ mice is impaired in both naïve neurons and in neurons transfected with expression plasmids, suggesting that transfection with the plasmids did not interfere with the cellular machinery of release. Our data indicate that the activity-dependent release but not the constitutive release of proBDNF requires the function of HAP1. As BDNF is critical for the survival and differentiation of many groups of neurons in the brain, the impairment of axonal transport and activity-dependent release of BDNF in HAP1$^{-/-}$ mice may underlie the death of neurons in the hypothalamus in these animals (Sheng *et al.* 2006, Li et al. 2003b) and explain the function of HAP1-A in neurite outgrowth (Rong *et al.* 2006, Li et al. 2002b).

The transport pathways of mature BDNF is different from that of proBDNF

Proneurotrophins can be cleaved intracellularly by furin or prohormone convertases (Edwards *et al.* 1988, Seidah et al. 1996) or extracellularly by plasmin or the metalloproteases MPP3 or MPP7 (Lee et al. 2001b, Smith *et al.* 1995). The activity-dependent secretion of BDNF is critical for various forms

of synaptic plasticity and the long-term regulation of synaptic structure and function (Katz & Shatz 1996, Lu 2004). After synthesis, unlike other neurotrophins cleaved within the trans-Golgi network (TGN) and packaged primarily into constitutive vesicles, proBDNF is mainly packaged into regulated secretory vesicles and then secreted in an activity-dependent manner as the mature form or pro-form (Goodman *et al.* 1996, Lou et al. 2005, Mowla et al. 1999). The neurotrophic actions are regulated by the two forms of the neurotrophins (pro- or mature) which are transported and secreted by cells (Hempstead 2006). In the present study, although we provide clear evidence that proBDNF transport is directly mediated via HAP1, the mechanisms by which mature BDNF is transported are not clear. Our pull-down assays showed that HAP1 interacts with the prodomain but not with mature BDNF. We found that mature BDNF indirectly binds HAP1 as mature BDNF binding proteins from rat brain homogenate containing HAP1-A (Fig. 1B). However, HAP1-immunoprecipitated materials did not contain mature BDNF (Fig. 2). Based on this data, it is reasonable to speculate that the motor accessory molecule HAP1 may transport mature BDNF by indirectly interacting with other molecules such as BDNF receptors. There are two conceptually different pools of mature BDNF within a neuron: synthesized, processed and ready-for-release mature BDNF and receptor-mediated internalized mature BDNF. It is unlikely that HAP1 is involved in the trafficking of the first pool of the releasable mature

BDNF as the co-transfection study showed that, after blocking extracellular BDNF with antibodies or its receptor p75NTR, HAP1 is not colocalized with endogenous mature BDNF. However, the exogenous fluorescently labelled mature BDNF added in the culture medium and internalized by neurons is highly colocalized with HAP1 (Fig. 4). These data suggest that the second pool of extracellularly derived mature BDNF may be transported by the HAP1-mediated mechanism. Whether HAP1 interacts with the BDNF receptors trkB, sortilin or p75NTR is not known, but our immunoprecipitation experiments showed that the HAP1 immunoprecipitation from the human brain contains sortilin (Fig. 9) and BDNF affinity purified materials contain p75NTR (Fig. 1D).

Thus, based on our current data and data from other studies (Li XJ, Gauthier et al) we propose models of BDNF transport within axons as depicted in the schematic diagram (Fig. 12). We propose that HAP1 is a cargo-carrying molecule which interacts with the molecular motor kinesin light chain and carries the BDNF prodomain and also transports proBDNF anterogradely from cell somata to nerve terminals or dendrites (Fig. 12A). For the retrograde transport of extracellularly derived-mature BDNF and -proBDNF, HAP1 interacts with p150Glued and may also carry the endocytosed cargo of BDNF/BDNF receptors by interaction with the receptors or endosome

components (Fig. 12B).

Val66Met mutation reduced the association between the prodomain and HAP1

20-30% of humans carry the mutation of a valine (Val) to methionine (Met) substitution at codon 66 in prodomain BDNF (Shimizu et al. 2004). Previous studies showed that the Val66Met BDNF mutation may associate with several neurodegenerative diseases (Momose *et al.* 2002, Chen et al. 2004). The Val66Met mutation leads to the reduction in activity-dependent secretion and impairs the intracellular trafficking of BDNF without affecting the constitutive release of BDNF (Egan et al. 2003, Chen et al. 2004). This mutation in humans also causes a reduction in hippocampal volume (Egan et al. 2003) and affects hippocampal processing of episodic learning and memory (Egan et al. 2003, Hariri *et al.* 2003, Rybakowski *et al.* 2003). This phenomenon suggests that the impairment of activity-dependent secretion of BDNF is responsible for dysfunction in hippocampal plasticity and for a number of human psychological disorders (Lu 2003). However, how the mutation results in a reduction in activity-dependent secretion and transport is not clear. In the present study we showed that this mutant form of the prodomain interacts with HAP1 with less efficiency compared to the wild type form. Mutant Htt further

reduces the interaction between HAP1 and the Val66Met prodomain. Our data suggests that the mutation in the prodomain may reduce activity-dependent release by impairing the cargo-carrying efficiency of HAP1. However, in the PC12 cell somata (Fig.11), the colocalization rate is almost the same between wt prodomain/HAP1 and Val66Met/HAP1, suggesting the mutation does not disrupt the sorting process. Whether HAP1 is highly colocalized with the Val66Met prodomain BDNF in axons and axonal terminals requires further study.

Htt and PolyQ-Htt affect the binding of HAP1 with proBDNF

Huntington's disease is a neurological disorder caused by mutant htt (PolyQ length >37). A large body of evidence suggests that mutant Htt abnormally interacts with HAP1. One of the pathophysiological mechanisms underlying neuronal death in HD is that mutant Htt down-regulates the expression and transport of BDNF. Several studies have already indicated that wild type Htt (PolyQ length from 17-36 Glutamines) is an anti-apoptotic protein that could enhance intracellular transport of BDNF, but mutant Htt in HD causes retardation of BDNF transport along microtubules (Humbert & Saudou 2005, Gauthier et al. 2004) and impairs the post-Golgi trafficking of wt BDNF, but not Val66Met BDNF (del Toro et al. 2006). However, how polyQ-Htt impairs

the axonal transport and post Golgi traficking of BDNF was not known. Our current study uncovers the mechanism by which mutant Htt may reduce the transport BDNF in HD. It is known that Htt interacts with HAP1 which interacts with p150glued. Mutant Htt decreases these interactions (Li et al. 1998b). We showed that mutant Htt significantly reduced the interaction between HAP1 and proBDNF (Fig. 7), suggesting that mutant Htt may disrupt proBDNF transport by interfering with the interaction between prodomain BDNF and its cargo-carrying molecule, HAP1. Further supporting this notion is the evidence that HAP1 in the brain of HD patients binds less proBDNF than that in the normal human brain (Fig. 8 and 9). The reduction in BDNF pull-down from HD brain could be due to two reasons: one is that the expression of proBDNF in HD could be reduced and the second is that the PolyQ-Htt may decrease the HAP1/proBDNF interaction. In a physiological setting both could act concomitantly with each other to be responsible for the lack of BDNF support in HD.

In summary, we have uncovered the mechanism underlying the neuronal transport of proBDNF and mature BDNF via interaction with the cargo-carrying molecule HAP1. Deletion of HAP1 blocks the axonal transport and activity dependant release of proBDNF. We also showed that mutant Htt reduces the interaction between HAP1 and proBDNF in HD and Val66Met

proBDNF interacts with HAP1 with a less efficiency than the wild type. Thus we conclude that HAP1 is essential for the transport and release of proBDNF and the reduced interaction between HAP1 and the prodomain of BDNF may underlie the reduction of transport and release of BDNF in HD and in the Val66Met polymorphism.

CHAPTER 3

PROBDNF INDUCES DEATH OF SENSORY NEURONS AFTER AXOTOMY IN NEONATAL RATS

1. Abstract

Brain-derived neurotrophic factor (BDNF) plays a critical role in the development of the central and peripheral nervous system and also in neuronal survival after injury. The actions of BDNF are mediated by its high affinity receptor TrkB and p75NTR. Recent studies have shown that proneurotrophins bind p75NTR and sortilin with high affinity, and trigger apoptosis of neurons *in vitro*. Some proBDNF is released extracellularly and biologically acts as mediator in TrkB phosphorylation, activation of ERK1/2, and neurite outgrowth. Pro-BDNF binds to and activates TrkB and could be involved in TrkB-mediated neurotrophic activity *in vivo* (Fayard et al. 2005). As proneurotrophins are a dominant form of gene products in developing and adult animals, it is essential to understand their physiological functions in animals. The research has shown that proNGF binding to p75NTR is responsible for the death of adult corticospinal neurons after lesion (Harrington et al. 2004), the the disagreement study has shown that proNGF exhibiting neurotrophic activity in vivo (Buttigieg et al. 2007). Here, we show that proBDNF plays a role in the death of axotomized sensory neurons. ProBDNF, p75NTR and sortilin are highly expressed in DRG neurons. We raised and characterized recombinant proBDNF which induced a dose-dependent death of PC12 cells and this death activity was completely abolished in the presence of antibodies

against the prodomain of BDNF. Exogenous proBDNF enhanced the death of axotomized sensory neurons, and neutralizing antibodies to the prodomain or exogenous sortilin-extracellular domain-Fc fusion molecule reduced the death of axotomized sensory neurons. Interestingly, antibody to the prodomain BDNF caused a significant increase in the number of sensory neurons in the contralateral unlesioned DRG. We conclude that proBDNF induces the death of axotomized sensory neurons in neonatal rats and the suppression of endogenous proBDNF rescued the death of axotomized sensory neurons and increased the number of sensory neurons in the intact DRG.

2. Introduction

Brain-derived neurotrophic factor (BDNF) belongs to the neurotrophin family which plays a role in the survival and differentiation of neurons during development. The requirement of BDNF signaling at the early stage of development of murine sensory neurons was demonstrated by the loss of approximately 30% of lumbar dorsal root ganglia (DRG) neurons in animals with a deletion of the gene (Jones et al. 1994). In addition to regulating peripheral nerve development, BDNF also plays an important role in regulating sensory neuron survival after axotomy of neurons (Zhou et al. 2005). BDNF expression switched from small to large axotomized neurons and anterograde

transport of BDNF was increased after peripheral nerve injury (Tonra et al. 1998, Li *et al.* 1999b, Zhou et al. 1999). The actions of BDNF are mediated by its high affinity receptor tropomyosin-related kinase B (TrkB) and p75NTR, a member of the tumor necrosis factor receptor superfamily. Our previous studies demonstrated that BDNF regulates the survival of sensory neurons, depending on p75NTR expression. BDNF prevents cell apoptosis in axotomized sensory neurons in DRG *in vivo* whereas BDNF promotes cell apoptosis of cultured neurons *in vitro* where p75NTR is upregulated (Zhou et al. 2005).

All neurotrophins are made first as precursor forms (proneurotrophins), which can be either secreted from cells or cleaved intracellularly to yield C-terminal mature neurotrophin (Chao & Bothwell 2002). Recently, these proneurotrophins were also recognized as functional proteins that distinctly activate the p75NTR but not the Trk receptor to mediate apoptosis of neurons (Lee et al. 2001b, Teng et al. 2005). ProNGF binds both sortilin, a type I transmembrane protein known as neurotensin receptor-3 (Mazella et al. 1998) and p75NTR with high affinity, inducing apoptosis of neonatal sympathetic neurons *in vitro* (Lee et al. 2001b, Nykjaer et al. 2004). ProBDNF is also recognized as being released in cultured cortical neurons and at hippocampal synapses (Pang et al. 2004, Teng et al. 2005). ProBDNF has a crucial role in long term depression (LTD) in the hippocampus enhancing NR2B-dependent

LTD and NR2B-mediated synaptic currents by activation of p75NTR (Woo et al. 2005). ProBDNF, similarly to proNGF, also induces neuronal apoptosis via activation of a receptor complex of p75NTR and sortilin in cultured sympathetic neurons *in vitro* (Chen et al. 2005). However, the effect of proNGF on the survival of sympathetic neurons is controversial as studies from a different group show that proNGF promotes survival of sympathetic neurons by phosphorylating TrkA but with a lower potency than mature NGF *in vitro* (Fahnestock et al. 2004). The intriguing question arising from this is whether proneurotrophins act as death factors *in vivo* under physiological conditions. In the present study, using axotomized sensory neurons of neonatal rats as a model, I examined the potential role of proBDNF in neuronal survival *in vivo*. The underlying mechanisms contributing to the effect of proBDNF were also investigated.

3. Materials and methods

Animals

All procedures involving animals were approved by the Animal Welfare Committee of Flinders University and undertaken according to the guidelines of the National Health and Medical Research Council of Australia. Neonatal

(postnatal day 1, P1) Sprague-Dawley rats were kept with their mother under standardized barrier-breeding conditions (12-h light/dark cycle). Food and water were provided *ad libitum*.

Sortilin gene was amplified from plasmid gp95/sortilin [encoding the cytoplasmic tail (aa 748-800)] (from Carlos R. Morales, McGill University, Montreal, Quebec, Canada) in pBK-CMV vector by PCR using primers to delete the transmembrane and intracellular domain and introduce an XhoI site at the 3' terminus and a BglII site at the 5' terminus. Then the construct was subcloned into the plasmid pcDNA3.1-Fc, which contains the sequence coding for the Fc region of human IgG1 between the XhoI and BglII site, and was bidirectionally sequenced. The confirmed constructs (plasmid pcDNA3.1-sortilin-Fc) were transfected into CHO cells and stable clones were generated after selection in media containing 0.5μg/ml G418. Medium from cells cultured in HyQ SFM4CHO (Hyclone, USA) was harvested for purification. Protein G sepharose beads (50% v/v slurry) were added into medium and incubated overnight at 4°C, then beads were collected into a column for chromatography. After the column was washed with washing buffer (150 mM NaCl, 10-20 mM Tris, pH 7.5-8.5 with 0.04% azide), the Fc-tagged sortilin protein was eluted with elution buffer (100 mM glycine-HCl, pH 2.5 with 0.04% sodium azide).

Eluted recombinant proteins were dialyzed against HBSS (Invitrogen, CA) and stored at-80°C until use.

The expression and purification of proBDNF were performed using Champion™ pET100 Directional TOPO Expression Kit**.** Briefly, the full length proBDNF was amplified by PCR from murine point mutant proBDNF plasmid [RR (amino acids 129 and 130) to AA] as a template (from Dr. Masami Kojima**,** Research Institute for Cell Engineering, National Institute of Advanced Industrial Science and Technology (AIST), Ikeda, Osaka) using primer pair: proBDNF (forward) 5'-TTAGCGCCGAACCCTCATAGA and proBDNF (reverse) 5'-CTACCTTCCCCTTTTAATGGT which could generate proBDNF furin-resistant recombinant protein. The fragments were cloned into pET100/D-TOPO directional vector according to the manufacturer's instructions, and the sequences were confirmed by sequencing. The plasmids were transformed into E. coli BL21, and the bacterial host was grown in 1000 ml LB media with 100ug/ml of ampicillin as a selective agent (300rpm, 37°C) until the O.D.580 reached ≈0.8. Isopropyl-b-D-thiogalactopyranoside (IPTG) was added to a final concentration of 0.5mM and shaken at 300 rpm overnight at 30°C. The bacteria were then centrifuged at 11,000×g for 20 mins at 4°C. The pellet was resuspended in 40ml of binding buffer (50mM K-phosphate buffer, pH 7.4, 0.3M NaCl, 10% glycerol, 0.005% Triton-X 100, 10mM

imidazole and 1mM DTT and 1mM of PMSF as a protease inhibitor). Lysozyme (Sigma) was added to the solution to a final concentration of 0.2mg/ml to lyse the cells and the solution was kept on ice for 25 mins. The solution was then sonicated 10 times on ice for 30 seconds each period at a power of 50 watts. The solution was then centrifuged at 11,000×g for 20 mins at 4°C and the pellet was resuspended with 50 ml of buffer I (20mM Tris pH 8.0, 0.2M NaCl and 1% deoxycholic acid sodium salt) and subject to agitation on ice for 30 mins. The suspension was then centrifuged at 3000g for 10 mins. The pellet was then resuspended in 50ml of cold buffer II (10mM Tris pH8.0, 1mM EDTA and 0.25% deoxycholic acid sodium salt). The solution was then centrifuged 3000×g for 10 mins. The pellet was washed using 40ml of buffer II 3 times as above. After the final wash, the proteins in the pellet were denatured and solublized in 40ml of 8M urea solution. The nickel column was prepared according to the manufacturer's instructions. The protein solution was centrifuged at 11,000×g for 25 mins at 4°C. The cleared supernatant was added to the column. After all the supernatant passed through the column, the column was then washed with the wash buffer (8M urea, 5mM imidazole and 0.5M NaCl). The OD of the wash eluate was monitored until it had dropped to the baseline. The elution buffer (8M urea, 1M imidazole and 0.5M NaCl) was added to the column to elute the target proteins. The collected proteins were subjected to commassie brilliant blue staining after separation by

electrophoresis. The elution solution containing proteins was 10 times diluted with refolding solution (0.75M L-Arginine, 5mM GSH, 0.5mM GSSH, 5mM EDTA and 0.1M Tris pH 9.5). After refolding, the protein solution was dialysed against 2L of PBS for 4 hours at 4°C, followed by 5L for 4 hours and then by 10L overnight. The final protein concentration was tested using BCA™ Protein Assay Kit (Pierce). For full-length proBDNF, supernatant lysate generated from buffer I (20mM Tris pH 8.0, 0.2M NaCl and 1% deoxycholic acid sodium salt) was used without urea and naturally refolded protein was affinity purified on the nickel column. All recombinant proteins were characterized by SDS-PAGE with Coomassie Blue staining and Western blot analysis.

Generation and characterization of antiserum to proBDNF

The prodomain fragment of proBDNF (500 μg) purified from E. coli was emulsified with complete Freund's adjuvant and injected subcutaneously into a sheep. Subsequently, the sheep was injected with the same antigen every two weeks with incomplete Freund's adjuvant. Antibodies in the serum were monitored with ELISA assays. The sheep was bled out one week after the fourth injection when the antibody titres reached 1/100,000. The antibody was affinity purified and characterized by Western blot, ELISA assays and bioassays.

Bioassay of proBDNF in PC12 cells and antibody neutralization

PC12 cells were maintained in DMEM supplemented with 10% fetal bovine serum, 5% heat-inactivated horse serum, 50 μg/ml streptomycin, and 50 IU/ml penicillin in a humidified atmosphere at 37°C and 5% CO_2 as described previously (Gueorguiev et al. 1999). 3 days before the experiment, the PC12 cells were plated on poly-lysine coated slides, cultured on differentiation medium (DMEM supplemented with 1% horse serum, 0.5% fetal bovine serum, 1% glutamine, 1% penicillin/streptomycin and 10ng/ml NGF). On the day of the experiment, triplicate cultures were rinsed five times with NGF-free medium and treated with proBDNF with 4 different dilutions of proBDNF protein (1ng/ml; 10ng/ml; 100ng/ml; 1μg/ml). For neutralization experiments, PC12 cells were cultured in 100 ng of proBDNF in the presence of different concentrations of antibodies to proBDNF or normal sheep IgG. After 48h, the PC12 cells were fixed in 4% paraformaldehyde and stained with 4', 6-diamidino-2-phenylindole (DAPI) (Sigma, MO) to visualize nuclei. The apoptotic nuclei and total number of nuclei were counted. 10 randomly selected fields were counted for each culture condition. The experiments were repeated three times. The percentage of apoptotic cells was calculated against the total number of nuclei counted. As there was a variation among different assays, we corrected the variation using the control value as 100% each time and the data

were calculated against the control.

Immunohistochemistry of p75NTR, sortilin and proBDNF

For sortilin and p75NTR immunohistochemistry, neonatal rats were perfused with 50% Histochoice (AMRESCO, Solon, OH, USA) containing 2% paraformaldehyde and postfixed in the same fixative containing 30% sucrose overnight. DRGs dissected from perfused animals were sectioned on a cryostat microtome at 20 μm. Sections on glass slides were blocked in 1% blocking solution (Roche, Switzerland) and incubated overnight in rabbit polyclonal antibodies against sortilin at 2 μg/ml (Abcam), and monoclonal antibody against p75NTR (MC192) at 1 μg/ml (Chemicon, CA). After extensive washing in PBS containing 0.1% Tween 20 (PBST), the sections were incubated with Cy3-linked or Cy5-linked secondary antibodies (Vector Laboratories, Burlingame, CA, USA) followed by DAPI staining for nuclei. After rinsing in PBS, slides were observed under fluorescence microscopy.

For proBDNF immunohistochemistry, DRG were treated as described above. Sections were incubated overnight at 4°C using rabbit antiserum to proBDNF (1μg/ml), followed by a 2h incubation with a rabbit anti-sheep antibody (1:1000, Sigma). Sections were washed in PBS and then incubated with ABC

complex reagents (Vector laboratories Burlingame, CA, USA). Following washes, these sections were developed in 3, 3-diaminobenzidine with nickel enhancement. Immunohistochemistry was performed on multiple samples and the specificity of staining confirmed in the absence of primary antibody.

Western blot of proBDNF, p75NTR and sortilin

The neonatal rat DRGs were homogenized in RIPA buffer (1% NP-40, 1% sodium deoxycholate, 0.1% SDS, 0.15M NaCl, 0.01 M sodium phosphate, pH 7.2, 1% Trasylol). The samples were centrifuged at 14,000×rpm. for 15 min at 4°C and the supernatant collected for SDS-PAGE. After SDS-PAGE, the proteins were transferred to a nitrocellulose membrane. The membrane was probed with sheep anti-proBDNF antibody at 1μg/ml, monoclonal antibody against p75NTR (MC192, 2μg/ml) and sheep anti-sortilin (2μg/ml), respectively. After further incubation in HRP-labeled rabbit anti-sheep antibody (1:2000) and HRP-labeled rabbit anti-mouse antibody for 1 h at room temperature, the membranes were developed by ECL.

Sciatic nerve transection and treatment

For anaesthesia, neonatal rats at P1 were wrapped with a piece of cloth and put

on ice. After 2 to 3 minutes, the mice were put on an ice cold plate. When the rat was motionless, an incision 2 cm long was made in the left thigh and the left sciatic nerve was exposed and transected. Immediately after the transection, a gel foam containing proBDNF, sortin-Fc (10μg) was placed on the lesion site of the sciatic nerve and the wound closed by sutures. BSA was used as a negative control. Animals were kept on a warm blanket for recovery. After recovery, the neonates were returned to their mother. In another group, the neonates were injected subcutaneously (s.c.) with antiserum to proBDNF or normal sheep serum (5ml/kg weight, twice a week) and normal sheep serum immediately after the transection. On day 8 after the sciatic nerve injury, the rats were killed with an overdose of sodium pentobarbitone and perfused with modified Zamboni's fixative containing 4% paraformaldehyde. L4 and L5 DRGs were dissected for stereological cell counting studies.

Stereological counting of total numbers of neurons in DRGs

The fixation and sectioning of dissected L5 DRG in neonatal rats were conducted as described (Zhou et al. 2005).

Statistics

Data are presented as mean±S.E. Statistical significances were calculated using Student's t-test for unpaired samples. Statistically significant difference was set at $p<0.05$.

4. Results

Expression of proBDNF and sortilin recombinant protein

Recently, it has been demonstrated that proBDNF-induced apoptosis is mediated by p75NTR and sortilin (Teng et al. 2005). To investigate proBDNF function and the relationship between proBDNF and sortilin, we cloned proBDNF into pET100/D-TOPO and sortilin into pcDNA3.1-Fc. ProBDNF was expressed in *E. coli*, purified and characterized. The recombinant extracellular domain sortilin protein fused with Fc was expressed in mammalian cells, purified and characterized. The purities of recombinant purified proteins are shown in the figure (Fig 1A and B). Commassie blue staining showed that proBDNF was over 85% pure and sortilin-Fc was 90% pure. The recombinant proBDNF and sortilin were recognized by specific antibodies against the prodomain of BDNF and sortilin (Fig 1A and B).

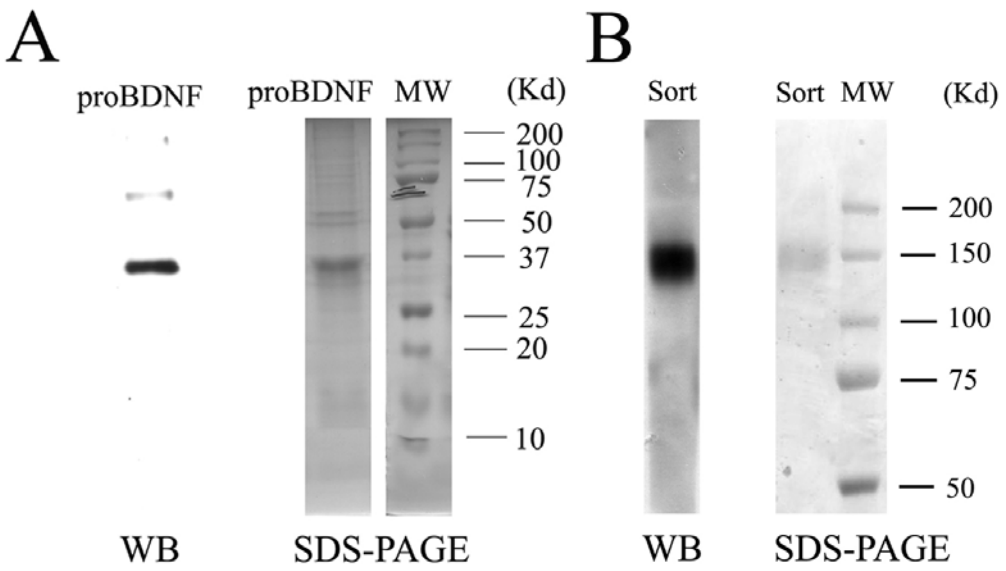

Fig. 1 Expression and purification of proBDNF and sortilin. (A) Western blot of purified proBDNF (MW 37 kDa). SDS-PAGE gel stained with Coomassie blue showing the purity of the recombinant proBDNF. **(B)** Western blot of purified sortilin (MW 140 kDa). SDS-PAGE gel stained with Coomassie blue showing the purity of the recombinant sortilin.

Characterization of sheep antibody to the recombinant prodomain BDNF

For the characterization of antibodies to the prodomain, the recombinant protein was conjugated to sepharose B. Sheep antiserum to the prodomain was passed through the column and binding antibodies were eluted from the column. As shown in Fig. 2A, the antibody specifically recognized the prodomain and full-length proBDNF but not mature BDNF. ELISA assay confirmed that the antibody binds to prodomain BDNF in a dose-dependent manner (Fig. 2B). The antibody did not recognize the recombinant prodomain NGF or prodomain NT-3 (Fig. 2C).

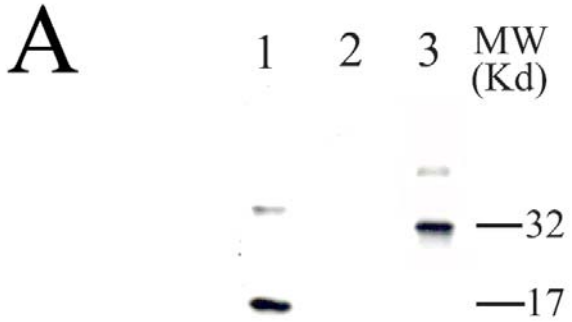
A
1
2
3
MW
(Kd)
32
17

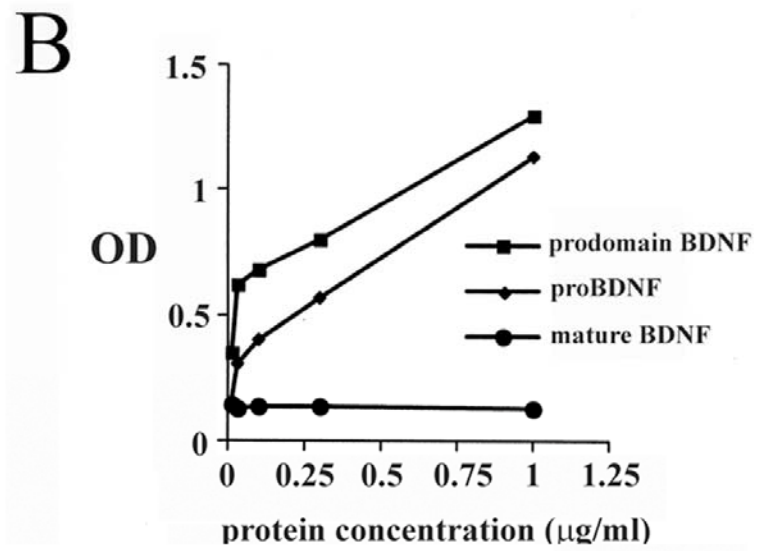
B
1.5
1
0.5
0
OD
prodomain BDNF
proBDNF
mature BDNF
0
0.25
0.5
0.75
1
1.25
protein concentration (μg/ml)

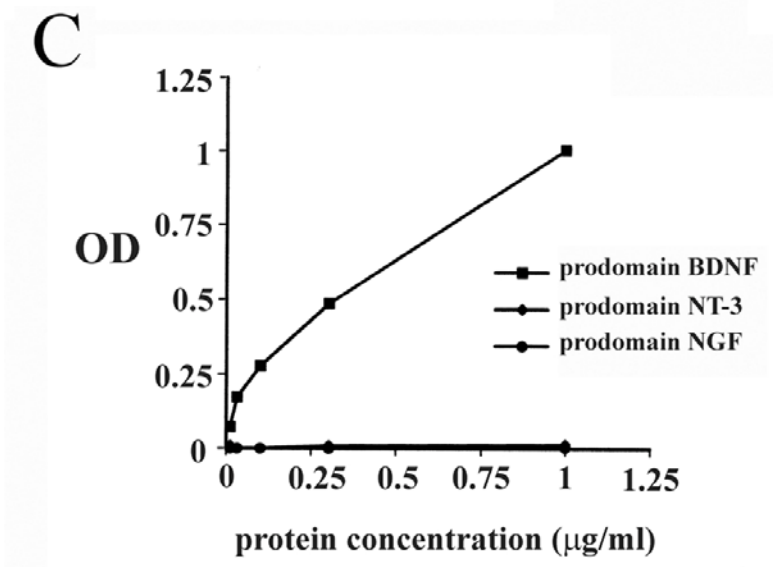
C
1.25
1
0.75
0.5
0.25
0
OD
prodomain BDNF
prodomain NT-3
prodomain NGF
0
0.25
0.5
0.75
1
1.25
protein concentration (μg/ml)

Fig. 2 Characterization of sheep antibody to the recombinant prodomain BDNF (A) using sheep anti prodomain BDNF antibody to probe prodomain BDNF (lane 1), mature BDNF (lane 2) and proBDNF (lane 3). **(B)** ELISA assay confirmed that the sheep anti prodomain antibody binds to prodomain BDNF in a dose-dependent manner. **(C)** The sheep anti prodomain BDNF antibody did not recognize the recombinant prodomain NT-3 or prodomain NGF.

Bioassay of proBDNF in PC12 cells and antibody neutralization

The interaction of proBDNF with both p75NTR and sortilin is required to induce neuronal apoptosis (Teng et al. 2005). To examine the bioactivity of recombinant proBDNF, co-expression of p75NTR and sortilin in PC12 cells was assessed with immunofluorescence labelling. The results illustrate that both p75NTR (Fig. 3A) and sortilin (Fig. 3B) were co-localized in PC12 cells (Fig. 3C and D). In the presence of proBDNF for 48 h, the number of cells undergoing death was significantly increased in a dose-dependent manner (Fig. 3G).

To further demonstrate biological activity of proBDNF and the biological activity of the antibodies against the prodomain, the affinity-purified antibody against the prodomain was added together with proBDNF. The cell death-inducing effects of proBDNF were abolished by different concentrations of antibody to proBDNF (Fig. 3H). The level of apoptosis was reduced in the presence of the antibodies to proBDNF in a dose-dependent manner (Fig. 3H). These results suggest that recombinant proBDNF has the biological activity of inducing the death of PC12 cells *in vitro*. These results also indicate that the antibody to the prodomain is biologically activite and can be used to investigate physiological functions of proBDNF *in vivo*.

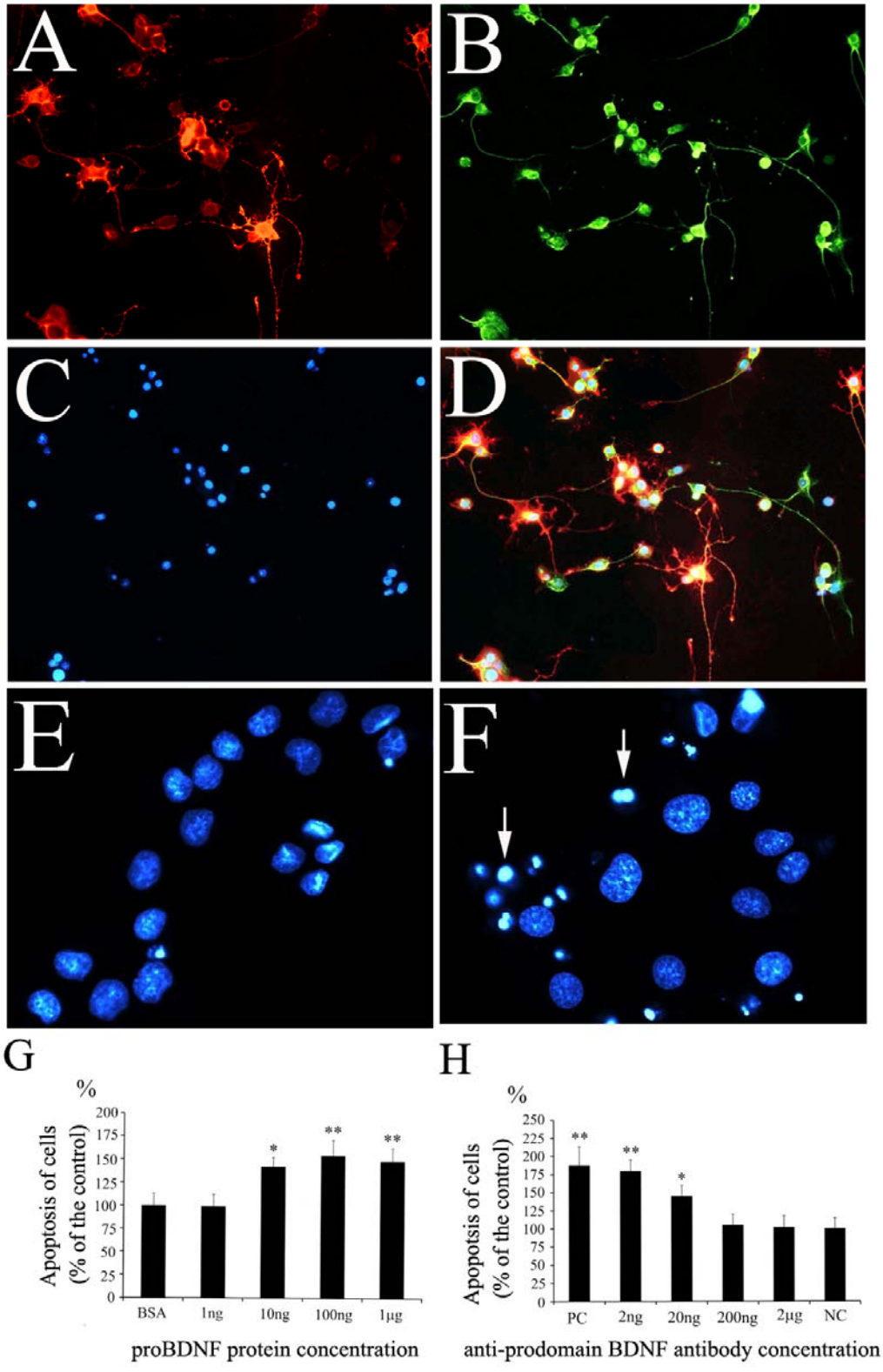
A
B
C
D
E
F
G
%
Apoptosis of cells
(% of the control)
200
175
150
125
100
75
50
25
0
*
**
**
BSA
1ng
10ng
100ng
1µg
proBDNF protein concentration
H
%
Apopotsis of cells
(% of the control)
250
225
200
175
150
125
100
75
50
25
0
**
**
*
PC
2ng
20ng
200ng
2µg
NC
anti-prodomain BDNF antibody concentration

Fig. 3 Bioassay of proBDNF in PC12 cells and antibody neutralization. (A-D) Double labeling of p75NTR and sortilin on PC12 cells **(A)** anti-p75NTR; **(B)** anti-sortilin; **(C)** DAPI; **(D)** merged. **(E)** DAPI labeling of control PC12 cells. **(F)** DAPI labeling of apoptotic PC12 cells (The white arrows point out the apoptotic cells.) **(G)** Recombinant proBDNF induces apoptosis in PC12 cells. In the presence of serial concentrations of proBDNF from 1ng/ml to 1μg/ml for 48 h, the number of PC12 cells undergoing cell death was assessed by DAPI labeling. **(H)** Affinity-purified antibody to proBDNF neutralized the effect of proBDNF. The antibodies against proBDNF at serial concentrations from 2ng/ml to 2μg/ml were added into culture medium prior to proBDNF administration. **PC**: proBDNF administration only; **NC**: No administration. Data are presented as mean ± S.E.M (*$p<0.05$; ** $p<0.01$)

Expression of proBDNF, p75NTR and sortilin in DRG

To test the function of proBDNF in sensory neurons *in vivo*, we firstly investigated the expression of proBDNF receptors (p75NTR and sortilin). p75NTR-immunoreactivity is mainly present in small- and medium-sized sensory neurons, and occasionally in axons (Fig. 4A). Sortilin is expressed in most neuronal cells (Fig. 4B), and it is also colocalized with p75NTR (orange/yellow) in a subpopulation of small neurons. Some sortilin-positive neurons do not express p75NTR (Fig. 4C and D). Western blot further confirmed the expression of p75NTR (Fig. 4E). Consistent with the immunofluorescence labeling, sortilin in DRG was also observed by Western blot.

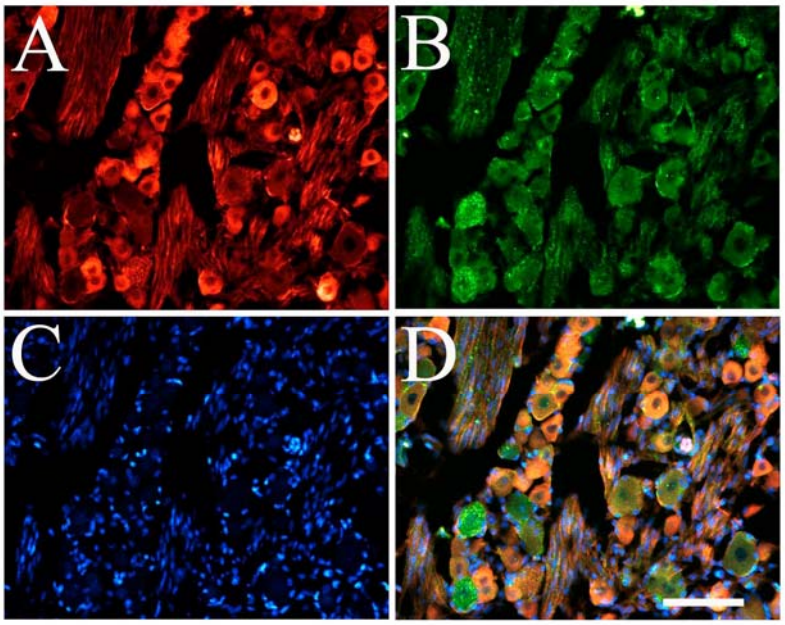
A
B
C
D

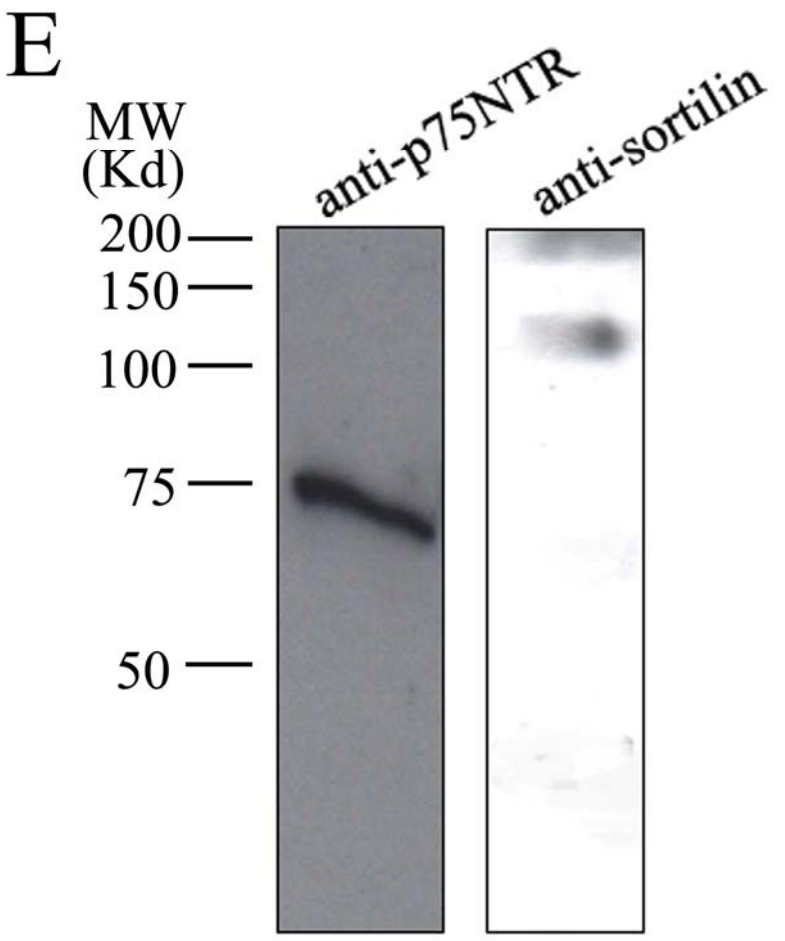
E
MW
(Kd)
anti-p75NTR
anti-sortilin
200
150
100
75
50

Fig. 4 Expression of p75NTR and sortilin in L5 DRG. (A-D) Double labeling of p75NTR and sortilin on DRG. **(A)** anti-p75NTR; **(B)** anti-sortilin; **(C)** DAPI; **(D)** merged (Scale Bar: 50μm); **(E)** Western blot analysis of p75NTR and sortilin in DRG.

Consistent with our previous studies (Zhou et al. 2004), proBDNF immunoreactivity was localized in cytoplasm of medium-sized sensory neurons in dorsal root ganglia (Fig. 5A). A specific band at about 32 Kd was recognized by proBDNF antibody in DRG homogenates conducted by Western blot, brain sample used as positive control (Fig. 5B).

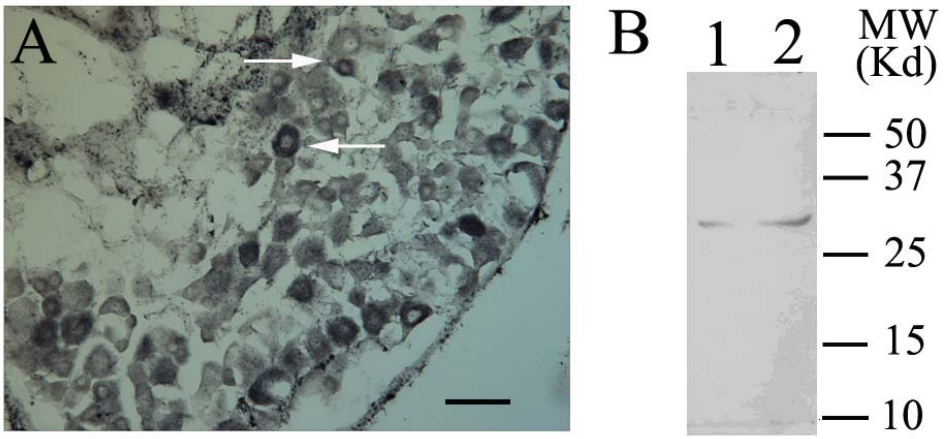

Fig. 5 Expression of proBDNF in DRG. (A) Image of proBDNF immunoreactivity in DRG. (Scale Bar: 50 μm). The white arrows point out the proBDNF positive staining cells. **(B)** Western blot analysis of proBDNF in rat brain homogenate (lane 1) and DRG homogenate (lane 2).

Exogenous proBDNF reduces the survival of sensory neurons *in vivo*.

To examine the effects of proBDNF in sensory neurons *in vivo*, proBDNF was point-mutated to generate furin-resistant proBDNF (Mowla et al. 2001). The recombinant proBDNF at 5 μg in 5 μl PBS was stored in gel foam and freeze-dried, and the dried gel foam was placed at the injured stump of sciatic nerve transected in P1 neonatal rats. 7 days after the treatment, the L5 DRGs were dissected and the numbers of the sensory neurons were stereologically counted. Results show that the average total number of neurons in ipsilateral L5 DRGs was significantly reduced compared to the contralateral side in both control and proBDNF treated groups (Fig. 6). The total numbers of neurons in ipsilateral and contralateral DRGs of control group (treated with BSA or normal sheep serum (NSS) were 7297±1271 and 13536±1570, while the total number of neurons in ipsilateral and the contralateral DRG treated with proBDNF were 4961±1154 and 12024±1739, respectively. The number of neurons in the ipsilateral DRGs treated with proBDNF was significantly lower than ipsilateral DRGs of the control group, suggesting that exogenous proBDNF exaggerated the loss of sensory neurons induced by axotomy.

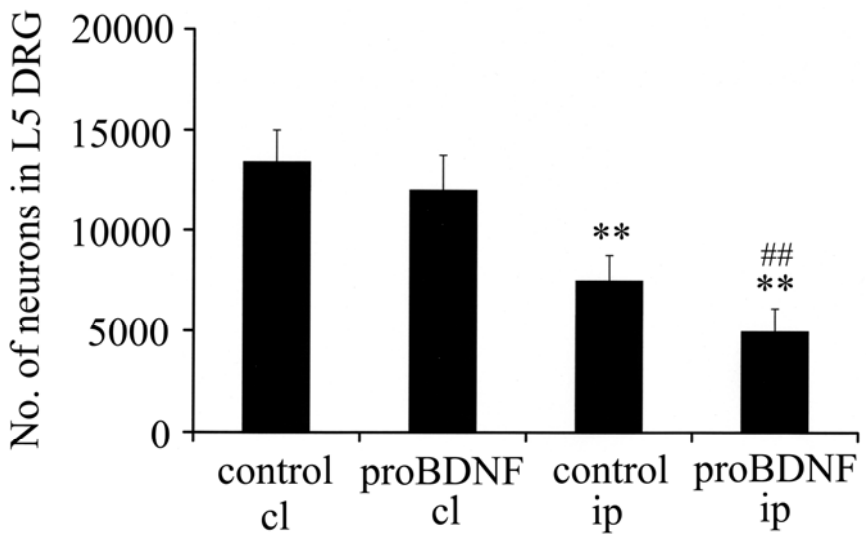

Fig. 6 Exogenous proBDNF reduced the number of sensory neurons in L5 DRG after sciatic nerve transection. The sciatic nerve was cut on P1 and recombinant proBDNF trapped into gel foams were placed in the injury sites (n=6). In control group, the gel foams containing BSA were placed in the injury sites or normal sheep serum group (NSS) was injected s.c. after sciatic nerve transaction (n=10). Total numbers of sensory neurons in bilateral DRG were counted stereologically. cl, contralateral DRG; ip, ipsilateral DRG. Data are presented as mean ± S.E.M., ** $p<0.01$ compared with the contralateral DRGs from the same animal. $^{\#\#}$ $p < 0.01$ compared with ipsilateral DRGs of control group.

ProBDNF anti-serum reduces cell death of axotomized sensory neuron *in vivo*

To investigate the function of endogenous proBDNF on the cell survival of sensory neurons after nerve lesion, specific serum against proBDNF was injected s.c. after sciatic nerve transection. The total numbers of neurons in ipsilateral and contralateral DRGs of control group (treated with BSA or normal sheep serum (NSS) were 7297±1271 and 13536±1570**,** while the average total numbers of neurons in ipsilateral and the contralateral DRGs treated with the antiserum to the prodomain of BDNF were 11297±613 and 17952±2156, respectively (Fig.7). The number of neurons in the ipsilateral DRGs treated with proBDNF anti-serum significantly diminished the loss of sensory neurons after the sciatic nerve transection, compared with the control group, suggesting that the neutralization of endogenous proBDNF could rescue the loss of sensory neurons induced by axotomy. There was no significant difference in the number of neurons between ipsilateral DRG treated with proBDNF antiserum and the contralateral DRG treated with NSS. Interestingly, the anti-proBDNF treatment in neonatal rats increased the total number of sensory neurons in the contralateral DRGs. Compared to the contralateral DRG treated with proBDNF antibody, the number of neurons in the ipsilateral DRG was still significantly reduced (Fig.7).

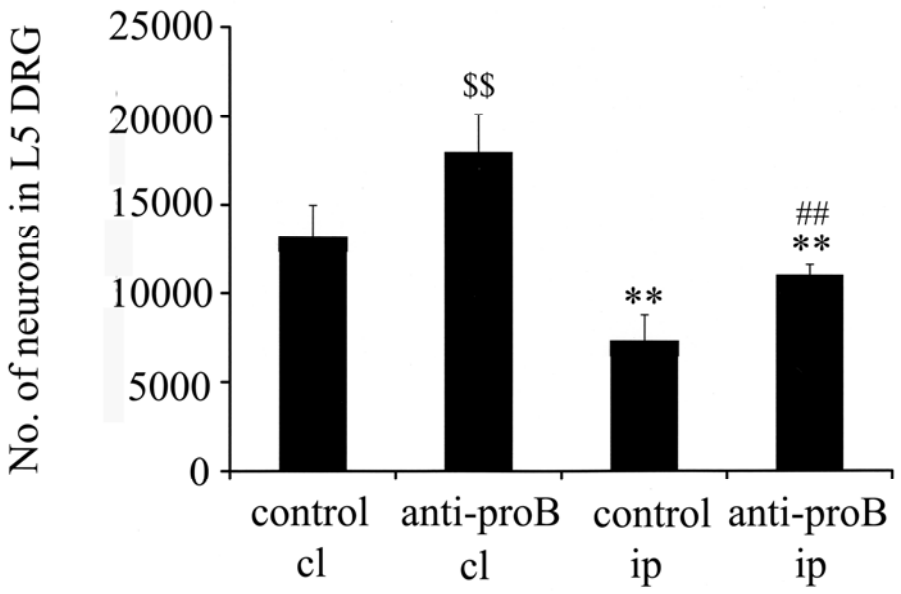

Fig. 7 proBDNF anti-serum increases the survival of sensory neurons in L5 DRG after sciatic nerve transaction. The sciatic nerve was cut on P1 and the antiserum to proBDNF (n=6) was injected s.c. In control group, the gel foams containing BSA were placed in the injury sites or NSS was injected s.c. after sciatic nerve transaction (n=10). Total number of sensory neurons bilaterally were counted stereologically. cl, contralateral DRG; ip, ipsilateral DRG. Data are presented as mean ± S.E.M. ** $p<0.01$ compared with the contralateral DRGs from the same animal. $^{\#\#}$ $p<0.01$ compared with ipsilateral DRGs of control group. $^{\$\$}$ $p<0.01$ compared with the contralateral DRGs of control group.

Sortilin-Fc protein increases the survival of axotomised DRG neuron

To further examine whether the apoptosis of sensory neurons after nerve transection is mediated by sortilin, the recombinant extracellular domain of sortilin-Fc was stored in gel foam and released persistently at the injury sites of sciatic nerve transection of P1 neonatal rats. 7 days after the administration of sortilin protein, the average total numbers of the ipsilateral and contralateral DRG neurons were 10394±1452 and 12542±1519 respectively. In control group, the average numbers of the ipsilateral and contralateral neurons of DRG were 7297±1271 and 13536±1570. Apparently, the sortilin-Fc significantly reduced the loss of neurons in L5 DRGs after sciatic nerve transection (Fig. 8). No significant difference in the number of neurons was found between ipsilateral and contralateral DRG treated with sortilin-Fc.

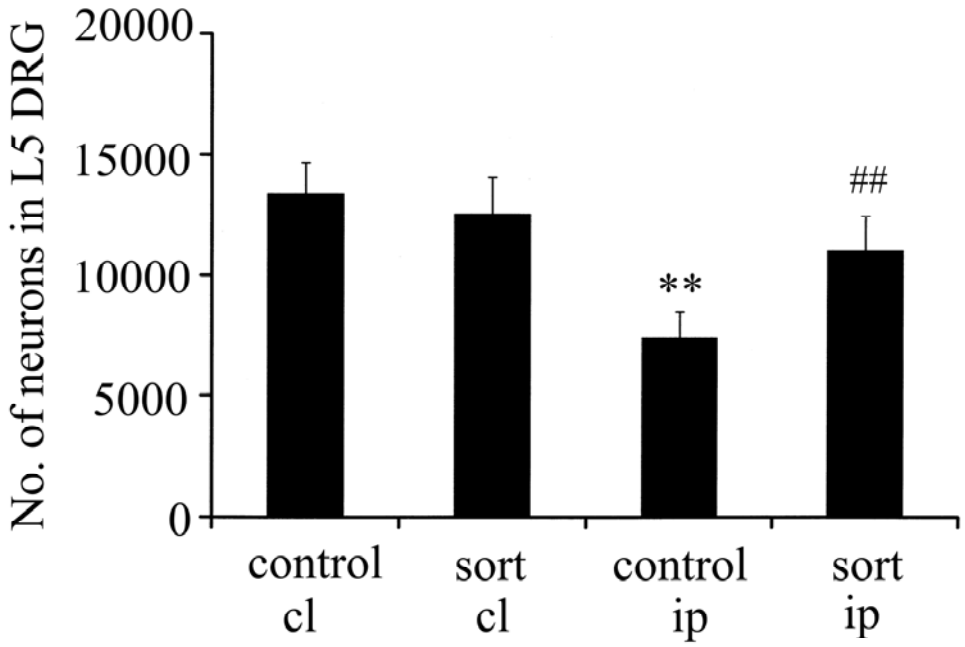

Fig. 8 Effects of sortilin-Fc on axotomised sensory neurons. The sciatic nerve was cut on P1 and recombinant sortilin-Fc trapped into gel foams were placed in the injury sites (n=6). In control group, the gel foams containing BSA were placed in the injury sites (n=10). Total numbers of sensory neurons in DRG were counted stereologically. cl, contralateral DRG; ip, ipsilateral DRG. **p<0.01, compared with the contralateral DRGs from the same animal. $^{\#\#}$ p < 0.05 compared with ipsilateral DRG of control group.

5. Discussion

In the present study, we have shown that recombinant proBDNF induces a dose-dependent increase in PC12 cell death which is abolished in the presence of a neutralizing antibody to the prodomain. With the biologically-active proBDNF and the neutralizing antibodies we have illustrated that exogenous proBDNF induces an increase in the loss of sensory neurons after axotomy in neonatal rats and that the treatment of neonatal rats with the prodomain antibody prevents the loss of axotomized neurons. We further showed that the soluble sortilin protein applied *in vivo* in the axotomized axons prevents the loss of axotomized sensory neurons. Our data suggest that endogenous proBDNF has a physiological function of inducing the death of axotomized neurons.

All neurotrophins are initially synthesized as precursor proteins containing a signal peptide with glycosylation sites and pairs of dibasic amino acids that are recognized by processing enzymes (Hempstead 2006). Mature BDNF is derived from proBDNF that is cleaved by the serine protease furin or other members of the prohormone convertase family (Lee et al. 2001b). Mature BDNF is essential for cell survival during the development of a subpopulation of sensory neurons (Altar et al. 1997, Conner et al. 1997) and axotomized

sensory neurons after the peripheral nerve injury (Zhou et al. 2005). The source of mature BDNF is the neuronal targets such as skin and visceral organs (Erickson *et al.* 1996, ElShamy & Ernfors 1997) as well as autocrine secretion from sensory neurons (Acheson et al. 1995). Sensory neurons highly express BDNF during development (Schecterson & Bothwell 1992) and the expression continues in adults (Zhou & Rush 1996, Zhou et al. 2005). This pattern of autocrine secretion of mature BDNF strongly suggests that proBDNF may also be expressed, transported and secreted by the sensory neurons in DRG (Wang et al. 2006). ProBDNF has been shown to be released from primary cultured cortical and hippocampal neurons of the CNS but this has not been examined in the peripheral nervous system. In the present study, we confirmed that proBDNF is expressed by sensory neurons in rat DRG. We observed that a subpopulation of neurons in DRG are proBDNF-immunoreactive (Fig.5A); the molecular weight of proBDNF assessed by Western blot is 30 kDa, consistent with previous studies that secreted proBDNF dimer is about 60 kDa and glycosylated in mammalian cells (Kolbeck *et al.* 1994, Heymach & Shooter 1995). Interestingly, p75NTR and sortilin, the functional receptors of proBDNF, are colocalized in sensory neuron in DRG. It is plausible that proBDNF may be an alternative ligand to modulate cell survival and cell death in DRG.

The prodomain of BDNF is highly conserved between species (Kolbeck et al. 1994, Heymach & Shooter 1995). The prodomain is required for correct folding and intracellular trafficking of BDNF (Egan et al. 2003, Chen et al. 2004). The Val66Met mutation in the prodomain causes dysfunction of BDNF transport, reduction in hippocampal volume and impaired episodic learning (Egan et al. 2003, Hariri et al. 2003). The mutation also causes a number of neurological disorders (Egan et al. 2003, Hariri et al. 2003, Bath & Lee 2006, Numata et al. 2006, Hashimoto 2007). It was reported that proBDNF is a potential proapoptotic factor, inducing sympathetic ganglion neuron apoptosis *in vitro* (Teng et al. 2005). In the present study, we confirmed that proBDNF induced cell death of cultured PC12 cells. These cells express p75NTR and sortilin on their cell surface. This effect was blocked by the antibody to the prodomain, suggesting the apoptotic effect is mediated via the prodomain but not the mature domain.

However, whether endogenous proBDNF has any physiological function *in vivo* is not known. Using the axotomized neonatal sensory neuron as a model, we examined whether proBDNF induces death of axotomized neurons. In neonatal rats, transection of sciatic nerve caused a loss of about 50% neurons in the L5 DRG and mature BDNF is required for the survival of a population of these neurons (Zhou et al. 2005). The proBDNF with a point mutation within

the cleavage site trapped in gelatin sponge further reduced the survival of sensory neurons. It is plausible that exogenous proBDNF activates p75NTR and sortilin is internalized and then transported retrogradely to sensory neurons to effect cell death. Indeed, proBDNF immunoreactivity accumulates in the proximal and distal segments of crushed sciatic nerve, suggesting that proBDNF can also be secreted and transported anterogradely and retrogradely (Wang et al. 2006). Labelled exogenous proBDNF injected into the sciatic nerve can also be transported anterogradely and retrogradely (Wang et al. 2006). To further investigate whether endogenous proBDNF elicits cell death after lesion, antiserum against the prodomain was injected after axotomy. The loss of sensory neurons in the ipsilateral DRG decreased significantly, indicating that endogenous proBDNF is responsible for the apoptosis of sensory neurons after the transection.

It has been reported that the induction of apoptosis of sympathetic neurons and glia by proBDNF is dependent on the p75NTR and sortilin coreceptors (Teng et al. 2005). Moreover, proBDNF is at about 10-20 times more effective at inducing apoptosis compared to mature BDNF. It was predicted that the access of proBDNF to its physiological targets must be strictly regulated (Teng et al. 2005). Their results showed that soluble sortilin can form a high-affinity complex with proBDNF and this preformed complex is ineffective in eliciting

death of cells co-expressing p75NTR and sortilin (Teng et al. 2005). To investigate the role of endogenous proneurotrophins in sensory neurons in DRG after axotomy, exogenous sortilin trapped in a gelatin sponge was placed into the injury site. Our data illustrate that the exogenous sortilin-Fc could also increase the number of neurons by about 42% compared to BSA/NSS treatment in DRG after lesion. As sortilin is also the receptor for proNGF which signals the death of p75NTR expressing neurons (Nykjaer et al. 2004, Volosin *et al.* 2006, Domeniconi *et al.* 2007), the protection of dying sensory neurons by soluble sortilin may be due to the formation of complexes with endogenous proBDNF or proNGF. Exogenous sortilin prevents the interaction of endogenous proBDNF or proNGF with their receptors on sensory neurons, blocks the ipsilateral retrograde transport and restricts the ipsilateral biological activity *in vivo*. As the NGF gene is upregulated in Schwann cells after sciatic nerve lesion (Frostick *et al.* 1998, Agthong *et al.* 2006), proNGF released from the Schwann cells at the lesion site may also induce the death of axotomized sensory neurons.

Previous studies from our group showed that mature BDNF reduces the rate of death of sensory neurons in DRG after peripheral nerve injury (Zhou et al. 2005); while this current study demonstrates that proBDNF increases cell death of axotomized neurons. These findings support the hypothesis that the balance

between cell death and cell survival may be determined by the ratio of proBDNF and mature BDNF in DRG after lesion. The present study demonstrates that exogenous recombinant proBDNF or anti-proBDNF administration may interrupt the balance of proBDNF and mature BDNF in sensory neurons after nerve transection. The prediction of this balance model has also been demonstrated by the differential effect of proNGF and mature NGF. proNGF preferentially activates p75NTR to elicit apoptosis while mature NGF preferentially activates TrkA receptor which negate this pro-apoptotic effect (Yoon et al. 1998, Lee et al. 2001b). The diversity of neurotrophin functions may be modulated by the regulated release of precursors versus mature proteins in the nervous system, or by the activity of proteases processing these precursors (Lee et al. 2001b). In addition, our data also suggest that the death of sensory neurons after axotomy is not only due to the lack of neurotrophic factors from their targets but also due to positive death signals released from neurons and injured nerves. Our study suggests that the administration of specific antibodies to the prodomain of neurotrophins or soluble extracellular domain of sortilin may have a therapeutic potential of rescuing apoptotic neurons after neurotrauma or other pathological conditions.